DESIGN AND DEVELOPMENT OF ROBUST HANDS FOR HUMANOID ROBOTS

Anand Vazhapilli Sureshbabu

Department of Bioengineering and Robotics and the iCub Facility

Università degli Studi di Genova with Istituto Italiano di Tecnologia

This dissertation is submitted for the degree of

Doctor of Philosophy in
Bioengineering and Robotics

Istituto Italiano di Tecnologia

March 2018

ANAND VAZHAPILLI SURESHBABU:
Design and Development of Robust Hands for Humanoid Robots

DOCTORAL SCHOOL:
Department of Bioengineering and Robotics (XXIX Cycle)

SUPERVISORS:
Dr.Alberto Parmiggiani
Dr.Giorgio Metta

To my Mom, who found the strength to encourage me as she lay beating cancer,
To Biene, whose love has given me a goal to run towards,
To my family, the greatest support and strength in my life.

Declaration

I hereby declare that except where specific reference is made to the work of others, the contents of this dissertation are original and have not been submitted in whole or in part for consideration for any other degree or qualification in this, or any other University. This dissertation is the result of my own work and includes nothing which is the outcome of work done in collaboration, except where specifically indicated in the text. This dissertation contains less than 65,000 words including appendices, bibliography, footnotes, tables and equations and has less than 150 figures.

Anand Vazhapilli Sureshbabu
March 2018

Acknowledgements

"A boy who won't stand up for himself becomes a man who can't stand up to anything." — Khaled Hosseini

"...talent means nothing, while experience, acquired in humility and with hard work, means everything." — Patrick Süskind

I would like to start by thanking all the reviewers in the past and present who put in their valuable time and painstaking effort of going through my publications and thesis, and for giving their invaluable feedback. I would also like to start off by saying that I have come across countless precious individuals, during my nearly four years in Genova. If I forget to thank you, forgive me.

My sincerest gratitude goes towards my advisors Giorgio and Alberto. Alberto, in particular has been a guiding force throughout these years, and having been his first student mentee, I guess we can say we grew up together to realise what a team needs to be, in both good times and bad. He was always there to criticize me and redirect my focus, when I went astray.

I would also like to whole-heartedly thank my reviewers, Dr.Marco Controzzi and Dr.Markus Grebenstein, your feedback was invaluable to me.

My PhD will not be where it is now without the help from our entire team at the iCub facility. In particular, I would like to thank Marco Maggiali, Luca Fiorio, Alessandro Scalzo and Roberto Puddu for providing their invaluable assistance. I would also like to thank Marcello Savoldi, my CREO and italian coach, who's guidance helped me both personally and professionally: *Grazie mille!*

I would also like to thank my current and past flatmates: Ninad, Silvio, Giovanni

and Emy, who fed me and made our house a home by providing endless entertainment and companionship to this outsider.

I also thank all my friends who supported me through good times and bad in the past three and a half years. My Vivlafrans group, for their unconditional support and the Party team for making Genova's social encounters all the more fun. Den, Sandy, Giulio, Yue, Chri, Mati, Louis, Fanny, Dave.. the list goes on.

I want to also thank my family. It has been 9 whole years since I left home. And not a day has gone by when I haven't wished I was closer to you. I thank them for their patience, it must be the toughest thing for any parent to do: to have your children live far away from you. Please know that, I would return in an instant, if the opportunity does so arise.

And finally, to Biene. For all her unconditional love and support these past two years, and for giving me a family that is just ours.

Abstract

Robotic hands have been among the most researched and oft used branch of humanoid robotics. At the forefront of every humanoids research problem, is the problem of grasping and manipulation. Designing a robotic hand that is efficient in cost, construction and performance is a very challenging task. Robotic hands are usually heavily customised within their requirements of cost, shape, function, features, platform, etc. This thesis aims at trying to identify the different aspects to robotic hand design and tries to find ways to do it well and in cost-efficient ways.

The first four chapters in this thesis sets up the problem, tries to identify the right inspirations when it comes to mimicking nature, goes through the different hands that exist in literature and tries to identify some of its key features which make it successful. An evaluation index is then proposed to compare hands across domains and to find where the key focus of these hands lie. It also acts as a list of 'best practices' when it comes to adding features in a robotic hand.

The core of the thesis aims at developing two diverse hands, connected by a similar design philosophy. The hands had to incorporate novel manufacturing technologies, accurate sensors and new features while making them extremely cost-efficient. First, a wrist is designed and constructed, which provides the requisite range of motion and the support required for the hand to be mounted upon. Later, a simple two digit underactuated hand is constructed with a plethora of cost-effective features and is studied. Both the wrist and the hand are built as part of a new humanoid robot, the R1.

Finally, the lessons learnt are noted and an experimental prototype hand for the iCub robot is designed and constructed. This aims at taking the features present in the R1 hand and adapting it for the iCub platform, while addressing the existing problems in the iCub hand. This experimental prototype introduces new technologies, never tried before on the iCub platform, all the while making the entire design process cost-efficient.

Contents

Contents xi

List of Figures xvii

List of Tables xxi

Nomenclature xxi

1 Introduction 1

1.1 Artificial Hands in Society and Science . . . 2

1.1.1 Medicine . . . 3

1.1.2 Domestic Robots . . . 3

1.2 Research Platforms . . . 5

1.2.1 The iCub Platform . . . 5

1.2.2 R1 Humanoid . . . 5

1.3 Research Objectives . . . 6

1.4 Thesis Structure . . . 7

1.5 Publications . . . 9

2 Hands in Nature 11

2.1 Animal Manus . . . 11

2.1.1 Special Features . . . 12

2.2 Human Hands . . . 14

2.2.1 The Human Wrist . . . 15

2.3 Human Hand Anatomy . . . 16

2.3.1 The Bones of the Human Hand . . . 16

2.3.2 Joints . . . 17

2.3.3 Pulley System in Fingers . . . 18

2.3.4 Arches . . . 18
2.4 Main Functions . . . 19
2.4.1 Prehensile Manipulation . . . 20
2.4.2 Non-prehensile Manipulation . . . 22
2.4.3 Communication . . . 22
2.4.4 Exploration . . . 24
2.5 Nomenclature . . . 25
2.6 Goals . . . 26

3 Review on robotic hands **27**
3.1 A General Timeline of Robotic Hands . . . 27
3.1.1 Robotic Hands . . . 28
3.1.2 Evolution of rapid prototyped robotic hands . . . 34
3.2 Types of Hands by Function . . . 38
3.3 A Qualitative Analysis on Robotic Hands . . . 39
3.3.1 The Key Features . . . 43
3.3.2 Comparison of Key Aspects . . . 48
3.4 Technical guidelines . . . 52

4 A New Evaluation Index **55**
4.1 Motivation . . . 55
4.2 A New Evaluation Index . . . 56
4.3 The FFP Index . . . 58
4.3.1 Form . . . 59
4.3.2 Control Features . . . 65
4.3.3 Performance . . . 69
4.3.4 Subjective Weighting . . . 72
4.4 A Case Study . . . 73
4.4.1 Form . . . 73
4.4.2 Features . . . 74
4.4.3 Performance . . . 74
4.5 Final Design Guidelines . . . 77
4.5.1 Technical Requirements . . . 77

5 The R1 Wrist **79**
5.1 Overview . . . 79

5.2 Conceptual Design . . . 80
5.2.1 Requirements . . . 81
5.2.2 Kinematic Structure Selection . . . 82
5.2.3 Load Path Analysis . . . 83
5.3 Embodiment Design . . . 85
5.3.1 Hardware . . . 85
5.3.2 Electronics . . . 87
5.4 Evaluation . . . 88
5.4.1 Cost Evaluation . . . 89
5.4.2 Payload . . . 89
5.4.3 Range of Motion . . . 90
5.4.4 Performance Analysis . . . 90

6 The R1 Hand **95**
6.0.1 Design philosophy . . . 95
6.1 Conceptual Design . . . 96
6.1.1 Kinematics . . . 97
6.1.2 Series Elastic Elements . . . 97
6.2 Embodiment Design . . . 101
6.2.1 Hardware . . . 101
6.2.2 Friction Management . . . 102
6.2.3 Coupling and Actuation . . . 102
6.2.4 Design of the Series Elastic Elements . . . 103
6.2.5 Electronics . . . 104
6.3 Evaluation . . . 107
6.3.1 Performance Analysis . . . 108
6.3.2 Grasp Force Sensing . . . 109
6.3.3 Load Response . . . 110
6.3.4 Grasping Analysis . . . 111
6.3.5 Robustness . . . 111
6.3.6 Weight . . . 112
6.3.7 FFP Evaluation - R1 hand . . . 112

7 The iCub Plastic Hand **115**
7.0.1 Lessons Learnt from the R1 Hand . . . 115
7.0.2 The iCub Hand . . . 116

7.1 Conceptual Design . . . 117
7.1.1 Kinematics . . . 118
7.1.2 Overall Design . . . 120
7.1.3 Transmission . . . 120
7.1.4 Finger Design . . . 123
7.1.5 Actuator and Motor Carrier Design . . . 124
7.1.6 Return Spring . . . 125
7.1.7 Series Elastic Module . . . 127
7.2 Embodiment Design . . . 131
7.2.1 Finger Design . . . 132
7.2.2 Palm Design . . . 134
7.2.3 Series Elastic Module Design . . . 137
7.3 Electronics . . . 138
7.3.1 Finger Flex Circuit Design . . . 139
7.4 Evaluation . . . 143
7.4.1 Force sensing . . . 143
7.4.2 Tactile Sensing . . . 144
7.4.3 Cost . . . 145
7.4.4 FFP Evaluation . . . 146

8 Conclusion **147**
8.1 Summary of Contributions . . . 147
8.2 Other Contributions . . . 148
8.3 Reached Goals . . . 149
8.4 Lessons Learnt . . . 150
8.4.1 On the Use of Polymeric Materials . . . 151
8.5 Future Work . . . 152
8.5.1 The FFP Evaluation Index . . . 152
8.5.2 The R1 Hand . . . 152
8.5.3 The R1 Wrist . . . 153
8.5.4 The iCub Plastic Hand . . . 153

References **155**

Appendix A FFP Index - Task list **167**
A.1 Grasping dataset for prehensile tasks . . . 167

A.2 List of non-prehensile tasks . . . 167
A.3 Manipulation tasks . . . 170
A.3.1 In hand manipulation . . . 170

Appendix B The R1 head display **173**
B.1 Conceptual design . . . 174
B.1.1 Printed optics module design . . . 175
B.2 Embodiment design . . . 176
B.2.1 Display Construction . . . 176
B.2.2 Head Construction . . . 178
B.2.3 Electronics . . . 178
B.3 Evaluation . . . 179
B.3.1 Expression perception . . . 179
B.3.2 Weight analysis . . . 180
B.3.3 Observations . . . 180

Appendix C A comparison of robotic hands **181**

List of Figures

1.1 Rossum's Universal Robots . . . 2
1.2 Pop culture robots . . . 3
1.3 Example of prosthetic hands . . . 4
1.4 Domestic robots . . . 4
1.5 Research platform . . . 5

2.1 Animal Manus . . . 12
2.2 Primate hands . . . 13
2.3 Human Hand . . . 14
2.4 Human wrist range of motion . . . 15
2.5 Hand bones . . . 16
2.6 Hand joints . . . 17
2.7 Finger pulley system. . . . 18
2.8 Hand arch . . . 19
2.9 Everyday use of hands with varying dexterity . . . 20
2.11 InHand Manipulation . . . 21
2.12 Non-prehensile manipulation . . . 22
2.13 Examples of sign language . . . 23
2.14 Examples of symbolic gestures . . . 24
2.15 Examples of conversational gestures . . . 24

3.1 General timeline . . . 28
3.2 Robotic hands timeline . . . 28
3.3 Robotic hands 80s and 90s . . . 29
3.4 Robotic hands early 2000s . . . 30
3.5 Robotic hands late 2000s . . . 32
3.6 Robotic hands 2010s . . . 33

3.7 Anthropomorphic rapid prototyped robotic hands 35
3.8 Anthropomorphic index 40
3.9 Dexterity index 41
3.10 Kapandji test 41
3.11 Cutkosky Grasp list 42
3.12 Hands DOF vs. DOA 49
3.13 Hands Weight vs. Payload 50
3.14 Hand weight vs. Number of actuators 51

4.1 A new evaluation index 57
4.2 FFP index - weights 59
4.3 Payload to weight 61
4.4 Human hand glabrous 63
4.5 Open and closed palm 64
4.6 Biased weights of the FFP index 72
4.7 FFP Index evaluation of the iCub hand 73
4.8 The iCub2 and INAIL-Rehab prosthetic hands 74
4.9 iCub sample grasps 75
4.10 iCub sample gestures 75
4.11 FFP Index: Rehab versus iCub 76

5.1 R1 wrist 80
5.2 The conceptual design of the parallel structure 83
5.3 Load analysis 84
5.4 The free body diagram of the platform 85
5.5 Wrist detailed design 86
5.6 Wrist detailed design 87
5.7 Completed wrist design 88
5.8 Wrist payload 90
5.9 Wrist range of motion 91
5.10 Wrist marker positions 91
5.11 Wrist repeatability 92
5.12 Radial force loading experiment 93
5.13 Radial force loading 93
5.14 Wrist accuracy 94

6.1 Kinematics of the R1 hand . . . 97
6.2 SEE module geometry . . . 98
6.3 SEE module stiffness selection curves . . . 99
6.4 Skin assembly . . . 101
6.5 R1 skin padding . . . 102
6.6 Tendon management . . . 102
6.7 Design of the SEE module . . . 104
6.8 The main control board of the R1 hand . . . 104
6.9 A layout of the electronics in the R1 hand . . . 105
6.10 R1 hand without covers . . . 107
6.11 Payload grasps . . . 107
6.12 Graph - Tendon force vs. SEE module deflection . . . 108
6.13 Graph - SEE module force sensing with FT sensor . . . 109
6.14 Graph - External disturbance response . . . 110
6.15 Key grasps of the R1 hand . . . 111
6.16 Form - R1 hand . . . 112
6.17 Features - R1 hand . . . 113
6.18 Performance - R1 hand . . . 113
6.19 FFP Index-iCub2 and R1 hand . . . 114

7.1 Basic Kinematics . . . 118
7.2 Detailed Kinematics . . . 119
7.3 Thumb positions . . . 120
7.4 Transmission mechanism . . . 122
7.5 Sliding pin distance selection . . . 125
7.6 Return spring selection . . . 126
7.7 Series elastic module 'k' value estimation . . . 128
7.8 Series elastic module spring stages . . . 128
7.9 Finger constructed . . . 131
7.10 Hard limits on joints . . . 132
7.11 Tendon routing in finger . . . 133
7.12 Return spring deflection . . . 134
7.13 Palm design of the iCub plastic hand . . . 135
7.14 Tendon friction force . . . 136
7.15 Palm tendon management . . . 137

7.16 Series elastic module: Estimated force deflection . . . 138
7.17 SEE-Linear . . . 139
7.18 Finger flex circuit architecture . . . 140
7.19 PCB slack maintenance . . . 140
7.20 Finger flex PCB assembly . . . 142
7.21 Hand CAD . . . 142
7.22 SEE module test setup . . . 143
7.23 Series elastic module: Real force deflection . . . 144
7.24 iCub old taxel distribution . . . 144
7.25 Form - iCub plastic hand . . . 145
7.26 Features - iCub plastic hand . . . 146

8.1 FFP Index: All hands . . . 148
8.2 R1 display . . . 149
8.3 R1 mockup hands . . . 152
8.4 R1 version 2 . . . 153

A.1 Communication - Gestures . . . 170
A.2 Translation and shift tasks . . . 171
A.3 Simple rotation task . . . 171
A.4 Complex rotation task . . . 171

B.1 The R1 display . . . 173
B.2 Printed optics module structure . . . 175
B.3 Proposed display structure . . . 176
B.4 Light pipe concept . . . 177
B.5 Internal structure of display . . . 177
B.6 Hardware architecture of the display . . . 178
B.7 Sample expressions . . . 179

List of Tables

5.1 Cost breakdown. 89

6.1 R1 hand - DH parameters 96
6.2 Tactile sensing information-R1 106

7.1 Finger kinematics 119
7.2 Thumb kinematics. 120
7.3 Tactile sensing information - iCub 141
7.4 Tentative cost breakdown 145

8.1 Validation of the designed robotic hands 150

A.1 Grasping Objects Dataset-1 168
A.2 Grasping Objects Dataset-2 169

C.1 Robotic hands 181
C.2 Robotic hands 182

Chapter 1

Introduction

Humanoid robotics is the field of robots that are anthropomorphic in their design principles. It is one of the most complex lines of research as it aspires to replicating the human condition physically and otherwise. This is an important step for the progress in human-agent and human-robot interaction. Making robots that look and behave like human beings, if done correctly, makes integration of robots into mainstream society easier, if done right. The end effectors in humanoid robots are more interesting because they are usually modelled after human hands. This thesis aims to study what constitutes a good end-effector or robotic hand, in the context of humanoid robots. A design of a good robotic hand that focuses on bringing the research domain of robotic hands into a commercial product is the end goal.

The main motivation of this thesis is to make cost-effective robot hands using modern manufacturing methods such as rapid prototyping, and employ lighter, more durable materials into everyday robotics. The field of robotics has come a long way in the past forty years. Humanoid robotics, especially has jumped out from science fiction pages onto reality. From the first play, Rossum's Universal Robots[26] (Fig.1.1), where the term robot was coined, to now where robots are slowly integrating into everyday life in society and science.

The rise of robots in popular culture was inspirational in the robot evolution as scientists started looking towards science fiction for inspiration. Robots such Evil Maria from Metropolis [2], Rosie from the Jetsons 1.2 and the robots R2D2 and C3PO from the Star Wars [3] franchise are some examples to name a few.

Humanoid robotics, in particular, has taken rapid strides in the past couple of decades. The iCub platform from the Italian Institute of Technology is an example of one such humanoid robotics platform. The objective of this thesis is to develop

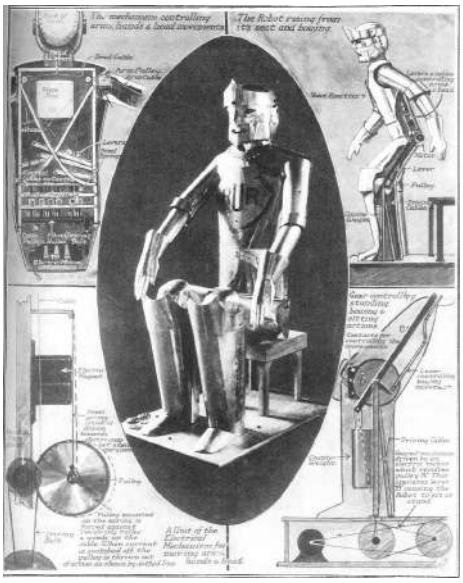

Fig. 1.1 A poster from the play adapted from Rossum's Universal Robots depicting a humanoid and it's working

a highly dexterous hand compatible with the iCub humanoid platform [118] of the Italian Institute of Technology. The iCub is currently undergoing a complete redesign with robustness and ease of manufacturing with an increased effectiveness in grasping in mind. Additional importance was given to achieve a fair trade-off between dexterity, manipulability and payload characteristics in order to achieve maximum possible grasps as defined by the taxonomy by Feix et al. [44].

1.1 Artificial Hands in Society and Science

The main motivation to create a good, affordable product does not only mean that it needs to be cost-effective to manufacture, but also easy to assemble, repair and eventually replace. The main uses of robotic hands, in particular, have been in prosthesis design and to a certain extent in grasping research.

Prostheses and functional prosthetic robotic hands have come a long way from the simple hook hands to advanced myoelectric prostheses. It is especially beneficial to amputee patients, who have lost their limbs due to a number of reasons such as accidents, line of duty, tumors, infections or neuroma, and are given a second chance at enhanced mobility. But a burgeoning field of interest has also been in domestic robots. The age where humanoid robots that can help around in domestic environments, to monitor and aid in the upkeep of the house, provide companionship to elders, assist

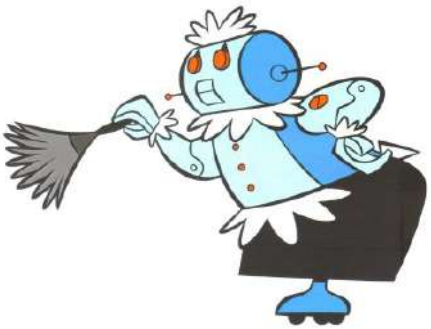

(a) Rosie the robot from “The Jetsons".

(b) C3PO from Star Wars

Fig. 1.2 Robots in pop culture. Shown in 1.2a is the home robot Rosie from The Jetsons. In 1.2b we can see the translation and diplomacy robot C3PO from the Star Wars movie franchise.

in day to day living, is not too far off.

1.1.1 Medicine

Robotic hands in medicine are generally in the realm of prostheses. To achieve a close-to-natural replacement for the lost hand, the user should be provided with an expansive gamut of sensory feedback, similar to what occurs naturally in the human body when grasping or manipulating an object. Ideal bidirectional hand prostheses should involve both a reliable decoding of the user’s intentions and the delivery of nearly “natural” sensory feedback through remnant afferent pathways, simultaneously and in real time. A number of companies and non-profit organizations dedicated to the development of advanced prosthesis have been on the rise, which deals with these issues. Some of the more notable works include [83] [111] (shown in Fig.1.3) [17].

1.1.2 Domestic Robots

Domestic robots are any type of robots that are used to aid in household chores, education, entertainment, therapy or in the service industry such as tellers and wait staff. Another interesting field in the use of domestic robots is telepresence. Home-telepresence robots can move around in a remote location and allow people to communicate with each other via its camera, speaker, and microphone. Through other remote-controlled telepresence robots, the user can visit a distant location and explore it as if they were physically present. These robots can, among other applications, permit health-care workers to monitor patients or allow children who are home-bound

Fig. 1.3 Prosthetic hands. An example of commercial prosthetic hands is the Prensilia IH2.

because of injuries, illnesses, or other physical challenges to attend school remotely. Meanwhile, a social robot is a robot whose main objective is human agent interaction in a social context, such as elderly care or companionship. Many of these robots are designed to help the elderly[100][58]. There has also been an increase in such type of robots in the public spaces such as malls and banks. There are also robots which are more recreational in nature [58, 99] which incorporate the navigation principles of a domestic robot, simplified human-robot interaction principles and aspects of telepresence robots to acts as companions around the house.

(a) Nao and Pepper from Softbank Robotics.

(b) Roomba from iRobot

Fig. 1.4 Domestic robots. An example of a house cleaning and mopping robot brand is the Roomba from iRobot. Robots such as Nao and Pepper are examples of domestic companion robots.(Pictures courtesy : Softbank Robotics and iRobot)

The simpler robots such as vacuuming, floor washing, pool cleaning robots etc., are of little significance to us. Lately, an increase in humanoid robots which are used

for the aforementioned objectives, while also doubling up as companions and “social" robots has been observed. Most of these applications require the robot to at least partially grasp or manipulate objects can also be observed.

1.2 Research Platforms

1.2.1 The iCub Platform

The iCub is one of the results of the RobotCub project, an EU-funded endeavor to create a common platform for researchers interested in embodied artificial cognitive systems. It is a bipedal robot which was originally conceived in 2007. Currently, the iCub robot has a total of 53 actuated degrees of freedom (DOF), 6 in each leg, 7 in each arm, 6 in the head, 3 in the waist and 9 for each hand[106]. It utilises tendon-driven joints for the hand and shoulder, with the fingers flexed by teflon-coated cable tendons running inside teflon-coated tubes. The hand tendons pull against spring returns and the fingertips are equipped with tactile touch sensors and a distributed capacitive sensor skin.

(a) The iCub humanoid platform

(b) The R1 humanoid

Fig. 1.5 The humanoid platforms. The iCub and the R1 humanoid act as the research platforms for the basis of this thesis.

1.2.2 R1 Humanoid

The R1 humanoid was conceived to be a robot that makes the iCub technology accessible to everybody. It is a wheeled robot that has 28 degrees of freedom with two 2 DOA hands. It took 16 months of development from its initial conception to the first working prototype. The R1 robot is designed to be very affordable, to allow for easy and natural interaction, to have an elegant and glossy look, to grasp, move and

manipulate objects, to operate switches and to open doors, and to be capable of safely navigating its environment.

1.3 Research Objectives

Starting from the generic objective of making a cost-effective hand and incorporating new methods and materials, some of the research objectives for this thesis is explored in more detail below.

- **Challenge 1**
  Large-scale integration of humanoid robots in society is uncommon and complex. There are many factors which are currently hindering progress in this field, one of them being the cost. Integration of the latest in manufacturing and material technologies can help overcome these barriers. A humanoid robot that is easy to assemble and repair, which also happens to be cost-effective is hence considered the main challenge of this thesis.

- **Challenge 2**
  Robotic hands in recent years have been progressing rapidly. There is a need for an objective evaluation of different types of these robotic hands. Most evaluation indices present in literature are based on control objectives or dated methodologies. A method of evaluating the key characteristics that make up a good robotic hand that can be objectively evaluated from a hardware perspective is hence required.

- **Challenge 3**
  Most anthropomorphic robotic hands aim at making a five-fingered hand which at most times does not even come close to the functionalities of the human hand. This thesis aims to achieve a middle ground between compactness, weight, sensor-less safety, actuation, dexterity and power of the hand. A trade-off between the number of actuators, the hand's dexterity and its payload should also be achieved.

- **Challenge 4**
  A common way of evaluating the performance of a robotic hand has been to either let it perform a certain number of grasps as defined in literature or to let it carry a certain number of objects. However, human hands are capable of

more than just prehensile tasks. They are also used to gesture, emote, sense and perform other types of non-prehensile tasks. This thesis aims at building a hand that can move beyond just the classical grasping methodologies and to being an effective agent for human-like interaction.

- **Challenge 5**
  Robots are expected to be an integral part of the human communal experience in the near future. Therefore, interacting with them in a safe manner becomes a priority. New and effective methods of sensor-less safety and inherent safety measures need to be explored. A robotic hand that aids safe human interaction by providing compliance and aiding in sensing the forces from its external environment and its internal system becomes mandatory.

- **Challenge 6**
  The integration of the robotic hand should be seamless, the iCub is a humanoid robot that needs to freely interact with its environment. Hence, the robotic hand should be able to integrate seamlessly with the rest of the robot, with its actuators and sensors completely self-contained within the robot.

1.4 Thesis Structure

The structure of the thesis is covered in three main segments, the introduction, problem definition and evaluation parameters are first defined, the R1 platform is then covered and the corresponding work done with the wrist and hand design is explained. Finally, the iCub hand design and evaluation is discussed. The breakdown of the structure is given in more detail below:

- **Chapter 1**
  This chapter aims to give a brief introduction on how robotics has become a part of our society through pop culture and is being slowly integrated into mainstream society. It aims to show the slow advent of robotics in medical and domestic scenarios. Some of the main challenges that the thesis hopes to address is then discussed and a corresponding thesis structure is formulated.

- **Chapter 2**
  The second chapter looks to nature for inspiration in making robot hands. It

discusses the functionality of animal manus in the evolution of different animals. It then looks into some of the special functionalities exhibited in different species of animals. Primate hands are then briefly discussed and compared with the human hand. The anatomical terms, functionalities and features of human hands are then explored, with its role in communication and interaction with its environment and society being discussed more in detail. A list of preliminary design guidelines that are favoured in robotic hands is then drawn as a starting point.

- **Chapter 3**
  The third chapter takes a deeper dive into what exists in literature, both research and commercial while drawing comparisons between the different robotic hands already in existence. An evaluation of features which are more favourable and aspects of robotic hands that are key to performance is then analysed. A list of desirable features are then drawn up and the final design guidelines are enumerated.

- **Chapter 4**
  The fourth chapter discusses the drawbacks in current evaluation methods and the problems in drawing a common baseline in literature for comparisons. A new type of evaluation is then proposed which lays out key features and how to weigh them. An analysis of the existing iCub hand is made as an example, which serves as a research baseline for the rest of the thesis.

- **Chapter 5**
  The first part of the research is on the R1 platform. This chapter discusses the design and construction of the R1 forearm and wrist assembly on which the R1 hand is mounted. The conceptual, embodiment and detailed design are discussed. The forearm is then evaluated in its performance against its design objectives.

- **Chapter 6**
  The force sensing R1 hand which was designed for the R1 humanoid platform is discussed in detail. The design objectives are modified and re-established for a domestic humanoid robot. The conceptual, embodiment and detailed design are explained. A preliminary evaluation of its key characteristics and performances are drawn against the design objectives. A preliminary score with the FFP

evaluation is also done and compared with the iCub hand.

- **Chapter 7**
  The second platform that required a design overhaul was the iCub humanoid. To this end, a prototype design of the iCub hand was developed. A key required characteristic in the iCub hand was force sensing. A brief look at the literature of force sensing in hands is done. The right design is then selected, designed and analysed. A final choice is then made to be integrated into the iCub hand. The design of the iCub hand is discussed in detail. The conceptual, kinematic, embodied and detailed design are all explained. Firstly, the finger design and the decisions that were made is enumerated. The same is then done for the thumb. Later, the development of a new PCB with flex circuit design encompassing the new tactile sensors and joint positioning sensors for the hand was discussed in detail. Finally, a detailed look at the integration of the different components was done. A detailed evaluation of the iCub hand was also done and a preliminary FFP evaluation was also drawn and explained.

- **Chapter 8**
  The goals achieved during the thesis is briefly enumerated. The lessons learnt are then listed and suggestions on how to improve are then given. The main contributions of the thesis are also listed. A discussion on the future work based off of the thesis is then discussed in detail.

1.5 Publications

This is a list of publications of the work that was carried out for the duration of the PhD. While a few other papers are in various stages of review, this is a list of published articles by this author up until December 2017.

- In *The Design and Validation of the R1 Personal Humanoid* by Parmiggiani et al. [96], a general introduction to the R1 humanoid platform was provided.

- In *A parallel kinematic wrist for the R1 humanoid robot* by Vazhapilli Sureshbabu et al. [121], is the work done on the R1 wrist that is discussed in Chapter.5.

- *Design of a force sensing hand for the R1 humanoid robot* by Vazhapilli Sureshbabu et al. [123], is the work done on the R1 hand that is discussed in Chapter.6.

- *A new cost effective robot hand for the iCub humanoid* by Vazhapilli Sureshbabu et al. [120], laid the foundation for the work discussed in Chapter.7.
- *Design of a cost-efficient, double curvature display for robots* by Vazhapilli Sureshbabu et al. [122], is the work done on the R1 display technology that is not part of the main topic in this thesis and is explained in Appendix.B.
- *Head and Face Design for a New Humanoid Service Robot* by Lehmann et al. [74] is a continuation of the work done on the R1 display.

Chapter 2

Hands in Nature

Nature provides a vast canvas when it comes to inspiration. Evolutionary traits and features in animals and human beings took thousands if not millions of years to be perfected. So inspiration from nature when it comes to modern problems has always been one way to look at for scientists.

It is not very different for the design in hands. Every animal has its own distinct set of features that it has adapted for its environmental constraints. In this first part of this chapter a few such examples are briefly discussed and key features are extrapolated, which serve as inspiration in the design of robotic hands in this thesis. In the following section, primate hands are then briefly discussed and its evolution to human hands are then explored, drawing comparisons between them both. Finally, the role of human hands as a tool for manipulation, emotion and interaction in society is discussed and the first user needs are drawn.

2.1 Animal Manus

The distal portion of the fore limb of an animal is termed as *Manus*. It is the part of the limb that includes the metacarpals and the digits (or phalanges) for grasping, manipulation etc. It can be represented by the hand in primates, hooves in horses, paws in rodents and monkeys, wings in birds, flippers in marine mammals or even the tentacles in octopi. The form and function of some of these manus' can prove to be inspirational in the design of end effectors.

2.1.1 Special Features

In addition to grasping, manipulation and non-verbal communication; some animals also use hands for locomotion. Primates in particular make use of hands for brachiation and knuckle-walking. Some other interesting functionalities in animal manus' are listed below:

Gecko

Geckos are reptiles that inhabit temperate ans tropical regions. Their feet have a number of specializations. The feet surface can adhere to most types of surfaces (except PTFE). This due to the fact that geckos have multiple microscopic protein structures which extrude from the body called setae. The setae increases Van der Waals forces between its feet and the surface.
Thoretically, the tokay gecko is capable of generating 1,200 newtons of shear force [9], in practice however, the gecko is attaching only 3 percent of its setae which accounts to about 20 newtons measured in whole-animal experiments. However, a gecko needs only 2 newtons to sustain its position. This gives the notion that gecko feet are over-engineered. But a prime example of its use is when the gecko is falling, it needs about a significantly larger amount of force to stick with the surface and to break its fall, at this point it is useful to have an over-engineered solution.
Another interesting fact about gecko setae is that they can adhere and unload in quick successions despite the large forces they are able to generate. This is due to the arrangement of its setae which allows it to become a sort of programmable adhesive.

(a) Gecko

(b) Tree frog.

Fig. 2.1 Special features on animal feet. Shown in 2.1a are protein protrusions called setae on gecko feet for adhesion. In 2.1b we can see wet adhesion in tree frogs.

Primate Hands

Primates such as bonobos and chimpanzees, being the closest relative to human beings, have a similar hand structure to that of ours. It lets them use have a semi-precision grip and have been seen on record employing sophisticated tool use. Opposable thumbs have given them an evolutionary edge and greater cognitive development. With minor variations between species, 35 joints accommodate the palm and fingers. Six layers of muscles produces movements resulting in effective gripping patterns and maintaining feeding and resting positions, securing an infant's hold on its mother, removing parasites from the fur, catching insects, plucking fruits, extracting foods from plants and trees, positioning objects for tactile, olfactory, and visual scrutiny.

Fig. 2.2 Different type of primate hands as compared to the human hand.

Almost all of the great apes have opposable thumbs, but none of them perform precision grips like humans. The gorilla's hand is the closest to that of the human hand when it comes to digit proportions. But chimpanzees and bonobos are more capable of performing precision grips akin to that of the human hand. This is due to the long opposable thumb, which performs a greater role in manipulating fine objects as compared to the other four digits.

Orangutan hands are similar to human hands; they have four long fingers and an op-

posable thumb. However, the joint and tendon arrangement in the orangutans' hands produces two adaptations that are significant for arboreal locomotion. The resting configuration of the fingers is curved, creating a suspensory hook grip. Additionally, without the use of the thumb, the fingers and hands can grip tightly around objects with a small diameter by resting the tops of the fingers against the inside of the palm, creating a double-locked grip.

A study of these animal hands and feet gives a good idea about the importance of smaller details. The kinematic properties of primate hands, the adhesion and gripping patterns in reptiles and amphibians which are highly evolved to suit the particular environment, the number of links, the spacing of the digits etc., all play an important role in obtaining a highly dexterous hand.

2.2 Human Hands

Human hands are the most important and oft-used appendage of our body which is not part of a human being's internal, involuntary body functions. It is a prehensile, multi-digit extremity located at the end of the forearm in human beings and usually consists of five fingers or digits which encompass a thumb which opposes the four other fingers. The human hand is divided into three main areas: the fingers, the palm

Fig. 2.3 A typical human hand

and the wrist. It contains an abundance of nerve endings making it the part of the body which we depend on most for tactile sensory feedback to carry out a number of tasks. It has long been one of the most significant part of human evolution due to its contribution in handling tools and manipulating objects. The evolution of the human hand to form the opposable thumb is considered one of the most important steps in human evolution. Opposable thumbs are required for efficient gripping of objects as well as performing fine manipulations upon them. As soon as man's tools evolved from

crude blocks of stone into more refined objects, the skill of refining objects with his hands on a tiny scale became indispensable to him. Without a thumb, it is unthinkable that man would have developed writing (as a thumb is indispensable in the act). Thus, he would not have devised a means of storing and passing on information in the long term, implying that he would still lead a largely primitive lifestyle not characterized by noticeable technological progress. The emergence of painting, sculpture, and music would have been unthinkable; people require thumbs to hold paintbrushes, chisels, and musical instruments.
It is also an indispensable part of human emotions since we express a range of emotions through our hands ranging from outright aggression to the most intimate expressions. Hence the role of the hand is clearly defined in human evolution and it's importance in the personal and societal standpoint of an individual.

2.2.1 The Human Wrist

The human wrist, also called carpus, is a complex joint between the five metacarpal bones of the hand and the radius and ulna bones of the forearm[1]. The range of motion of the wrist as shown in Fig.2.4 is discussed more in detail below.

Wrist Flexion/Extension

Forward bending of the wrist is called flexion. This motion is needed for daily activities such as styling hair, writing, getting dressed, using a screwdriver and lifting heavy objects. Normal wrist flexion is approximately 70 to 80 degrees. Extension, the act of backward bending of the wrist, is necessary for opening car doors, pushing a door closed, pressing up on the arms of a chair and driving. Normal wrist extension is approximately 55 to 75 degrees.

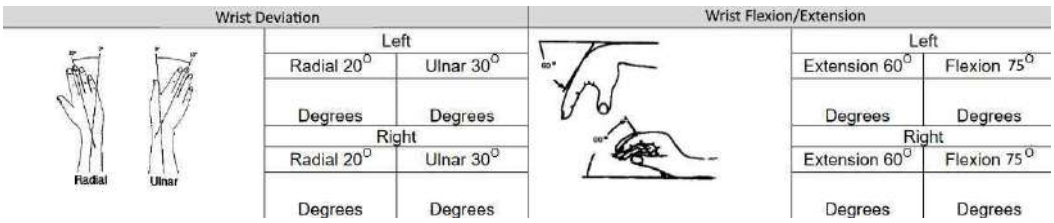

Fig. 2.4 The range of motion of a typical human wrist

[1]https://www.britannica.com/science/wrist-anatomy

Wrist Deviation

The wrist joint also deviates or tilts from side to side, this can also be called as the wrist abduction-adduction motion. Ulnar deviation tilts the wrist toward the pinkie side of the hand. Radial deviation tilts the wrist toward the thumb side of the hand. These movements are used frequently during the day to type, write, get dressed and talk on the phone. Normal ulnar deviation is approximately 25 to 40 degrees, while radial deviation is approximately 15 to 25 degrees.

2.3 Human Hand Anatomy

The anatomy of the human hand is incredibly intricate and complex. Its structural amd functional integrity is absolutely essential for everyday functional living. It is discussed more in detail in the following sections.

2.3.1 The Bones of the Human Hand

It consists of 27 bones, not including the sesamoid bone. 14 of which are the phalanges (proximal, intermediate and distal) of the fingers. The metacarpals are the bones that connect the fingers and the wrist. Each human hand has 5 metacarpals and 8 carpal bones.

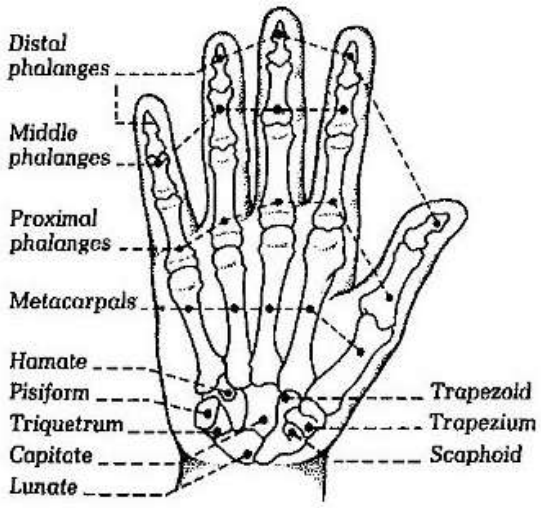

Fig. 2.5 Bones in a typical human hand [47]

The skeletal structure of the hand is naturally divided into three different types of

bones, shown in Fig.2.5. From the wrist, the carpus is the subgroup of 8 bones that makes up the wrist and base of the hand. The fingers are connected to the carpus and are composed of metacarpal and interphalangeal segments and joints. The latter segments are further subdivided into proximal, middle, and distal phalanges. The wrist is the most complex joint in the body. It is formed by 8 carpal bones grouped in 2 rows with very restricted motion between them. From radial to ulnar, the proximal row consists of the scaphoid, lunate, triquetrum, and pisiform bones. In the same direction, the distal row consists of the trapezium, trapezoid, capitate, and hamate bones.

The hand contains 5 metacarpal bones. Each metacarpal is characterized as having a base, a shaft, a neck, and a head. The first metacarpal bone (thumb) is the shortest and most mobile. It articulates proximally with the trapezium. The other 4 metacarpals articulate with the trapezoid, capitate, and hamate at the base. Each metacarpal head articulates distally with the proximal phalanges of each digit.

2.3.2 Joints

The wrist joint is a complex, multiarticulated joint that allows wide range of motion in flexion, extension, circumduction, radial deviation, and ulnar deviation. The distal radioulnar joint allows pronation and supination of the hand as the radius rotates around the ulna. The radiocarpal joint includes the proximal carpal bones and the distal radius.

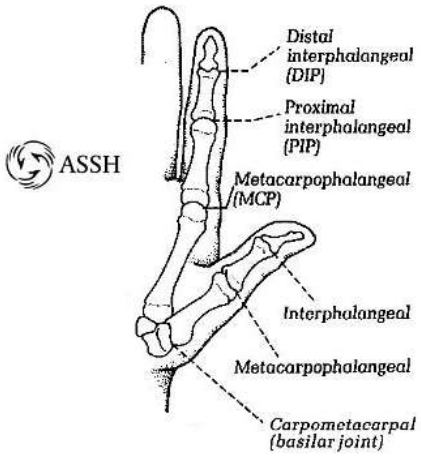

Fig. 2.6 Joints in a typical human hand [47]

At the metacarpophalangeal joints, lateral motion is limited by the collateral lig-

aments, which are actually lateral oblique in position, rather than true lateral. This arrangement and the shape of the metacarpal head allow the ligaments to be tight when the joint is flexed and loose when extended (ie, cam effect).
At the interphalangeal joints, extension is limited by the volar plate, which attaches to the phalanges at each side of the joint. Radial and ulnar motion is restricted by collateral ligaments, which remain tight through their whole range of motion.

2.3.3 Pulley System in Fingers

The pulley system is critical to flexion of the finger. The retinacular system for each of the fingers contains 5 annular pulleys and 4 cruciate pulleys. The thumb has 2 annular pulleys and 1 oblique pulley. In the finger, as shown in Fig.2.7 the second and fourth annular pulleys (A2, A4) are critical pulleys. The oblique pulley is the critical pulley in the thumb [66].

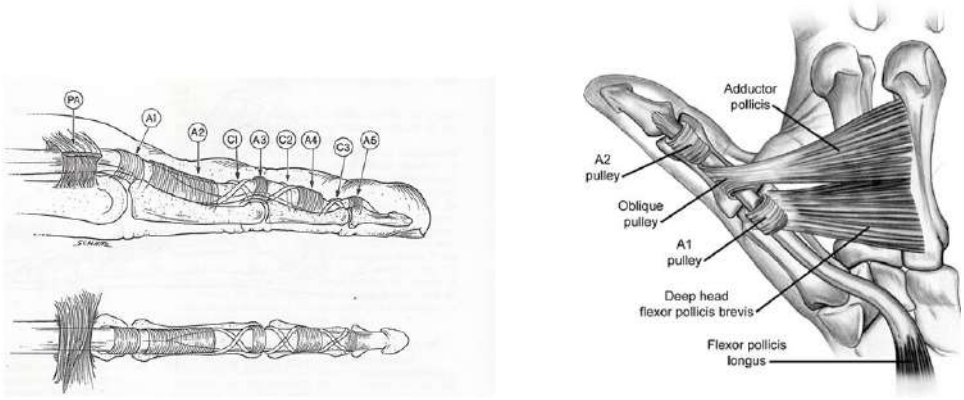

Fig. 2.7 Finger pulley system. The finger tendons act as sort of virtual pulleys to actuate the fingers. On the left is shown the pulley configuration for the fingers and on the right is the pulley articulation for the abduction and adduction of the thumb.

Deficiency of the pulley system can result in less active flexion of the digit for a certain tendon excursion.

2.3.4 Arches

The fixed and mobile parts of the hand adapt to various everyday tasks by forming bony arches: longitudinal arches (the rays formed by the finger bones and their associated metacarpal bones), transverse arches (formed by the carpal bones and distal ends of the metacarpal bones), and oblique arches (between the thumb and four fingers)

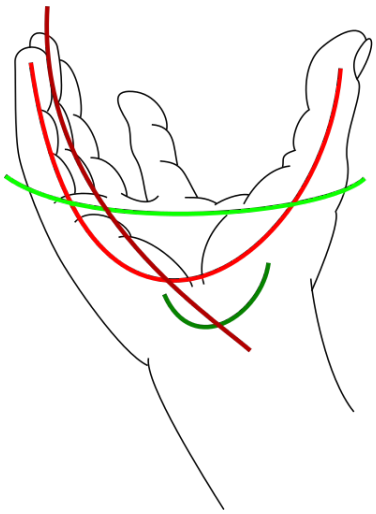

Fig. 2.8 Arches of the hand. Red: one of the oblique arches Brown: one of the longitudinal arches of the digits Dark green: transverse carpal arch Light green: transverse metacarpal arch [34]

Of the longitudinal arches or rays of the hand, that of the thumb is the most mobile (and the least longitudinal). While the ray formed by the little finger and its associated metacarpal bone still offers some mobility, the remaining rays are firmly rigid. The phalangeal joints of the index finger, however, offer some freedom in movement to its finger, due to the arrangement of its flexor and extensor tendons. The carpal bones form two transversal rows, each forming an arch concave on the palmar side. Together with the thumb, the four ulnar fingers form four oblique arches, of which the arch of the index finger functionally is the most important, especially for precision grip, while the arch of the little finger contribute an important locking mechanism for power grip .

2.4 Main Functions

The main functions of human hands are for grasping and manipulation of objects in our surroundings. The same applies for robots which need to handle objects of different sizes and also to explore its environment. We shall broadly classify the hand functions as 1. Prehensile manipulation 2. Non-prehensile manipulation 3. Exploration and 4. Communication, which will be discussed in detail in the following sections.

2.4.1 Prehensile Manipulation

"Prehensile" means capable of grasping, prehensile manipulation or just "manipulation" as it is commonly known is the ability to move the hand or both hands into a favourable position which facilitates the grasping or holding of objects. This can be used to move objects from one place to another or to manipulate them in any way desired.
Prehensile manipulation can happen in varying degrees in our everyday life. A number of factors are counted when defining the type and complexity of the grasp performed.

(a) Operating a smartphone

(b) Threading a needle

(c) Steering wheel grip for driving

(d) Gripping a baseball

Fig. 2.9 Everyday use of hands with varying dexterity

Even in this type of manipulation, we can classify it as fingertip manipulation or whole-arm manipulation. As the name suggests, the term fingertip manipulation refers to the activities which make use of only the displacement of the fingertips and hand (includes the wrist) to perform the particular actions whereas whole-arm manipulation makes use of the hand and arm system together to perform these actions. We shall now explore the types of hand manipulations.

In-hand Manipulation

In-Hand Manipulation skills refers to the ability to move and position objects within one hand without the assistance of the other hand. Only the fingers are used for manipulation along with the support of the palm. There are three components of

(a) Translation

(b) Rotation

in-hand manipulation: translation, shift, and rotation. Some manipulations use only one of these components, others require a combination of them.

Translation: The ability to move an object from the palm to the fingertips, or from the fingertips to the palm. An example of this type of manipulation can be placing and removing screws in an assembly where you hold a number of screws before placing them in slots or vice-versa where you remove the screws from slots and hold them in the hand. Fig.2.10a shows this movement as the fingertips manipulate and shift the pencil from the palm to the fingertips.

Shift: The ability to move an object on the fingertips in a linear movement (thumb moves across fingertips)

Fig. 2.11 Shift

Examples include repositioning the pen in the fingers to position for writing or fanning playing cards in the hand. Fig.2.11 shows this movement as the fingertips slide along the surface of the shaft of the pencil.

Rotation: The ability to rotate an object using the fingertips of the thumb and index finger, as well as the side of the middle finger. Fig.2.10b shows this movement as the fingertips are used to rotate the pencil around the middle finger. It can vary such as turning an object around in the pads of the fingers and thumb (simple rotation) or turning an object from end to end (complex rotation) such as flipping a pencil from writing end to eraser.

2.4.2 Non-prehensile Manipulation

Non prehensile manipulation is the ability of a system to manipulate an object without directly grasping it[73]. It can be done directly or indirectly by either pushing, hitting, blowing, twirling or through non-direct grasping where the object is not in direct contact. Eating with a spoon or fork is an example of non-prehensile manipulation.

Fig. 2.12 Playing the piano is one example of non-prehensile manipulation

Prehensile manipulations involves a passive force on the object being manipulated, there is no active grasping taking place. Examples of non-prehensile manipulation include typing on a computer keyboard, doing push-ups, push buttons on the telephone or playing the keyboard as shown in Fig.2.12.

It is not usually preferred in robotics since the manipulation is not directly connected to the manipulable part of the robot and usually requires extensive planning algorithms to indirectly manipulate the end artifact.

2.4.3 Communication

Communication is any act by which one person gives to or receives from another person information about that person's needs, desires, perceptions, knowledge, or effective states[82]. Communication using hands plays a vital role in human interaction where they can accompany vocal communication or even replace them entirely as in sign languages. They can be further classified into the following:

Verbal

Verbal communication consists of building up of words to make phrases or sentences. In the cases of hands this is made possible using sign languages or manually coded languages. This doesn't mean sign languages limit the role of communication to hands. There is an involvement all parts of the body including the arms, head and other

parts of the body. But the predominant role is played by hands. The use of fingerspelling(Fingerspelling (or dactylology) is the representation of the letters of a writing system, and sometimes numeral systems, using only the hands) is a prime example of how hands are used to communicate complete words and phrases through hands although they are predominantly used by deaf and mute people.

(a) American sign for *"eat"*

(b) American sign for *"How much?"*

Fig. 2.13 Examples of sign language[1]

Body Language/Gestures

Gestures can also be categorized as either speech independent or speech related. Speech-independent gestures are dependent upon culturally accepted interpretation and have a direct verbal translation. A wave or a peace sign are examples of speech-independent gestures. Speech-related gestures are used in parallel with verbal speech; this form of nonverbal communication is used to emphasize the message that is being communicated. Speech-related gestures are intended to provide supplemental information to a verbal message such as pointing to an object of discussion.

Adapters They consist of manipulations either of the person or of some object (e.g., clothing, pencils, eyeglasses)—the kinds of scratching, fidgeting, rubbing, tapping, and touching that speakers often do with their hands. It has been suggested that adapters may reveal unconscious thoughts or feelings [80] , or thoughts and feelings that the speaker is trying consciously to conceal[42].

Symbolic At the opposite end of the lexicalization continuum are gestural signs—hand configurations and movements with specific, conventionalized meanings—that we will call symbolic gestures[16] . In contrast to adapters, symbolic gestures are used intentionally and serve a clear communicative function.

Conversational The properties of the hand movements that fall at the two extremes of the continuum are relatively uncontroversial. However there is considerable

(a) Symbolic gesture for *"Victory"*

(b) Symbolic gesture for *"Okay"* or *"Alright"*

Fig. 2.14 Examples of symbolic gestures

disagreement about movements that occupy the middle part of the lexicalization continuum, movements that are neither as word-like as symbolic gestures nor as devoid of meaning as adapters.

(a) Italian gesture for *"What?"*

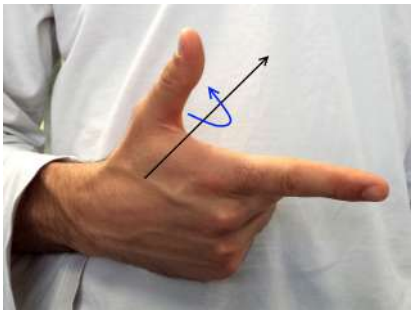

(b) Italian gesture for *"No more"*

Fig. 2.15 Examples of conversational gestures

2.4.4 Exploration

Exploration is the ability to gain knowledge about objects through sensing. Human hands have numerous nerve endings in the palm and fingertips which give sensory feedback of different kinds using tactile sensing through the skin. In robotics, hands are coupled with encoders in the joints to get an exact position of the various links. Tactile sensors are also used to provide touch and pressure feedback to judge the material and the rigidity of the artifact to be manipulated. It can also provide information on the obstacles in the environment. Touch forms the most complex human sensory system and is capable of detecting a diverse range of parameters including: frequency

and intensity changes (for pressure and texture/slip perception), thermal changes (for safety and in object identification) and pain sensors for system protection.
In humans as well as in humanoid robotics, tactile sensing is vital to provide vital sensory inputs that enhance safety and general information on the embodied agent and its environment. It also helps in interaction with environment and any all equipments to quantify overloads and to detect contact with harmful material/objects. It is suggested that the minimum specification for generalized tactile sensing should be included as defined in [23][38]:
Contact pressure/force : to ensure a firm grip but at the same time to prevent excessive force and damage.
Object texture Object texture: grip force is often regulated using knowledge of the surface nature and aids in object identification.
Slip: Detecting slip is important in material handling where it gives information on the stability of the grip.
Hardness: Detecting the hardness of an object ensures soft objects are not excessively compressed and aids identification by touch.
Profile: Profile or shape and size sensing provides details on how flat an object is, or the extent of curvature, i.e., information on the objects' physical characteristics. This helps in conformity to shape.
Temperature: Knowledge about the temperature characteristics of both objects and the environment is vital in safe human-agent interaction. And in humanoid robotics, it is very similar and prevents damage to the gripper from excessively high or low temperatures.
Thermal Conductivity: Thermal conductivity differs for every object and material. This is extensively used to aid material identification by touch.

2.5 Nomenclature

In the following chapters, the following nomenclature will be used to refer to the different parts of the robotic hands under investigation.

The distal link of the finger will be referred to as the distal phalange (DP), the proximal link as the proximal phalange (PP), and in the presence of an intermediate link, the intermedial phalange (IP). The support link for the finger (the metacarpal in the human hand) is called as the metacarpal phalange (MP). The corresponding joints

are named as the Metacarpophalangeal joint for the joint between the metacarpal phalange and the proximal phalange (MCP joint), the Proximal Interphalangeal joint (PIP joint) in the presence of a joint between the PP and IP, and finally the Distal Interphalangeal joint (DIP joint) between the IP and the DP or between the DP and PP in the absence of an intermedial phalange. The thumb has an additional rotational joint and a corresponding link, which will be called as the Carpometacarpal phalange (CP), similar to the nomenclature in human hands, and the joint, simply referred to as the rotation joint of the thumb.

2.6 Goals

Based on the knowledge of the type of hands in nature and about the human hand, the following list of desired features base on user needs are drawn:

- The robotic hand should be able to pick a water bottle, preferably from a table. It should be able to fully grasp and support the water bottle.
- It should be compliant and safe enough to not cause damage to any interacting agent or the environment.
- It should be relatively lightweight to move around and should not weigh more than its target payload i.e., 500 grams.
- The robotic hand should be able to perform basic functions, both prehensile and non-prehensile. Like opening doors, toggle switches, carry objects etc.
- It should be sufficiently dexterous to carry out basic non-verbal communication to aid in human-robot interaction.
- It should have some sort of force sensing capabilities, to aid in perceiving the environment, objects it interacts with and itself.
- The should be robust and not be prone to frequent breakdowns

This serves as a baseline for all the research that follows. The user needs are then refined and the corresponding technical objectives are extracted in the following sections.

Chapter 3

Review on robotic hands

The last decade has seen a huge spurt in the design and manufacture in the number of anthropomorphic hands for robotics and prosthetics. Performing an extensive study on all the artificial hands in the academic and patent literature is beyond the scope of this study since there are more than a hundred hands currently in employ.

In this chapter a review of the performance specifications of a wide range of commercial and non-commercial robotic hands is done through a thorough review of published literature. An overview of performance characteristics of all types of robotic hands is done. A detailed breakdown of the major hands is given in Appendix.C. Both the physical performance specifications (when available), as well as a justification for their form and functions is discussed wherever available. Finally, a comparison of key features and potential mechanical design trade-offs in the current state of the art in robotic hands is done to extract technical objectives relevant to this thesis.

3.1 A General Timeline of Robotic Hands

An overview of robotic hands show how the technology has evolved over time and what has stayed in relevance. Some of the more prominent hands over these past four decades are shown in Fig.3.1.

The past decade in particular has seen an explosion in the research of hands due to the ease in manufacturing methods and the speed at which the design iterations are cycled. This is in part due to the advent of rapid prototyping techniques that have come to the fore in this decade. Methods like 3D printing, selective laser melting and sintering, fused deposition modelling, stereolithography etc., have really accelerated the speed at which we prototype objects.

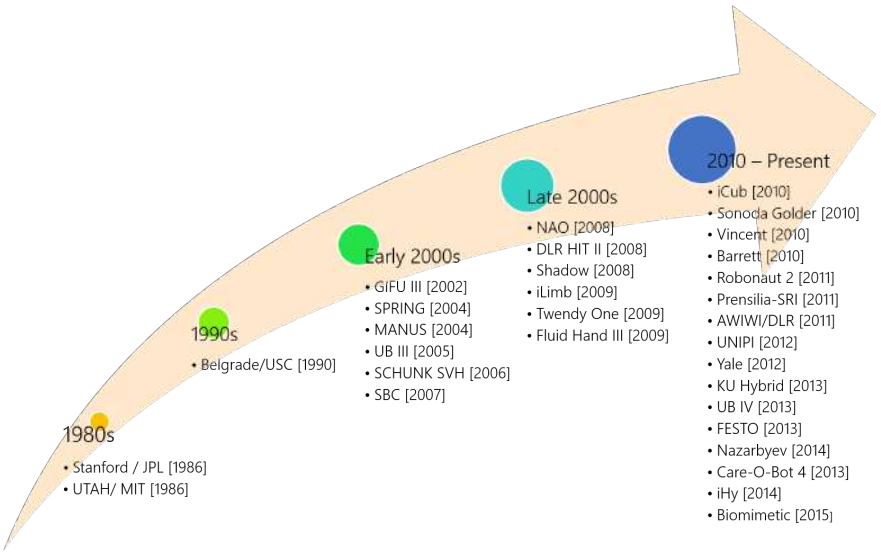

Fig. 3.1 Evolution of robotic hands over time

3.1.1 Robotic Hands

A list of relevant robotic hands (Fig.3.2) have been selected by the number of citations they have acquired over time. Some other robotic hands have been selected due to their relevance when it comes to innovating the field, since they were recently published. But all these robotic hands have moved towards the progression of the field by innovating in entirely new directions with its design and manufacturing decisions.

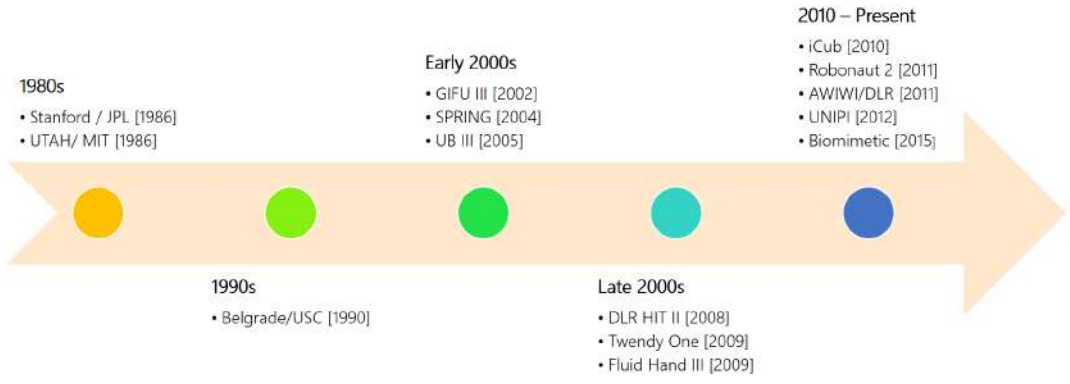

Fig. 3.2 Breakthrough robotic hands over time

These robotic hands are vital in identifying key features that are important to designing a functional and good end-effector. They are discussed in more detail below.

Stanford/JPL [1983]

The Stanford/JPL [103] dexterous hand, designed by Dr. J. Kenneth Salisbury Jr., is a three-fingered robotic hand containing nine joints. Each finger is identical containing three revolute joints, with the first joint rotating perpendicularly to the consecutive joints. The three fingers are positioned as two fingers and an opposing thumb.

The hand is significant since it was one of the first hands to introduce the concept of a fully formed robotic hand and laid the foundation for what would be the modern age of articulated robotic hands.

(a) Stanford-JPL (b) UTAH-MIT (c) USC-Belgrade

Fig. 3.3 Robotic hands from the 1980s and 1990s

It also introduced the concepts of mobility, force-application accuracy, singularities, noise propagation etc., in articulated robotic hands. Iterative improvements on this hand still exist to this day and is being pursued by Salisbury Robotics Lab at Stanford.

UTAH/MIT [1983]

The UTAH/MIT hand [61] was a research hand that was first developed in 1983. It has 16 DOF and three fingers with four active DOF each, plus a thumb with four DOF. The fingers each have a proximal joint that allows for abduction/adduction. The last version was actuated by graphite pistons and transmitted via tendons and pulleys. It is tendon (belt) driven, and is a highly integrated hand with 38 antagonistic drives with tendon tension control. The thumb has a rotational DOF parallel to the index finger metacarpal enabling thumb opposition/reorientation.

It is supported by tendon tensioners, joint position sensors and damping systems. It remains one of the most pioneering robotics research hands today.

Belgrade/USC [1990]

The Belgrade/USC hand [11] is a non self-contained, underactuated hand introduced in the 1990s. It was one of the first robotic hands that used underactuation principles and referred to underactuation as "internal synergy". It consists of five fingers, the little and ring finger are coupled while the index and middle finger are also coupled in the same way using a whiffletree mechanism. It is supported with position sensors and force sensing resistors built into the hand.

GIFU III [2002]

The Gifu Hand III [87] is a self-contained, light, titanium robotic hand for dextrous object manipulation. The Gifu hand is equipped with a thumb and four fingers, with 20 joints and 16 controlled degrees of freedom (DOF) in total. The predecessors of Gifu Hand III were the well-known robot hands, Gifu Hand and Gifu Hand II from the Kawasaki and Mouri Laboratory, at Gifu University in Japan.

Gifu Hand III is equipped with DC servomotors, built into the finger and palm components of the hand. The use of satellite gearboxes and face-gear in transmission leads to a high level of stiffness and lower backlash rates.

(a) GIFU-III (b) SPRING (c) UB-III

Fig. 3.4 Robotic hands from the early 2000s

Gifu Hand III is designed in such a way that 6-axis force sensors can be attached to the fingertips. In addition, a tactile sensor is also attached to the hand. It also has a lighter, plastic version codenamed the KH SAND S1.

SPRING[2004]

The SPRING hand [27] is a three fingered, eight DOF hand, but the hand has only one motor that drives all the joints. A DC Minimotor has been selected to obtain a

10N pinch force at the finger tip. The index and middle fingers are composed of a base, fixed to the palm, and of three phalanges connected by rotational joints. The thumb has a fixed base to the palm, but it is composed of only two phalanges, as in the human hand. The palm acts as the centre for actuation and transmission systems. It is supported by force sensors, two strain gauges that are mounted on the differential mechanism and hall effect position sensors.

UB III [2005]

The University of Bologna has been long developing a series of hands and the UB III [79] was the third in the series. It is a remotely actuated, five fingered hand. It has four identical fingers and an opposing thumb covered by soft tissue. It focuses on reducing the complexity from the previous versions while increasing functionality and dexterity.

It has an endoskeletal articulated frame with elastic joints and springs in the middle. The linear motion of the drives is transmitted to the finger joints through sheath routed tendons. The index finger is the only fully actuated finger, and the number of actively actuated joints is different in every finger. It is supported by a strain gauge in series with the spring bending which aids in measuring spring deflection and consequently, the joint position.

DLR HIT II [2008]

The DLR HIT Hand II [77] from HIT (Harbin Institute of technology) and DLR Institut for Robotics and Mechatronic is the second iteration of their first collaborative work: the DLR HIT Hand I. It is self contained hand with five identical fingers with four joints and an aluminium open skeleton structure with injection moulded plastic shells.

In contrast to the DLR HIT Hand I the new DLR HIT Hand II has five modular fingers with four joint and three active degrees of freedoms and is still lighter and smaller. It is a modular, belt driven hand and each finger has a differential bevel gear-cardan MC joint allowing abduction/adduction in the first axis and flexion/extension in the second. The HIT II hand is used on the space robot called Space Justin from the DLR institute and is a humanoid robot setup for grasping objects with shared autonomy. It is fully observable with joint position and torque sensors, motor position sensors and dedicated Force-Torque sensors along with temperature sensors.

Twendy-One[2009]

The Twendy-One hand [60] is a self-contained, four fingered hand built for the Twendy-One robot by Waseda University. It has a passive compliant design. It has a spring loaded passive DIP joint. All the surfaces of the finger and palm are overlaid with visco-elastic silicone materials. It passed the Kapandji test which is discussed more in detail in the following sections. It comprises a sensorized tactile skin, a six-axis force sensor on each fingertip and position sensors, giving it an efficient force feedback system.

(a) DLR-HIT II (b) TwendyOne (c) Fluidhand III

Fig. 3.5 Robotic hands from the late 2000s

FluidHand IV [2008]

The Fluidhand IV [49], [8]is fourth in a series of *Fluidhands* made by Forschungszentrum Karlsruhe. It is a remotely actuated, human sized, five fingered robotic hand. It was built for the ARMAR robot and is described as "a new hybrid concept of an anthropomorphic five fingered hand and a three jaw robotic gripper"

It is equipped with position sensors on all of the 11 joints. The hand is also fitted with tactile sensors based on cursor navigation sensor elements, which allows it to have grasping feedback and the ability for exploration

Robonaut 2 [2011]

The Robonaut 2 [40], [19] hand is a remotely actuated, five fingered robotic hand built for the Robonaut humanoid to be used in space applications. Developed as part of a partnership between General Motors and NASA. A key aspect to the hand's improved performance is the use of lower friction drive elements and a redistribution of components from the hand to the forearm.

(a) Robonaut 2

(b) AWIWI

(c) UB IV

Fig. 3.6 Robotic hands from the 2010s

The hand categorizes its parts as grasping fingers (ring and little finger; mainly used to grasp objects), dexterous fingers (index and middle finger; used for manipulation tasks also), the palm and the thumb. It has 18 DOF actuated by 12 motors. The actuation of each active joint is accomplished by a flexible conduit, implying a linear motion transmitting the linear motion of the motors to a nut that converts it into rotary motion. The robustness against collisions is enhanced by allowing a buckling of the cables connecting the lead screw and the finger segments and additionally shock mounts between the fingers and the palm. The hand is supported by joint position sensors, tactile load cells on each of the phalanges and tendon tension sensors to keep the Vectran tendons' tension in check.

AWIWI (DLR Hand-Arm system) [2011]

The AWIWI hand [54] [55] which is a part of the DLR Hand Arm System and is a remotely actuated, five fingered anthropomorphic hand that contains highly dynamic and fully integrated mechatronic system. The fingers are protected against overload by allowing subluxation of the joints.

The system is driven by 52 embedded variable stiffness actuators (VSA) that are able to adjust joint stiffness on-line, avoiding the trade-off between robustness and accuracy typical of serial elastic actuators (with predetermined and fixed stiffness). The use of antagonistic drives tackles any problems of tendon overstretching and slackening that are commonly encountered in tendon driven mechanisms. The possibility of storing energy in the elastic elements of the drive opens new opportunities to perform dynamic actions. The hand itself has 38 actuators allowing for 19 DOF with an additional 6 motors for a 3DOF wrist.

The fingers are actuated via ServoModules. Fingers have four independent DOFs,

except for the ring and the little fingers which present coupled PIP and DIP joints. Also the thumb has four independent DOFs, eliminating the 5th DOF of the human thumb dedicated to the in-ward orientation of the serial chain on the opposing fingers during abduction. The overall systems weighs 13.5kg. The hand itself weighs about 4kg without the forearm mechanisms.

It is supported by a bevy of sensors, including joint position hall effect sensors, and custom-designed magneto-resistive sensors in the series elastic deflection mechanism.

UB IV [2013]

The UB IV hand ([84], [93]) or the DEXMART hand, as it is more commonly known, is a remotely actuated, five fingered, anthropomorphic hand developed by the University of Bologna and is the successor of the UB III hand. It makes of the so called twisted-string actuation system . The basic concept of this actuation system is that the overall length of the transmission is reduced by twisting the tendons at one end by means of the motor, resulting in a linear motion at the other end of the tendon.

It is supported by an LED–photodetector couple with a wide angle-of-view. It is used as joint position sensors. The sensory apparatus is also augmented by a tactile sensor based on discrete surface-mounted optoelectronic components. This sensor allows direct data acquisition (without any amplification circuit) by measuring the deformation of soft pads mounted above the sensor grid.

3.1.2 Evolution of rapid prototyped robotic hands

In this section, robotic hands designed and built through rapid-prototyping techniques. Robotic hands from the previous sections are often expensive, customized for specific platforms, and difficult to modify. It is typically impractical to experiment with alternate end-effector designs. This results in researchers needing to compensate in software for intrinsic and pervasive mechanical disadvantages, rather than allowing software and hardware research in manipulation to co-evolve. Hardware iterations are also intrinsically longer than typical software cycles. One way to make up for this drawback is to incorporate easier manufacturing technologies. While advances in rapid prototyping have made it easier and faster to build custom parts, there has been a corresponding increase in the use of such techniques in robotic hands.

- PISA Synergy [28] [2012]

- Washington [126] [2013]
- Pepper [100] [2014]
- Openbionics [70],[129] [2015]
- Brunel [5] [2015]
- ALPHA [29][2016]
- Colorado [71] [2016]
- SSSA-Myhand [35] [2017]

Typically, most of them are underactuated robotic hands that use tendons to drive their joints (although this is not always true). An added advantage of rapid prototyping hands is the ease of building complex structures and making the design a lot more integrated than what is possible with traditional manufacturing means. Some examples of such robotic hands are discussed in the following sections.

University of Pisa-IIT Synergy [2012]

The UNIPI Hand [28](Fig.3.7a) is a self-contained structure. It is simple, lightweight and cheap. One motor drives its 19 DOFs; four per finger and three for the thumb. Robustness and safety are inspired by soft-robotics approaches. It is a highly integrated prototype of human hand which conciliates the idea of adaptive synergies with a human form factor. The transmission mechanism is composed of several pulleys and

(a) UNIPI - Synergy (b) Biomimetic hand (c) Openbionics

Fig. 3.7 Robotic hands from the 2010s

a closed-loop Dyneema cable routed through all joints. When the last is pulled, fingers

flex and adduct, while elastic elements restore fingers to a stretched configuration at rest. Finger joints for flexion/extension implement rolling contacts compliant in flexion and stiff in traction, inspired by Hillberry joints. Despite the integrated pulleys, friction ultimately limits the number of joints that can be actuated by a single motor. This phenomenon is contained by the tendon actuation which is realized from both ends, allowing the implemented hand to perform satisfactorily.

Washington Biomimetic [2015]

The biomimetic hand [125](Fig.3.7b) from Washington University was built to mimic the human hand physiology in its entirety. The biomimetic hand is 3D printed and the muscles, ligaments and support structures are imitated through a series of tendons and textile crotchets. Silicone and rubber sheets are then cut to be made as support structures.

The hand is actuated by 10 Dynamixel servos and can imitate most hand postures of the human hand.

Openbionics [2016]

The Openbionics prosthetic hand [70](Fig.3.7c) is an anthropomorphic, underactuated robot hand that utilizes a selectively lockable differential mechanism. However, the differential locking mechanism is not automated and needs physical user intervention. All phalanges are stitched on flexure joints that are implemented with silicone sheets of different widths. For each finger, extension is mechanically implemented in a passive fashion through the use of appropriate elastomer materials, while flexion is implemented with cables (Dyneema fishing line), driven through low-friction tubes. The joints are made from silicone or polyurethane sheets, so as to be lightweight but also stiff enough to produce a force range that corresponds to everyday life tasks.

Upon contact of one finger with the environment or object surface, a whiffletree mechanism facilitates the motion of unconstrained fingers. Tis way the whiffletree allows one motor to control multiple fingers in a coordinated fashion.

Notes on anthropomorphic hands

The kinematic design and actuation of five fingered hands also vary vastly according to the type of tasks to be performed. We see that in the past decade the design of hands has bifurcated into two groups: the first focusses on generic gripping with

minimal actuators and the second concentrates on fine manipulation skills and grasps using multiple actuators. The method used to incorporate generic grasping can vary greatly, such as the synergy hand developed by the University of Pisa and IIT i.e: the UNIPI Hand [28] to the very simple mechanically compliant open-close hand [48]. These hands use mechanical compliance to perform grasps. Fine finger manipulation is also nearly impossible due to a lack of force control and due to the use of single motor actuation.

Hands such as the NU hand [65], Harada [67] and the Milano hand [112] provide for a fair trade-off between in-hand manipulation, finger manipulation and the number of actuated DOF. Alternative types of actuation which move away from the traditional DC motors have also been successfully tried in hands. Some examples include the highly dexterous Shadow Hand[104],[56] which employs air muscles to hands using hydraulic actuation [49],[50],[109], pneumatic air cylinders [61],[49],[8] and even shape memory alloys [31]. It is also of particular interest to observe that the FRH IV Hand [8] employs complete palmar flexion of its four fingers opposing its thumb to provide high power grasp capabilities.

Innovation in the transmission of force from the source actuator to the joints have also been a major part of hand design. By classifying them according to transmission, it is seen that they vary from traditional transmission systems such as spur, bevel and worm gears [111],[112],[43] to harmonic gearing [30],[54],[83]. It can also vary widely using alternative transmission systems such as hydraulic bellows [49],[50] to novel actuation methods such as twisted wire tendons [93]. These type of hands transmit force through pressure, friction and tension which are all parameters that are generally difficult to quantify consistently. Also pneumatic and hydraulic actuation or transmission systems are prone to leaks and need scheduled maintenance or frequent re-calibration.

Some hands employ stiff steel cables [106], Spectra wires [126], Dyneema wires [30][72], simple Poly-ethylene tendons [84], [43] etc. Steel cables are usually enclosed in sheaths and used as bowden cable which are known to have comparably higher friction losses and reduced life cycle when compared to other tendons. Dyneema and Spectra wires, in comparison, are relatively more flexible with very good friction parameters. However, they can be used only with agonistic-antagonistic actuation which would mean twice the amount of actuators or backdrivable motors or a return mechanism.

3.2 Types of Hands by Function

Hands can be classified according to the function or purpose they are intended for. Robotic hands can be built for the market to be sold as part of a package or standalone systems intended to be part of an integrated system, or in rehabilitation, prosthetics or simply to be proof of concepts of advances in the technology. Depending on the purpose they are built for, hands can be categorized as the following:

- Robotic research
- Prosthetic
- Commercial

Each type will be discussed briefly in the following sections.

Robotics Research

Research hands are typically "one-off" prototypes that are developed to realize novel concepts or part of a specific research objective the designer is trying to achieve. It often focuses on a single feature and does not adhere to the "commercial viability" of a product. It can be further classified into humanoid hands (which are part of a humanoid robot) or standalone hands.

Stand alone hands Standalone robot hands are typically designed to be multi-purpose hands. The technology used in these hands are usually generic enough to be tested across various platforms. Hands like the Shadow hand, the DLR HIT II hand, the KU Hybrid hand and the UB hands are examples of such hands.

Humanoid robot hands These hands were developed as part of a humanoid robot. They are specific in their needs, i.e; they are in accordance with the needs for which the robot that they are a part of were built. Some examples of humanoid robot hands include that of the TwendyOne robot, the RoboRay hand, the HRP-3 and HRP-4 hands, the iCub hand etc.

Each of these hands are in accordance with the design philosophy, price and functionality of their corresponding robots and are hence highly customised.

Prosthetics

Prosthetic hands are aimed at restoring partial or complete mobility to human beings who have lost hand function either through accident, paralysis, amputation or other means. Although prosthetic hands can technically fall under both the commercial or research section, we still keep it as a separate category for the sake of clarity.

Prosthetic hands almost always share a list of desired features with robotic research hands such as having a combination of high functionality, durability, adequate cosmetic appearance, and affordability whilst being lightweight and highly anthropomorphic in nature. Usually, self-contained robotic hands are preferred in prosthetics since remote actuation is most often not an option.

Commercial

Commercial robotic hands can be standalone, prosthetic or part of a humanoid robot. But they all have similar objectives, which are: easy to produce, robust and cost-effective. They usually have a good weight to payload ratio and employ relatively simplistic manufacturing practices. They tend to opt off the shelf components for the sake of production in big numbers. Some examples of commercial robot hands include The Shadow Hand, the Bebionic hand, the iLimb, the Pepper hand, the UNIPI hand etc.

All the aforementioned types of hands can be either self-contained (comprising all required actuators and electronics in self) or remotely actuated (the electronics or actuators or transmission systems or all are placed outside the main structure of the hand).

3.3 A Qualitative Analysis on Robotic Hands

Analysis of robotic hands in literature has been highly subjective. There are a number of evaluation tests and indices that exist in literature. One such is by Biagiotti et al. [12] where they try to define “a quantitative measure of the distance of a generic robotic end-effector from the ideal target". This measure which is the result of several aspects, are said to contribute to the real dexterity of a robotic hand. Therefore, this measure has been expressed by means of some indices and refers to the degree of anthropomorphism with the human hand serving as the base concerning aspects of form and function. It also serves as a baseline to evaluate the level of dexterity,

resultant from the kinematic configuration, the sensory apparatus and the control system. The objective is to outline trends and open problems in robot hand design, in an integrated perspective, which considers mechanical aspects, sensing capabilities and control issues.

Anthropomorphism Index

In the paper from [12], the nature of anthropomorphism in robotic hands is explored and tries to answer if it is better to call a hand anthropomorphic if it fits the form better without replicating its functions or vice-versa. An anthropomorphism index, which aims at explaining these questions is proposed. It takes into account the kinematics

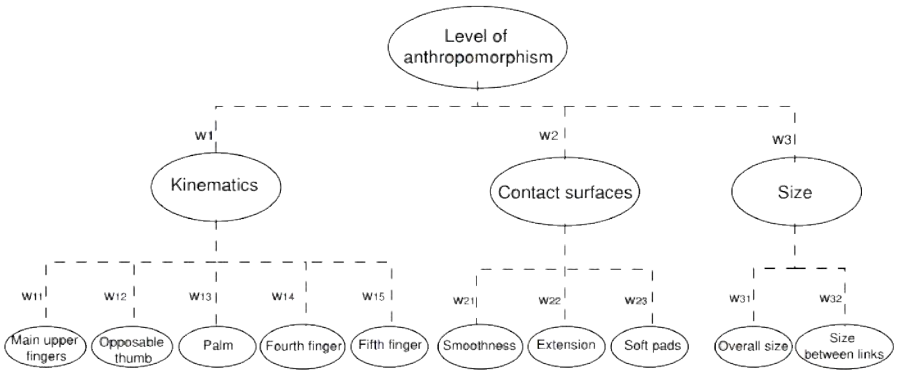

Fig. 3.8 Evaluation of anthropomorphism in robotic hands as proposed by [12]

of the hand, its contact surfaces and size, with a weightage for each. It breaks down each of these three categories into sub-components with a weight for each. This is demonstrated in Fig.3.8.

Dexterity Index

A separate index also defines dexterity as the amount of useful work that can be done with a presented hand. It gives weights to each kind of prehensile, non-prehensile and manipulation tasks that can done by the robot. Since this tasks is a combination of the morphological features, the sensory equipments, control algorithms etc., it provides a good idea about what features goes into making the hand "dexterous". A complete breakdown of the dexterity index can be seen in the Fig.3.9.

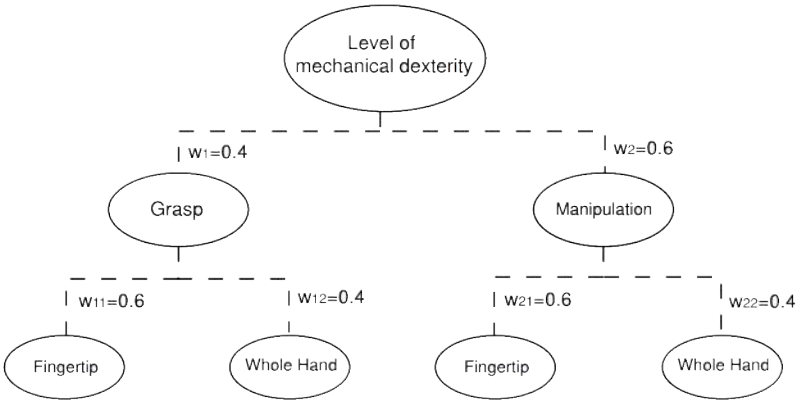

Fig. 3.9 Evaluation of dexterity in robotic hands as proposed by [12]

Kapandji Test

The Kapandji test or Kapandji score was originally proposed by Ibrahim A. Kapandji ([64]) in 1985 as a tool for assessing the opposition of the thumb based on where the thumb tip (in red) can access or touch various parts on the hand (in blue).

The opposition test consists of touching the four long fingers with the tip of the thumb: the score is 1 for the lateral side of the second phalanx of the index finger, 2 for the lateral side of the third phalanx, 3 for the tip of the index finger, 4 for the tip of the middle finger, 5 for the ring finger and 6 for the little finger. Then, moving

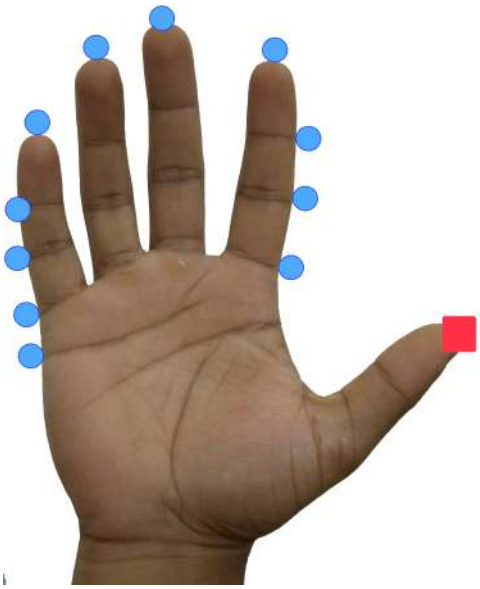

Fig. 3.10 A score for thumb dexterity.

the thumb proximally along the volar aspect of the little finger, the score is 7 when it touches the DIP crease, 8 on the PIP crease, 9 on the proximal crease of the little finger and 10 when it reaches the distal volar crease of the hand. This test is valid only if the first stages are possible: a crawling thumb in the palm is not an opposition motion. The counter-opposition test (or reposition test) needs the other hand as a reference system.

This test has been used in various robot hands[54][29] as a way of evaluating the dexterity of the thumb.

Grasping

Grasping, as defined in [12] is intended at constraining objects inside the end-effector with a constraint configuration that is substantially invariant with time (the object is fixed with respect to the hand workspace). Throughout the study in [12], the terms

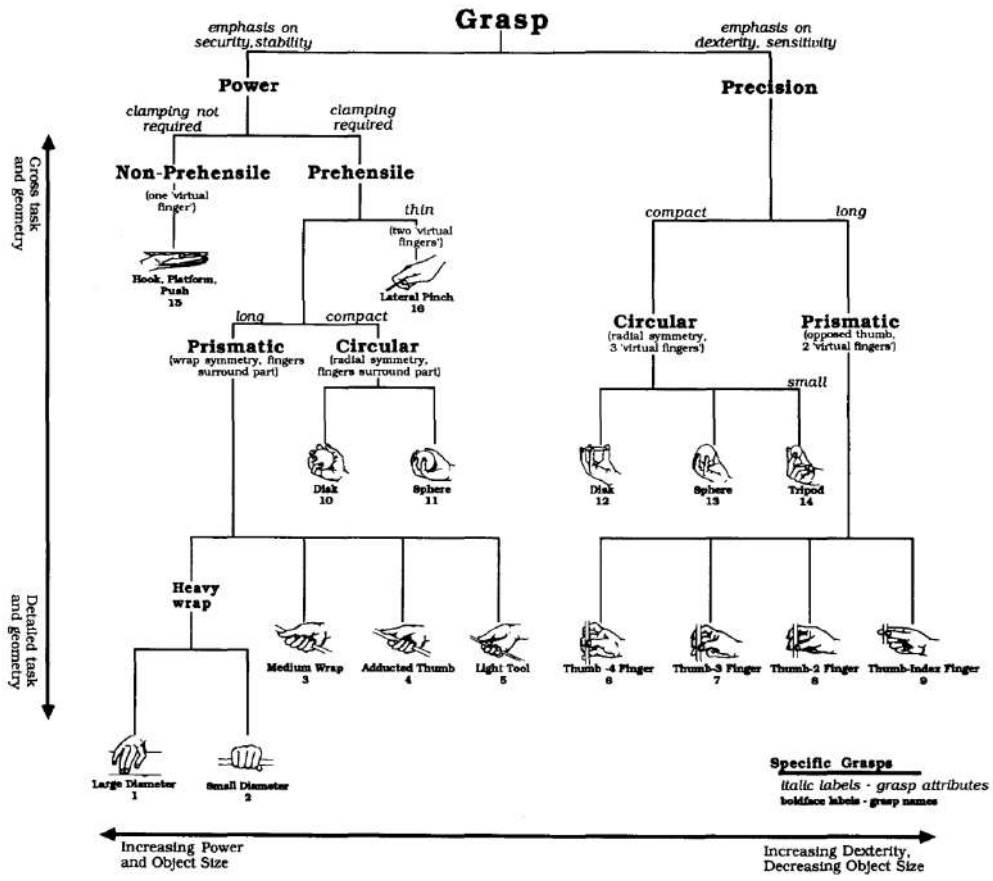

Fig. 3.11 The grasp terminology as defined by Cutkosky [37].

for grasping are taken from the original Cutkosky grasping terminology and combined

it with the one done by Feix et al.[44] [45].

3.3.1 The Key Features

Robotic hands are never the same or follow a standardized design procedure. Each type of end-effector is almost always different, depending on the project's specific goals. But there can be some key features that can be identified and parametrized. The findings based off of the empirical data from the evaluated hands are briefed in the following section. The key features that are discussed below were selected based on literature and the amount of importance each feature has played in making it a successful hand and what role it plays in making it best suited for a particular domain.

Kinematics

The simplified kinematics of the human hand consists of 22 DOFs. The corresponding proportions, lengths and angle deflections are briefed by [22] using X-Ray data. There are a number of methods and criteria for the evaluation of robot hand kinematics in literature. Some of the major ones include:

1. Dexterous workspaces ([36])
2. Manipulability ellipsoids ([101])
3. Grasping stability ([7])
4. Grasping simulations ([86])
5. Grasping indices ([44],[37])

Actuation Packaging

Actuation in a robotic hand means, in a robotic hand system having a plurality of fingers, each having a plurality of joints pivotally connected one to the other, with actuators connected at one end. This can be remotely actuated from a different part of the robotic system, completely removed from the structure of the hand or completely contained within the structure of the hand. There usually then exists transmission systems which connects the actuation mechanism to the joints of the fingers for actuating the fingers.

Both remote actuation and contained systems come with their own advantages and disadvantages.

Size and Weight

The human hand weighs in at about 400g or about 0.6% of a human body's weight. But what is often overlooked in the design of hands is that the human hand is supported by a complex layering of skeletons over muscles and ligaments. Constructing a standalone hand that is not well integrated can lead to fatigue in human prostheses and a cantilever effect in robots. Hence, a lightweight hand is usually preferred in both cases. A survey done by [14] found that prosthetic hand users rated the weight of the hand at 70 on a scale from 0 to 100 (being most important) when it came to design priorities in the design of a prosthetic hand.

Another major observation was that due to the fact that the amputation level of a person varies from one subject to the next, prosthetic hands have a preference of keeping the majority of the mass contained within the hand. This rules out remote actuation in most cases. Humanoid robots are not limited by such constraints and the more dexterous of humanoid hands go for remote actuation and offset their weight by placing the actuators in their forearms, thereby reducing the overall weight of the hand structure.

Hand size should usually be proportional to the body size of the subject it is built for. Be it human or a humanoid/robot.

Payload

The difference between payload and grip force is often misunderstood. Since the selection of these two parameters for robot end effectors is really important, it is crucial to understand the difference between them. It is also important to calculate them properly in order to make accurate choices and decisions for the right applications. Payload is the maximum mass that can be attached or supported by the end-effector. It usually does not include the mass of the end-effector and its mounting mechanism. This is usually the mass of the object that must be moved by the robotic system.

Gripping force is the maximum effort applicable by the end-effector. As robot end effectors are not all alike, different terms exist. Grip force is normally used for less advanced end effectors, representing the force that the "fingers" can apply on a part. Grip force is normally expressed as a force unit. In the following sections, one of the two will be used interchangeably wherever there is a lack of the payload parameter (especially in non-anthropomorphic and semi-anthropomorphic end effectors) since not all evaluation is done based off of payload performance. It can also be argued that

payload and gripping force are related since payload depends on the gripping forces when geometric closure is not obtained.

Compliance

The term "compliant motion" or compliance refers to manipulation tasks which involve contact between manipulator and environment, and during the execution of which the end-effector trajectory is modified by occurring external forces [39]. There exists two types of compliance. The first in which the control system may be programmed to react to force sensor inputs is called active compliance (e.g:Grebenstein et al. [53]). The second type called passive compliance is when the flexibility due to the shape or transmission or the actuation system gives a compliance generates trajectory modifications when come into contact with external forces.

In passive compliance of many robotic hands [113] [17] [56] [107], the mechanism is equipped with a mechanical element that allows for a certain level of compliance in the flexion direction. This type of feature helps to prevent the fingers from breaking under any inadvertent contact, forcing the fingers to close.

Thumb Design

The human thumb is the most complex articulating digit in the human hand. Work done by [51] gives the five link kinematics of the thumb based on cadaver analysis. A number of thumb designs have been explored in the previous sections. The working of the thumb with other key features of the hand such as the wrist, other digits and the palm, play a key role in the functionality of the hand. The relationship between actuation axes of the wrist and that of the rotation axis of the thumb determine the workspace trajectory of the thumb, which is essential for determining most kinematic features of the grasp. Including fingertip spatial position at contact, specific finger paths, finger and thumb path distances, finger and thumb peak tangential velocities, and individual joint rotation magnitudes. Providing an opposable thumb is a key aspect as a design requirement in most anthropomorphic hands. Opposability to most digits (except the index/index-middle) was considered optional since it does not play a key role in grasping.

From a purely design point of view, how the thumb is actuated also plays an important role. A number of hands [118] [35] [71] [108] [43] have the actuator placed inside the hand for the rotation axis of the thumb. Remote actuation of the rotation

axis is relatively rare in all the hands observed. Except in the cases of pneumatic actuation.

Actuation/Grasp Speed

Actuation speed here refers to the speed of closure of all joints to its hardware limits. This can be most effectively correlated with grasping speed i.e., the speed at which the robotic hand conforms to an object that it intends to grasp. Human hands were studied for this task[59] in particular and were found to be achieving full flexion of the fingers at an average of around 1 second every time. Even though the human fingers are capable of flexing faster than this, the grasp speed is what is taken into account for the purpose of this study and is treated as the base line for naturalistic human behaviour.

Sensors

Sensors in hands vary nearly as much as there are robotic hands. It is impossible to narrow them down to a select few. It is always a trade-off when it comes to the sensor parameters that are at the disposal to control the hand effectively. Over-actuated hands, typically require less sensors while underactuated hands usually integrate a lot of sensors to gather information and make up for the lack of absolute position control they have over their platforms. Sensors for joint position sensing and motor position sensing are considered vital in underactuated robotic hands. In addition to that, force sensors such as force-torque assemblies, series elastic modules, tactile feedback sensors [25], strain gauges and optical fibers [78] are also currently employed. Another set of useful sensing is distance, velocity and acceleration sensing in robotic hands. The use of accelerometers [27], miniature distance sensors such as IR, SONAR with even RGBD sensors [69] and LIDAR technologies have been on the rise in recent years in robotic hands research.

Material

Material research and progress in robotic hands has completely changed in the wake of innovative new manufacturing methods. In the previous decades, design was limited by traditional manufacturing methods and materials. The materials were mostly metal based that tended to be more expensive and limited in its manufacturing scope. The advent of rapid prototyping practices has scaled the possibilities much higher. As with

other products in society, the move towards plastics has been the pioneering change in robotic hand design. The use of both machined and rapid prototyped polymeric materials has been on the rise. Polymeric materials have an added advantage of being more lightweight, and in some cases, as durable as metal components.

Rapid prototyping methods have not only revolutionized polymeric material design, but also metal such as stainless steel, titanium, gold and silver. Some research groups [5] [126] [125] [65] [70] [28] have built hands that are entirely 3D printed with novel parts that would have been otherwise hard to be built. Material decisions have, however, not been confined to mechanics design in robotic hands. They have also revolutionized the sensor industry by providing novel interfaces, printable conductive layers, soft-actuation etc.

Manufacturing Methods

Material and manufacturing progresses go hand in hand. Robotic hands have been manufactured by a number of methods such as from traditional means of manufacturing such as CNC machining, lathe operations, casting and molding to the advent of rapid prototyping technologies in recent years such as fused deposition modelling (FDM), Vat polymerisation techniques (SLA), powder bed fusion for polymeric materials (SLS) and metals (SLM, EBM) to material and binder jetting methods. This generally involves manufacturing a component layer by layer by different means. This gives the opportunity to manufacture components that are highly customized, robust and more organic in shape.

Rapid prototyping materials are usually structurally weaker than parts produced by traditional means. This is mainly due to the fact that very often, the bond strength between the different layers is always lower than the base strength of the material.

Cost

The last key factor that plays a major role in the design of any robotic system is the cost of the device. Robotic hands are incredibly intricate designs which often require highly customized parts. A good balance is achieved when the prototype costs are lowered by using rapid prototyped parts and the scaling up of commercial hands cuts down on overall costs to a great extent. But it remains a key factor on deciding which features go into a robotic hand and to what extent. The iCub hand, for example, costs about €8,000 for each hand. The SANDIA hand costs about €10,000 each, the

Shadow hand costs about €90,000, while the Openbionics hand is said to cost only about €1200.

3.3.2 Comparison of Key Aspects

Limitations on size and weight for robotic end-effectors, and its performance trade-offs between various design options, must be addressed by the designer. A general comparison of some of the key trade-offs needs to be done to better understand how every key parameter influences every other parameter in the study of end-effectors. Following is a list of the typical trade-offs encountered in hand design processes

- Number of actuators vs. Number of joints
- Hand weight vs. Payload
- Hand weight vs. number of actuators
- Number of sensor inputs to number of actuators

Number of Actuators to Number of Joints

The rise of underactuation in recent years in robotic hands has been due to the rise in the quality of manufacturing methods, innovative materials and the exponential increase in sensor and sensing tools. One of the biggest problems in underactuation has been control, this gap has been bridged in recent years due to the advent of new and innovative sensors which provide with information needed for robust control. However, looking into literature, it is seen that the higher the actuated DOF, the better it is in terms of control. This, however, also makes the hands more complicated to design and increases computing requirements. Most of the grasps as defined by [21] can in theory be performed by an end-effector with an opposing thumb, i.e., two fingers with 2 DOFs. While to go beyond these functions, a more dexterous hand is needed depending on the functions it has to perform. It can be seen from the Fig. 3.12, in general, completely actuated or over-actuated hands tend to be research hands such as the DLR hand arm system and the UB IV. In some commercial cases such as the Shadow hand, it is remotely actuated and the complexity greatly increases. Prosthetic hands require the system to be lightweight, and adding more actuators tends to increase the complexity of the hand and its weight greatly.

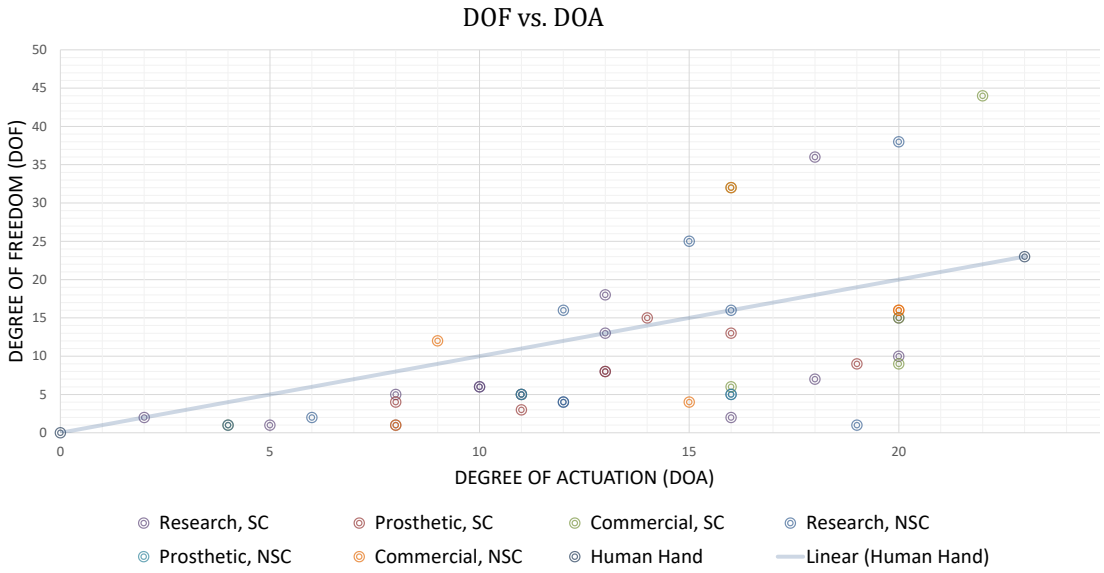

Fig. 3.12 Comparison in the type of actuation in robotic hands

From Fig.3.12, we see the robotic hands that lie on the line are commercial hands which have a single actuator for each joint that it controls. The hands that fall above the line are the underactuated hands which have some sort of coupling between the joints. Prosthetic hands tend to be on the lower side in the number of degrees of freedom and actuation, they are usually underactuated or have a one to one actuation ratio since absolute control is not required in prosthetic systems as there is a human in loop.

Research hands usually have a range of sensors and are generally remotely actuated. They are not limited by the lack of space in other types of robotic hands that have to make accommodation for other joints while respecting size and shape parameters. However, even these kind of robotic hands have been observed to limit the number of joints that are independently controllable, this shows that underactuation is generally a better trade-off. They are usually in the range of 10-20 joints that are usually underactuated and approach the same number of joints as that of a human hand. Novel distribution and transmission mechanisms as used in [29] [70] can be employed to distribute the actuation forces in a planned manner in a fully observable system, to actuate the joints in a pre-planned fashion and reduce the need to over actuate a given system.

Hand Weight to the Payload

The hand weight is greatly influenced by a number of factors such as the number of actuators, number of joints, transmission system, materials used etc. But a good trade-off in determining a good hand would be the ratio between its weight and payload. The human hand can carry great loads mostly due to its skeletal structure and its integrated muscle strength that runs all along its arm. Making a direct comparison in this case would be difficult.

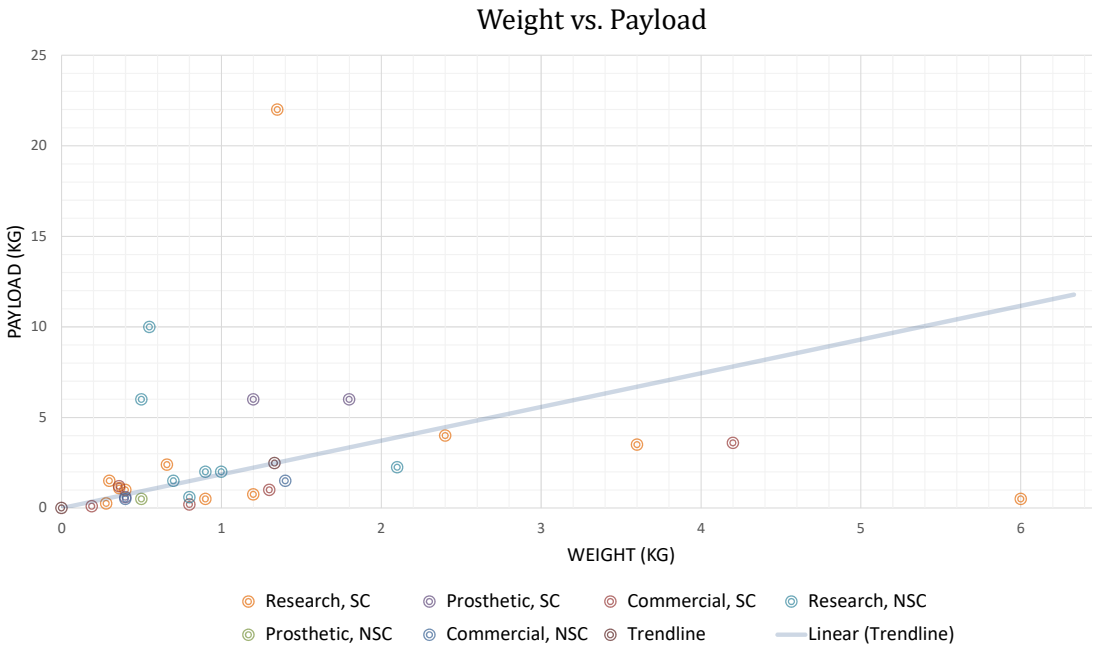

Fig. 3.13 Comparison between the hand weight and its corresponding payload in robotic hands

A good comparison would be to assume a 1 to 1 ratio, i.e., the hand should be able to lift as much as it weighs. Payload lift as defined here, would be complete grasp of the object with the open part of the palm along gravity, with the object securely held by the hand. Keeping this in mind, we can refer to the Fig.3.13. We can see that prosthetic hands don't weigh too differently than their quoted payload. This is due to the fact that prosthetic hands need to be lightweight in order to be useful to the wearer. Hence they are limited to lifting everyday objects. They are also most often than not, aren't remotely actuated.

Robotic research hands do not suffer from this limitation. They can be remotely actuated and hence allows for displacement of the actuators. But an interesting thing of note is that, even though they have a distinct advantage in this case, they still

suffer from a poor ratio between their weights and payload. Limitations in actuation strategies, motor capabilities and transmission systems are some of the reasons for this. Another telling factor is cost, since the complexity and performance levels of all these aforementioned factors are limited by cost.

Most robotic hands are clustered around this ratio, the line represents a linear fit line of the ratio observed in all hands. On average, a well cited robotic hand is capable of carrying 1.8 times its own weight. It can be seen that the only robotic hands that go above the line are mostly commercial or prosthetic or both. The average payload is between 200 grams to 1 kilogram. The commercial hands which performed way above average than the rest of the hands were usually fluidic or pneumatic cylinders without the pump weight taken into consideration. From this we can estimate a good ratio to be achieved between the weight of the finished hand and the weight of the payload it can carry is a minimum of 1 to 1.5 ratio. Clearly, the higher the ratio, the better.

Hand Weight to the Number of Actuators

Another interesting analysis is the comparison of hand weight to number of actuators being employed by the hand. Even underactuated hands tend to be heavy if motors are housed within the hand. For a fair comparison, when we refer to weight, we include any type of actuation system, be it remotely actuated or self-contained (as mentioned in literature). Another interesting factor in this would be the transmission systems

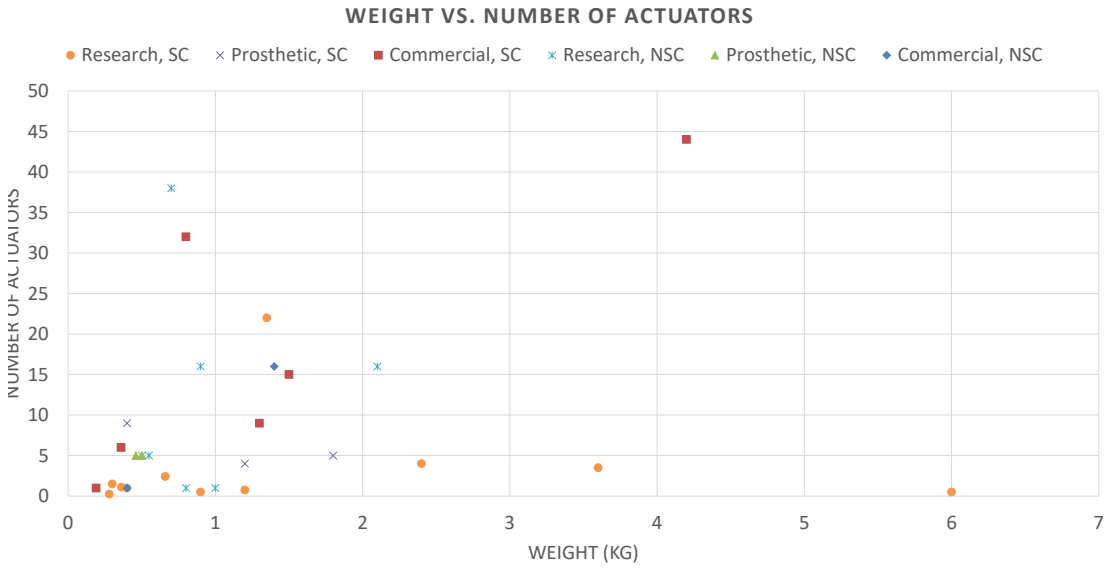

Fig. 3.14 Comparison between hand weight and number of actuators in robotic hands

in the actuation methods. Since even in underactuated hands, there is still a high level of coupling between joints, which account for more weight in the system. As can be observed in Fig.3.14, we can see that the robotic research hands are consistently heavier than their prosthetic counterparts. The lowest on this scale are the commercial self-contained hands since they focus on cost reduction and ease of manufacture.

But it can be noted that the weight of the hand and the number of actuators plays no significant role in the ratio. All self-contained and remotely actuated hands are clustered close to each other in the graph, which shows that the number of actuators in the robotic hands play no significant role in determining the overall weight of the system. This could be due to the transmission systems, the type of actuation, the distribution mechanism (in underactuated hands) and the type of sensors that are employed in the hand, to name a few.

Number of Inputs to Number of Actuators

Although a statistical analysis of this is harder since the exact number of sensor inputs is not completely defined, it would be interesting to note the number of different type of sensors that are put into the robotic system. Although adding more actuators is not necessarily always better, the same design principle works for sensors. Providing a large amount of sensory data is almost always beneficial to better control the robotic hand. This holds especially true in underactuated hands, where the advantages of underactuation: where the distributing force contacts are better and over a larger area, increased adaptability, resistance to external disturbances due to compliance etc., are slightly under served due to the problems that arise in controlling them. But having enough sensory data to make the state of the robotic hand fully observable tips the advantage to underactuated systems. This is especially true off late due to the rise in machine learning techniques and deep neural learning systems which require more inputs to overcome minor disadvantages in the hardware system.

3.4 Technical Guidelines

The previous chapter outlined user needs for the robotic hands. This section aims at outlining the key technical guidelines of the system. Based on the previous sections, the following technical guidelines were enumerated to facilitate the conceptual design of the robotic hands:

- The hand has to be underactuated
- The ratio of hand weight to payload should be at least 1 to 1.5
- It should be a highly sensorized system that makes the robotic hand completely observable
- The hand should have a thumb with at least two degrees of actuation
- It should be anthropomorphic in shape and size
- The hand should not cost more than 10 percent of the total cost of the robot
- The robotic hand should have a mechanism to sense forces and make the fingers compliant (active or passive)
- The hand should be robust, easy to assemble and repair

Chapter 4

A New Evaluation Index

4.1 Motivation

From the previous chapter, it can be observed that there is a lack of a standard set of tests to evaluate multiple design aspects of a robotic hand. There does exist a lot of different benchmarks and evaluation indices which mostly focus on the grasping capabilities of the hand based off of the work done by Cutkosky [37] and Feix et al. [44]. There also exists other methods such as the Kapandji test [64] for quantifying thumb opposability and the anthropomorphism and dexterity index proposed by Biagiotti et al. [12].

All these benchmarks and indices give either different objects that best represent the Cutkosky grasps or give a specific grading to certain aspects of the hand. The usefulness and versatility of a robotic end-effector depends not only on the diversity of grasps it can accomplish but also in its form and the complexity of the control methods required to achieve them. While evaluating literature, there arose a need to quantify hands in a better way. All the robotic hands that were studied usually had specific features that were required due to specific user needs of the platform under investigation. However, an objective benchmark is necessary to provide guidelines which aid in making a particular end-effector platform better while also acting as a types ofguide for best practices in the design of these hands.

Hence, a new form of evaluation index is proposed that is mainly intended to be performance oriented, while also considering the hardware capabilities of the hand. When it comes to performance evaluation, the grasping of objects is key, but it is not completely defined by just that. It has several aspects associated with it as defined by Cutkosky [37], they include:

- Compliance
- Connectivity
- Force closure
- Form closure
- Grasp isotropy
- Internal forces
- Manipulability
- Resistance to slip
- Stability

Since most of these aspects are heavily tied to the control of a given robotic hand, the results drawn are not only a result of design decisions that went before it.

There is then the need to separate the hardware features in robotic hands from the performance aspects, at least in the initial stages. Certain features and parameters in robotic hands can help in improving the overall design. This can consequently aid in effectively controlling the hand. Robotic hands are no longer manufactured for the sole purpose of grasping a set of standard objects. Nor are they made to look entirely anthropomorphic. This kind of disparities have to also be taken into account during evaluation.

A direct comparison is not possible, nor would it be fair. Each type of robotic hand is manufactured specifically for a given need. If there exists a way to evaluate every hand such that the focus of the hands' purpose is inherently highlighted, that would be of a greater significance.

In the following sections, a new evaluation index based on tests that address these limitations are proposed to help evaluate major aspects of hand design and their performance.

4.2 A New Evaluation Index

As mentioned in the previous sections, robotic hands are not built exclusively for the sake of grasping. Human-Robot interaction has led to the need for incorporating

communication and interaction aspects into hands. Additionally, robotics hands also need to be capable of performing simple manipulation tasks as the need for increasing the mobility in prostheses increase.

Also of importance is the type and amount of sensors that need to be incorporated into the hand. Myoelectric hands have been on the rise in prosthetics which focusses on a more natural input from the user. While in humanoid robotics, the use of force-feedback and tactile sensing is increasing in importance as ways of handling objects better, once they are grasped.

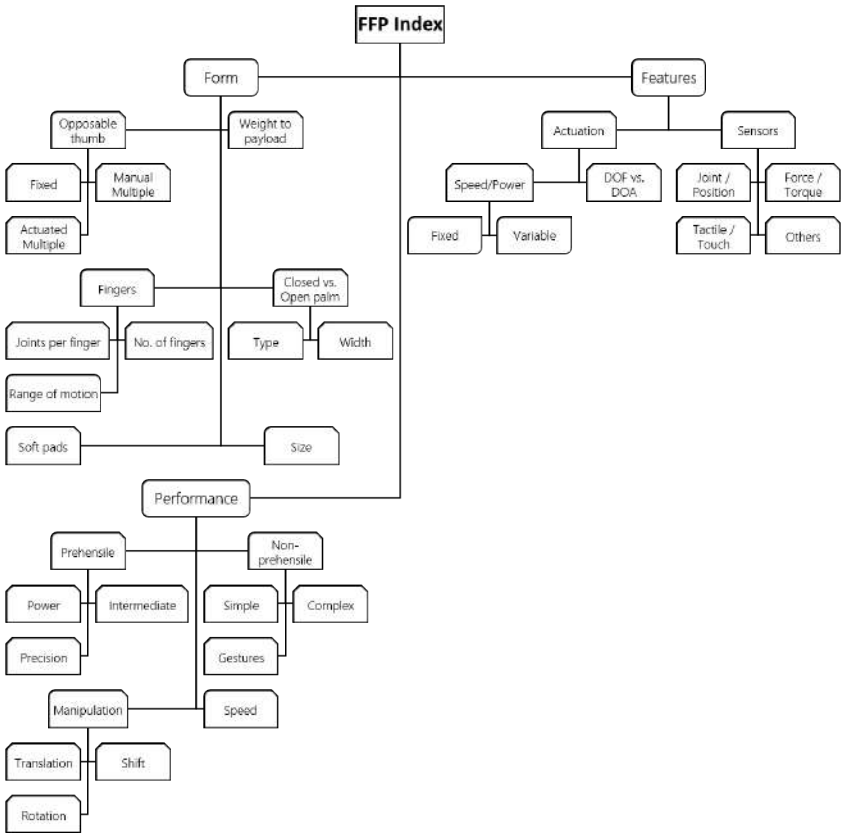

Fig. 4.1 The FFP index. It is a new, holistic way of evaluating research hands. It comprises three main sub-categories, the form: how anthropomorphic a hand is, the features: how many features are available to control the hand effectively and performance: how well the hand performs prehensile, non-prehensile or even manipulation tasks.

The other aspect of robotic hands would be its shape and form. Anthropomorphism is a tricky subject as the importance now lies on the user perception of the look of a robotic system. An anthropomorphic shape is considered favorable in prostheses, while current research in humanoid robotics has gone beyond traditional anthropomorphic

hands. Humanoid robotics are no longer exclusively bound by the conventional design paradigms that anthropomorphism entails.

Hence, rating a hand strictly by its anthropomorphic constraints seems primitive, since function precedes the form. Some robotic hands that perform exceptionally well for a dedicated purpose might fall low on the form scale and vice versa.

To bridge this discrepancy, a new index for evaluating hands which treats the form, features and the performance aspects of a given hand as loosely tied, with separate scores for each, all the while interacting with each other is proposed as given in the following sections.

4.3 The FFP Index

The FFP index or the Form-Features-Performance index is an evaluation method, wherein different aspects of the hand can be evaluated. As shown in Fig.4.1, the FFP index is composed of multiple sub-categories. This is not a strictly weighted index, the three main categories in this evaluation can be weighted equal in the first step. This gives an idea about how a given hand performs in each of the dedicated categories of form, feature and its performance. As a second step, weights are assigned to each of the three categories as and how important it is deemed by the user. By doing this, an estimate of the amount of importance that goes into the design of each aspect of the hand can be determined. The main motivation behind this type of evaluation is to act as a good guideline for building effective hands and to draw a common denominator across all the robotic hands that are there in the market. By drawing a common baseline, comparison of different types of robotic hands is made easier. While assigning a unique weight for each application domain gives a customised score depending on the application of the robotic hand.

It also acts a good indicator of what the main motivation behind a particular design had been. For eg., if a proposed hand weighs in at 0.9 in Form, 0.6 in control and 0.7 in performance, it can be derived that importance went into the look of the hand and the design was focussed on making it as anthropomorphic as possible.

As an example, a set of weights is proposed for each category that is considered optimal to design a functional anthropomorphic hand for a domestic robot, as shown in Fig.4.2. These weights put a higher priority to a hand's performance over its other aspects.

The weights suggested here, although seemingly arbitrary, are drawn from a num-

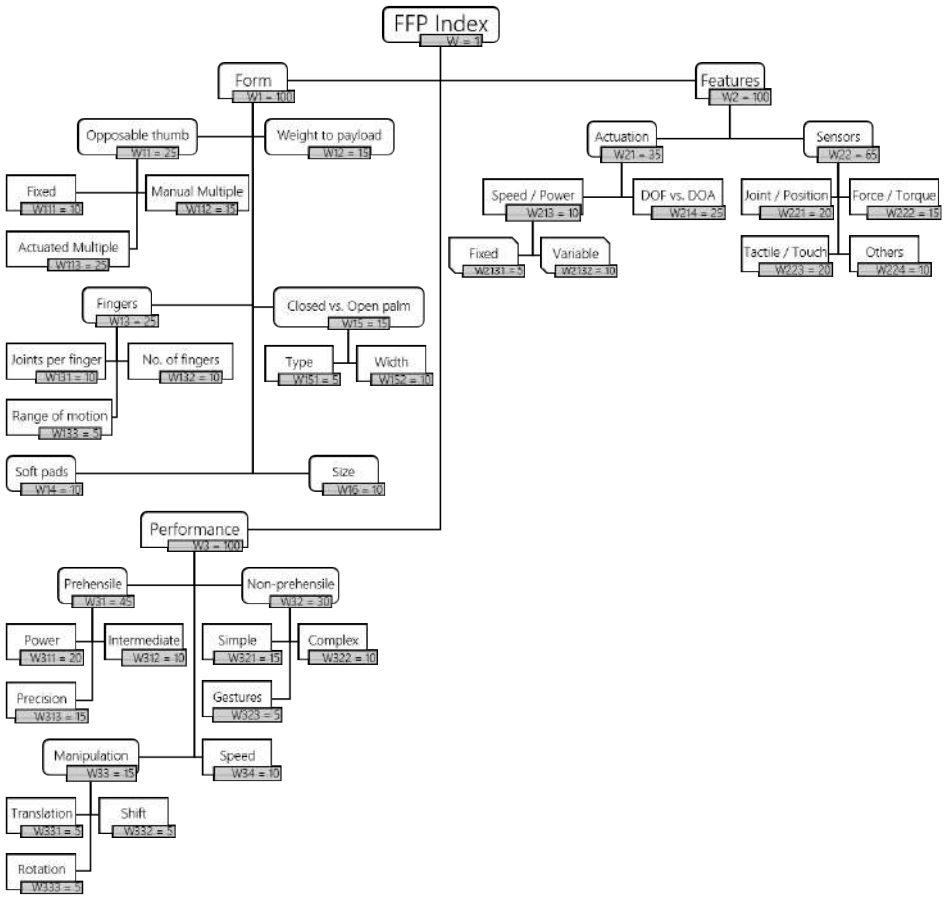

Fig. 4.2 A weighted FFP index. Each main sub-category has multiple sub-categories which cumulatively earn a score of 100% and are then compared with the other two, to gain a relative view of the design. This helps to gain an insight into where the design focusses on.

ber of factors such as features that are found common in the most cited hands in literature, and some other features are drawn from existing evaluation practices. The weight assignment is intuitive and biased but based on all the research done from literature. Each of the categories and its sub-categories is discussed more in detail in the following sections.

4.3.1 Form

Anthopomorphism, in this case, is defined as the presence of five unique digits that aim at replicating the look of the human hand, an opposable thumb and has similar size and weight ratios to that of the human hand. Biagiotti et al. [12] defines anthropomorphism in robotic hands as *"the capability of a robotic end-effector to mimic the human hand,*

partly or totally, as far as shape, size, consistency, and general aspect (including color, temperature, and so on) are considered".

Anthropomorphism might be a key factor in prosthesis since subjects wearing it have a degree of comfort factor to the anthropomorphic form. But even that is not considered the crucial factor when it comes to deciding for or against the use of prostheses according to the work done by Biddiss and Chau [13]. According to the survey[13], the most prominent factor for prosthesis rejection was that users considered themselves as having more or less the same level of functionality without the prostheses or it was too heavy or hot or even that the sensory feedback obtained from it was not enough.

Only about 70% of the total said that the look was even a factor and the level to which it was a factor, was around 1 (on a scale from 0 to 3, 3 being most important). This shows anthropomorphism is not high on the list of requirements even in prosthetics.

Research hands on humanoid robots are highly function specific. Since the anthropomorphic shape is not always chosen in humanoid robots, it is considered very low on its importance scale and almost always is preceded by its functionality. This does not mean that the form doesn't matter whatsoever. Some key features in the form of hands are deemed important and are explained below. In the FFP index, anthropomorphism is given a weight of 20%.

Opposable Thumb

In the book by Napier and Tuttle [89], thumb opposition is defined as *"probably the single most crucial adaptation in our evolutionary history.."* and that loss of thumb opposition could *"..put back 60 million years in evolutionary terms.."*. Thumb opposition is perhaps the most important movement of the human hand and is a major underlying factor when it comes to any kind of skilled actions performable by the hand.

Indeed, as can be seen in literature, almost all hands have an opposable digit that takes the role of the thumb or its part in opposition. *How* the hand performs this opposition is a different case. The best score of 25% is given to the presence of an opposable, articulated thumb. The presence of a single position (no rotation, but opposable) thumb gets a score of 10%, a manually articulated thumb which requires human intervention to lock its position gets a score of 15%, while the lack of a thumb gets an automatic zero.

An articulated thumb is when the thumb can facilitate apprehension tasks by mov-

ing out of its default opposable position, either through rotation, abduction/adduction or a combination of the two.

Payload to Weight

The weight of the hand is considered to be an important factor in the design of a robotic hand. It is considered to be a key design parameter in prosthetics according to the survey done by Biddiss and Chau [13]. It also plays a significant role in the design of humanoid robots since the final articulation and manipulation skills depend on the end-effector of the robot. A heavy hand can increase the cantilever effect in

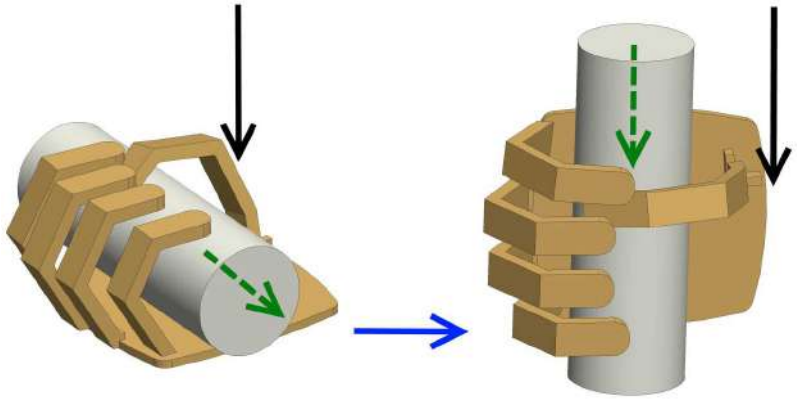

Fig. 4.3 Payload to weight ratio. The measurement of the payload the hand is carried out in two distinct steps. The hand has to completely support the payload with the palm oriented perpendicular to the gravity vector. In the second step, the hand has to turn with the payload in hand till the palm is in line with the gravity vector.

all manipulators and can make the robot structurally weak. In classical definition of "payload", it is defined as the maximum mass that can be attached or supported by the wrist of a robot arm. A payload is usually expressed as a weight unit (kilograms [kg] or pounds [lbs]). A more useful parameter would be the gripping force of a robotic hand. Gripping force can be defined as the maximum effort applicable by the end-effector on an object under its grasp. As robot grippers are not all alike, different terms exist. Grip force is normally used to define the force that the "digits" can apply on a part.

However, such distinctions exist widely in literature. For the purposes of this research, the robotic hand is treated as a separate robotic system and the payload here is the maximum weight the hand is capable of lifting given its link lengths, actuation type and its friction parameters. To achieve success in lifting a payload, the

hand should be able to perform a successful grasp. It should grasp the object and be able to completely turn it with only the hand supporting the object. This should be done from a position where the object being grasped is perpendicular to the gravity vector and turned till the hand is parallel to the gravity vector while maintaining a firm grasp on the object in one continuous motion as shown in Fig.4.3.

What is referred to as "weight" of the hand in this evaluation includes the actuation setup (be it remote or self-contained) and "payload" refers to the maximum weight that can be held by the hand as explained before.

This is given a 20% as a perfect score. From the previous chapter, if the ratio is 1.5 or higher, the hand gets a full score, if the ratio is 1.5 or higher excluding the actuators from the weight but higher otherwise (remotely actuated hands), the weight is cut by half to 10% and a no score for all other values.

Fingers

A finger is a type of digit, an organ of manipulation and sensation found in the hands of humans and other primates [34]. Fingers can be flexed or straightened at their respective joints between phalanges. They can also move side to side with respect to the centre of the hand; this movement is called abduction/adduction. Fingers in a human hand refer to four individual digits and a thumb. But it need not necessarily be the case in a robot hand. For this evaluation, a weight of 25% is assigned to a robotic hand that has all five fingers and an appropriate number of phalanges that is classical for a human hand. The breakdown of the different aspects that influence the form of the finger is discussed below.

Joints per finger: The number of joints per finger is deemed extremely important since it provides the hand with conformance to shapes, a contact surface for gripping and a support structure for grasps. A minimum of two joints is considered important in most cases for effective grasping.

A score of 10% is given if the hand has a minimum of two active joints(physically distinct) and a score of zero otherwise.

Number of fingers: From literature, it can be seen that hands can perform very well with just two[18] or three[88] digits. Some of them even outperform anthropomorphic hands. The performance also highly depends on the control and overall achievable posture of the robotic hand. In essence, robotic hands need not be necessarily anthropomorphic, but an increased number of fingers (be it in underactuated or fully actuated hands) give it more grasping surface and increases conformity to shapes.

However, the number of fingers plays a major role in the degree of anthropomorphism in hands[14].

Keeping this in mind, a score of 10% is assigned for the overall evaluation score for five fingers (four fingers, one thumb), 8% for four fingered hands and 5% for three fingered (minimum of two fingers, one thumb) end effectors and zero otherwise.

Range of motion: The metrics for the range of motion is derived from Becker and Thakor [10]. Performing an average of range of motion of each of the phalanges across the four main digits of the hand, it can be observed that the range of motion is best when the MCP joint is between $75° - 85°$, the PIP joint lies between $100° - 110°$ and finally the DIP joint when it lies between $65° - 70°$. Hence, a maximum score of 5% is given for fingers that achieve or exceed a range of motion as described and zero otherwise.

Soft Pads

The soft padding on the palm and fingers in the front side of the human hand is called the glabrous, it is tightly stretched with flexure lines in specific areas to accommodate folding and stretching. The glabrous is covered by papillary ridges or fingerprints, which provide the necessary friction and also acts a sensor to micro-vibrations. This kind of soft-padding is considered important since it allows for conformity to objects and also gives rise to compliance. Friction surfaces also provide the hand with extra support during both prehensile and non-prehensile tasks.

Fig. 4.4 The glabrous of the human hand with flexure lines and papillary ridges acts as both soft padding and as a friction surface for efficient grasping and manipulation.

Drawing from this, it is clear that the presence of compliant paddings and friction surfaces are very useful in providing a good grasp. A weight of 5% is assigned for the presence of soft padding and 10% to a dedicated friction surface such as commercial

gripper material, or high-density neoprene, leading to a total of 15% for this subcategory of the evaluation.

Closed vs. Open Palm

Another feature which has been sparingly explored in the evaluation of robotic hands is the approach of the hand to a grasp. Human hands have an offset thumb making the hand more "open" in its approach. Traditional grippers and a number of hands in literature, however, have an opposing digit in the centre of its palm. This could also be defined as the classical gripper form versus the anthropomorphic/semi-anthropomorphic hand.

(a) A closed hand, courtesy:Robotshop (b) An open robot hand

Fig. 4.5 The different configurations of the hand, on the left is the closed palm (seen from the side), with a central thumb as compared to the offset thumb in the right, which constitutes an open palm design.

The human hand works tightly with the rest of the body to perform a lot of actions. Actions such as opening doors can be highly complex and require the coordinate motion of the entire torso. Same holds true for humanoid robots. Hence, the approach to handling objects and its planning is a lot easier when the thumb is offset or the palm has more space to approach the object and wrap around it.

Type of Palm

The offset thumb also provides increased, effective contact surfaces for object grasping and manipulation. Sometimes, this can be compensated with longer digits and decreased palm surface, but this makes in-hand manipulation more difficult.

Therefore the type of palm design warrants a separate, albeit small weight in the evaluation scale. It is given 5% of the total form evaluation score for an open palm,

with an offset thumb design while a no score for closed palm, since the anthropomorphic form is favored in humanoid robotics and prostheses.

Width of Opening

The width of opening of a hand can be defined as the minimum distance between the tip of the palmar digits to the tip of the thumb when the hand is fully open. This plays a vital role in grasp approach, volume, fidelity and strength. When designing for prostheses, hand function emphasis is generally on variable opening of the hand. For non-dominant hand function, where the hand is used essentially as a portable vice with objects being placed into it, a wide opening becomes more important. As given by [124], an artificial hand should be able to open at least 10 cm (3.5 to 4 in).

Hence a robotic hand that is capable of achieving a hand width opening of more than 10cm is considered as the best option, while anything between 5 and 10cm is deigned acceptable. The scores are assigned accordingly for each.

Size

For prosthetic robotic hands, it is only natural to have a human hand size or a proportional size to whom the prosthetic is being fit. Same holds true for humanoid robots. A hand proportional to the size of the robot, keeping with human proportions should be selected. Human hand proportions can vary due to a number of reasons as explored by [81]. For the purposes of this work, the size here refers to a proportional scaling for height of the 95th percentile hand as referred to by Dreyfuss et al. [41]. This feature is given a weight of 10% in the Form part of the evaluation, if the hand is within ±15% of its proportional human size. And a no score for all other values.

4.3.2 Control Features

Control features in this context means parameters that would enhance the amount of data available to control the hand effectively. This means that the robotic system should have all tools to make itself completely deterministic, fully observable and actuated at its disposal. Control features are also weighted separately, along with Form and Performance.

Actuation

Fully observable systems compensate for the drawbacks to underactuated systems to a great extent keeping this in mind, actuation features are given a slightly lower weight than sensor system. Actuators have a completely different set of constraints. Human hands vary greatly in their speed and grip force and are capable of reaching up to 400 N on average in every day tasks[76]. This kind of actuation characteristics is next to impossible with the current motors in the market, if they are to be housed within the hand. Hence, remote actuation seems to be the stop-gap solution for now. Finding miniaturized actuators that would fit into the finger phalanges or at least into the palm of the hand, is a constraint apparently shared with nature. This necessitates the use of actuators placed in the forearm and using tendons to transmit forces to the finger joints.

Variable Speed/Power Takaki and Omata [116] state that it is difficult to improve the speed and power performances simultaneously if the reduction ratio of a finger joint drive is constant. One added feature in robotic hands that could prove to be useful is the option to vary the power and speed of actuation of finger joints. A weight of about 10% is given to this feature.

Fixed transmission: This is the most common type of transmission in robotic hands. It is also the default where the speed and power is fixed. Most robotic hands tend to drift towards this configuration as the space constraints inside the hand limit the variable transmission capabilities within the hand. Since this tends to be the most common type, it is given a score of 5%

Variable transmission: A good feature to have in robotic hands would be to select the power and speed at which fingers are actuated depending on the object to be grasped or the task to be performed. A variable transmission is a solution to this problem because low reduction ratios enable quick motions and high reduction ratios enable powerful motions[116]. Therefore, any robotic hand that has variable transmission is given a full score.

DOF vs. DOA: In physics, the degree of freedom (DOF) of a mechanical system is the number of independent parameters that define its configuration. It is the number of parameters that determine the state of a physical system[34]. The degree of actuation on the other hand can be defined as the number of actuators required to fully actuate and control a given robotic system. A robotic system can be fully actuated, where each degree of freedom has an actuator controlling it or underactuated: where the system has a lower number of actuators than degrees of freedom or over-actuated where a

single DOF can be controlled by more than one actuator. These robotic hands in which you have more actuators than the systems' degrees-of-freedom are called over-actuated systems. In the case of robotic hands, the use of such actuators can vary greatly. They can typically be used to control the impact and force load response of the system, or can be used in systems that used agonist-antagonist actuation etc. It is usually case-specific, but they almost always have the number of operable control greater than the controlled variables. These marginal advantages do warrant a slightly better score than that of fully actuated systems.

There are however perils to equating the number of degree of freedoms directly as the number of joints. In some robotic hands such as the prosthetic hands explored in Odhner et al. [92] where different joints are rigidly coupled together using links (typically four bar mechanisms). In such cases, the number of joints increase while the DOF is reduced. In such cases, the system must be considered individually and the appropriate DOF must be taken into account.

However, much of this research goes into the study of underactuated hands, where such distinction is negligible, and all the tendon driven underactuated hands are considered to have the same number of DOF as joints.

This is a difficult parameter to evaluate considering the efficacy of the system depends if the system has enough sensors and adequate controllable parameters to make the system fully observable. Keeping this in mind, a weight of 10% is assigned to underactuated hands, while a fully actuated robotic hand is given a score of 20% while overactuated systems are given a full score of 25%.

Sensors

Sensors are what robotic systems use to get useful data of its own state or the environment it is placed in. It can be partially or fully observable to play any role in the control of the hand. Robotic hands are basically puppets without the use of sensors, since open loop control of robotic hands requires a human in the loop all the time. Hence, sensors play a major role in the development of a hand, and some of the key types of sensors are discussed in the following sections. The category as a whole carries an increased weight of 60% as compared to actuation in the features part of the evaluation. The breakdown of the weights in each of the sub-categories is as shown in Fig.4.2.

Joint / Position: Joint position sensing is critical in robotic hands as they give feedback on the link and joint position in the robot's workspace. In underactuated

hands, it also provides feedback on the grasp as it conforms to the shape of the objects being handled. In the absence of force sensors (which is usually the case), it can prove vital to grasp quality.

Force / Torque: A very useful feature to have in robotic hands is information on the amount of force being applied by the hand on its environment or even the forces and torques that are present within the system itself. This can provide useful information on tendon tension in tendon actuated hands, it can provide force and torque parameters that are critical in force-closure and form-closure control. It can also be key in aiding human-robot interaction and promoting safety. In the case of prosthetic robotic hands, myoelectric sensor inputs are used for intent learning and are also considered to be part of this category and carry the same weight of 15% as that of force feedback, even though it is a sensor that gives an input for actuation response rather than being a status monitor affected by the actuation.

Tactile / Touch: An expansive review of tactile sensors was done by [127]. The minimum functional requirements for a robotic tactile sensing system mimicking human manipulation was summarised as:

- Detect the contact and release of an object.
- Detect lift and displacement of an object.
- Detect shape and force distribution of a contact region for object recognition.
- Detect contact force magnitude and direction for maintaining a stable grasp during manipulation.
- Detect both dynamic and static contact forces.
- Track variation of contact points during manipulation.
- Detect difference between predicted and actual grip forces necessary for manipulation.
- Detect force and magnitude of contact forces due to the motion of the hand during manipulation.
- Detect tangential forces due to the weight and shape of the object to prevent slip

Hence any type of feedback sensor that fulfils most or all of the above requirements, falls under the category of tactile feedback. It is essential for the above-mentioned reasons. And as technology advances in this direction, there has been an increasing amount of robotic hands that has been incorporating this as part of their design [106][46][117].

Others: This could be sensors providing information on temperature, olfactory, vision, any type of depth sensing, stress, strain, twist etc. These are considered tertiary level sensors and although they might be function specific and aid in enhancing the features of the robotic hand, they are not considered to be mandatory as a general guideline.

4.3.3 Performance

The most common way of grading hands has been to make it grasp objects of different shapes and sizes. The first attempts to make a standard set of grasps that well define and categorize a hand grasp comes from Cutkosky [37] which was later improved upon by Feix et al. [44],[45].

Biagiotti et al. [12] state "Grasping is intended as constraining objects inside the end-effector with a configuration that is substantially invariant with time (the object is fixed with respect to the hand workspace), while internal manipulation means controlled motion of the grasped object inside the hand workspace, with constraint configuration changing with time." By this definition, simply grasping an object is not sufficient to completely grade all of the qualities in a robotic hand. Some benchmarking techniques also suggest carrying out manipulation tasks and non-prehensile tasks.

Performance Benchmarking in Literature

When it comes to evaluation of hands, grasping of objects is the standard. However, there does not exist a standardized set of objects that are grasped in these evaluations. Therefore, there does not exist a uniform comparison across platforms. There exists a variety of objects' models: some use 3D model meshes, some provide just images while some others give real world objects in the form of commercial kits that can be bought or in the form of a shopping list that can be used for buying the objects from any commercial outlet.

These grasping benchmarks supposedly represent the set of objects that best en-

compasses all types of grasps or even tasks that a robotic hand should perform. The more famous ones are from GeorgiaTech and ones from Yale University. A review of all available benchmarks was carried out by [24]; the interested reader is invited to consult it for further details.

A major shortcoming in any kind of grasping dataset is that it is inherently biased or too expansive, which in turn does not give a very intuitive view on the overall performance of the robotic hand under evaluation.

Keeping all this in mind, a list of objects that are used in daily events in a domestic environment was made. This was done by sourcing research done by GeorgiaTech [32] and their study with ALS patients, objects used daily in a home environment and objects most often used in elderly care homes.

For performance metrics, the weights are assigned as shown in Fig.4.2 for all sub-categories.

Prehensile

The prehensile tasks are based on the work done by [37] while proposing a new set of objects for grasping. We came up with a list of 65 objects which uses all types of grasps as enlisted by [37][45]. It also tries to balance a wide range of textures and weights on real world objects which are also used in everyday life.

For the sake of simplicity the type of grasps were divided into either Power, Intermediate or Precision grasps.

Power: The power grasp encompasses grasps that require both large and intermediary grasp forces. These type of grasps focus on the stability of the grasp and are usually imparted on larger objects that need a secure clamping action. These are most often used in scenarios where the object being grasped needs to be moved from one place to the other and usually does not involve manipulation of the object.

Intermediate: These are the “in between” state of grasps that are represented within the taxonomy since it is between power and precision in its state [57].

Precision: Precision grasps require lower force and higher accuracy in positioning and control. It is typically characterized with thumb opposition to the distal joints of the other fingers. These are used in the grasp and manipulation of smaller objects.

Non-prehensile

Non-prehensile manipulation is generally categorised as the handling of any objects without straight grasping. This kind of manipulation might be done in a number of ways such as: pushing, squeezing, twirling, tapping, rolling etc. A set of non-prehensile tasks are also proposed in the following sections based on everyday activities.

Simple: These kind of tasks involve displacement of a single object placed within or outside the hand from its current state , eg: lifting a cup.

Complex: These are manipulation tasks that involve interaction between two distinct objects excluding the hand, and changing their current state eg: pouring water into a glass.

Gestures: With the rise in Human-Robot and Human-Agent interaction, non-verbal communication has become an important part of the development of robotic hands. A simple set of gestures is hence recommended in the FFP index to evaluate the basic gesture performing capabilities of the hand. Since hand gestures vary according to culture, fields and regions; five distinct hand signals which are universally accepted for their respective action intents are listed.

In-hand Manipulation

A major distinction from most performance metrics of robotic hands is that the emphasis on the in-hand manipulation aspects of the hand. Since this aspect of performance analysis is heavily dependent on the control robustness of the system, we limit it to a few simple tasks which can be done using open loop position control.

Translation: It is the ability to move objects from the fingertips to the palm or vice-versa.

Shift: It is the ability to move an object in a linear manner with the fingertips

Rotation: It is the ability to turn an object around the pads of the fingers and thumb

Speed

Human-like speed in normal every day grasping is not impossible to achieve, as is the case with grasping force. It is however mandatory to 'react' quickly and to perform grasps in an efficient manner. Hence it is given a weight of 10% for complete flexion and extension is carried out within one second. A score of 5% is given for a speed

anywhere between 1 to 1.5 seconds for flexion/extension which is near human speed, and a no score for anything below those prescribed speeds.

Tool use

Additionally, tool use in robotic hands is a useful yet redundant task when it comes to design of robotic hands for prehension and manipulation tasks as they involve, to a great extent, robustness in control. The tasks listed in the Appendix are recommended but not necessary in the FFP evaluation of robotic hands.

4.3.4 Subjective Weighting

An added feature of this evaluation index is tuning the weights of all three major aspects of design and making it inter-related. By assigning weights each of the three categories: Form, Feature and Performance; it is possible to acquire a single score that rates the efficiency of the hand for a particular purpose.

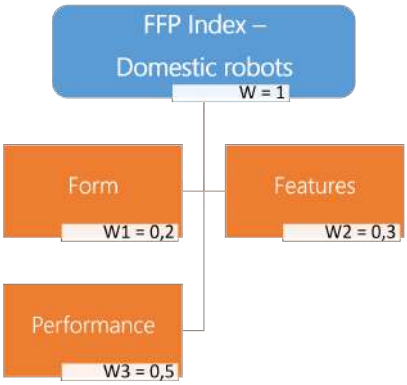

Fig. 4.6 Subjective evaluation - Suggested weights for a domestic robot

As an example, the iCub hand is graded with subjective weighting of that recommended for a domestic robot. The weights are distributed as shown in Fig.4.6 This works by multiplying the results obtained for each of the three categories by the suggested weights and then summing it up against 100. This is explained with an example in the following sections.

4.4 A Case Study

The iCub hand is used as a preliminary baseline to evaluate other hands and to compare against. The evaluation is done by means of an online questionnaire form[1] where users can fill in a questionnaire based on the hand that is being evaluated. The hand will be benchmarked if the user sends video proof in the form of pictures and videos to the iCub department at IIT.

This was done for the iCub hand and some sample pictures of the performance characteristics are shown where the iCub is grasping a series of objects (Fig.4.9) and performing a series of gestures (Fig.4.10).

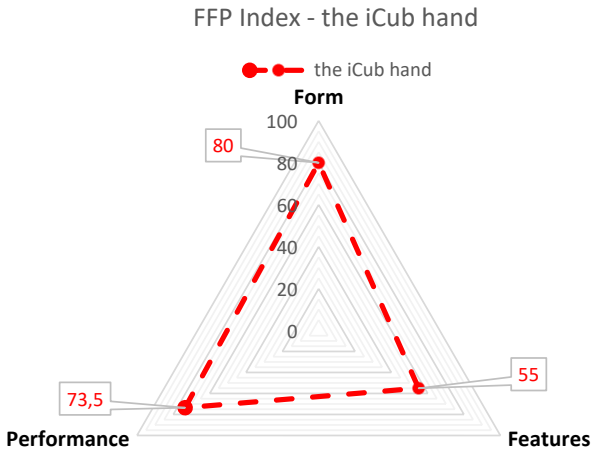

Fig. 4.7 FFP Index evaluation of the iCub hand. The iCub hand is a research platform that needs to perform adequately overall. The FFP evaluation shows that it is a good anthropomorphic hand that performs well for most tasks but is lacking in features.

4.4.1 Form

The iCub has an open form, anthropomorphic, five-fingered and underactuated hand. It has three phalanges to each of the fingers. It has an opposable, articulated thumb. The tactile skin is covered with a dielectric layer and a second conductive layer: electrically conductive Lycra for the palms, electrically conductive silicone for the fingertips. This layer is connected to ground and enables the sensor to respond to objects irrespective of their electrical properties. This gives it a thin layer of compliant material with

[1] available at https://goo.gl/7hJcVv

minimal friction properties. The iCub hand scored an 85% for its Form characteristics, which is a good indication that the hand is highly anthropomorphic.

(a) The iCub2 hand (b) The hand from INAIL-Rehab

Fig. 4.8 The iCub 2 hand and the INAIL-Rehab hand from IIT are evaluated with the FFP benchmarking index.

4.4.2 Features

The iCub hand (Fig:4.8a) has hall effect position sensors at each of its joints, it has motor position sensing and a tactile skin on its palm and fingertips. The actuation of all these joints is obtained using 9 DC motors (resulting in 9 DOAs) 7 of which are embedded in the forearm and 2 in the hand. Therefore, certain DOFs are obtained by coupling different joints (either tightly or elastically) so that they are moved by a single motor. The iCub hand has a total of 20 DOF[106].

It has minor issues with the joint position sensing as it tends to be non-linear and is not a fully observable system. It scored a 55% on the features part of the FFP evaluation.

4.4.3 Performance

The performance analysis of the iCub was done on all three sub-categories. It performed well when it came to almost all types of grasps (as shown in Fig.4.9) and gestures (as shown in Fig.4.10). It was, however, not the ideal hand for manipulation and non-prehensile tasks. One of the major issues is the thumb being too long to manipulate the objects in-hand effectively. It scored an average 61.5% in its performance evaluation.

A sample comparison is with the prosthetic hand from the INAIL-Rehab lab (Fig.4.8b) in the Italian Institute of Technology. The hand is defined as a prosthetic

Fig. 4.9 FFP Evaluation grasps. Some of the sample grasps that were performed as part of the FFP evaluation

hand aimed to be easily used, strong, easy and cheap but with a capacity to reach a high level of grasp like a human hand. An additional line of research is dedicated

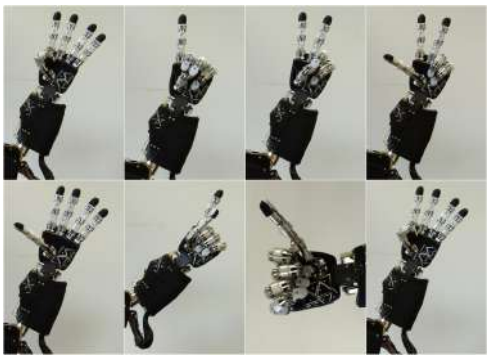

Fig. 4.10 FFP Evaluation gestures. Some of the sample gestures that were performed as part of the FFP evaluation

to the development of advanced EMG (Electromyography) devices as an additional input and well-integrated techniques to better control the prostheses.

An added advantage this hand has on the iCub hand is having a human in the loop. This allows for complicated grasps to be performed with relative ease as the compounded degrees of freedom capable by a human is impossible to match for the iCub. But this is exactly the comparison that needs to be done to show the influence of different parameters when designing a hand. A robotic research hand differs from a hand built for a commercial robot which yet again differs from a prosthetic hand.

And the FFP evaluation gives an idea on where the design motives lie in the form of a graph which gives a brief overview on all these distinct and disconnected domain characteristics.

This is achieved in the above comparison, as it can be observed that importance went more into the look of the hand (anthropomorphism) than any other single domain. A hand that is actuated with a single motor cannot be expected to perform complicated manipulation tasks, and the lack of sensors on the hand can also be compensated to a great extent by putting a human in the loop, deeming a fully observable system unnecessary to a great extent.

Readjusting the weights of the iCub hand against the need of a domestic robot using the subjective evaluation as explored in the previous section (refer to Fig.4.6), it is possible to obtain a score which gives an idea of how well it would perform when used on a domestic robot. The iCub scored a 19 for form, a 16.5 for features out of a maximum 30 and 29.5 for performance against a maximum 50. Adding it up, the iCub scored a 65% in its subjective weighted evaluation as a hand used in a domestic robot.

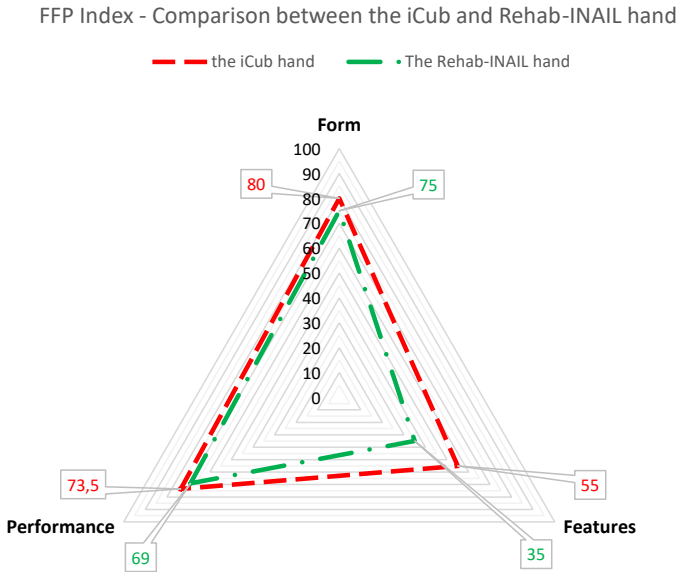

Fig. 4.11 FFP Evaluation and comparison between the prosthetic hand from the INAIL-Rehab group from the Italian Institue of Technology against the iCub hand

4.5 Final Design Guidelines

Drawing from the previous sections, it is possible to list desirable guidelines for the development and design of hands. However, design decisions are almost always limited by the cost, resources and functionalities specific to the hand being developed. For the two platforms, the iCub and the R1, that are relevant to this research, there arises a common set of higher level user needs and technical requirements. This is refined from the primary challenges, objectives and now the evaluation examination of the iCub hand. It is discussed in more detail in the following paragraph.

4.5.1 Technical Requirements

The updated list of technical requirements comes from combining the ones set in the previous chapter and refining it using the things learnt from the previous sections to make a more clearly defined set of technical requirements desirable in the robotic hands being developed. These can be tweaked and changed to suit the individual requirements of the two platforms being investigated.

- The robotic hand should have a mechanism to sense forces and make the fingers relatively compliant (active or passive)
- if the hand is tendon driven, it should preferable have some of tendon tension monitoring system
- the robotic hand should have linearly variable position sensing at all joints
- the hand should have a tactile sensing skin, preferably on all its grasping surfaces
- the hand should have a minimum of two phalanges on all its fingers/digits
- an articulated thumb is generally preferred
- the hand can be underactuated as long as it is fully observable
- the thumb should have at least two distinct degrees of actuation and degrees of freedom
- the ratio of the weight of the hand to its payload should be at least or less than 1.5

Keeping these guidelines in mind, the development of new hands and its associated assemblies are addressed in the next chapter. A brief introduction to the R1 humanoid is given, followed by a discussion on the development of its wrist, on which the hand will be mounted.

Chapter 5

The R1 Wrist

The R1 robot was a new project to make iCub technology accessible in a more cost-efficient, commercial platform. The high level goal of this project was to demonstrate the feasibility of an affordable humanoid platform with good grasping and manipulation capabilities. The design requirements were derived from a list of higher level user needs.

In this chapter, the R1 wrist platform, on which the hand will be mounted, is discussed. An overview of the motivations behind the design of the wrist is first given, followed by the conceptual design, where the design decision that went into selecting a parallel mechanism for the wrist is discussed and the corresponding theory is presented. Finally, the design is discussed in detail and each aspect of the design is evaluated.

5.1 Overview

In humanoid robotics, the internal volume in forearms is often exploited to house the actuators needed to operate the robot end-effector. This approach was adopted in robots such as iCub [95], Robonaut [40] and DLR's HASY [54].

There are examples of the conservative approach of choosing not to integrate any DOF in the robot wrist; this option is generally preferred by those developing entertainment robots mostly for human-robot interaction (HRI) such as Nao [52] or Pepper[110].

On the other hand, most robots' arms are comprised of 2DOF wrists. For example, the ball-screw design developed by Kim et al. for the Roboray wrist [68], the belt design developed by Albers et al. [6] for the ARMAR IV humanoid , and the Harmonic

Fig. 5.1 The completed and mounted forearm-wrist of the R1 humanoid robot

Drive based design with linkage transmission developed for the HRP4 humanoid robot [63]. Three DOF wrists are less common [62] [94] but they do exist with the rotation, flexion/extension and abduction/adduction arrangement.

The application of parallel mechanisms in wrists are few and generally constrained by limitations of space, cost or complexity in control. Some prosthetic wrists [128] make use of such mechanisms to mimic the human range of motion in the wrist. However, they have distinct drawbacks in the fact that they have limited range of motion, sub-optimal workspace and pronounced singularity problems. Another interesting approach is the design developed by Lemburg et al. for DFKI's AILA humanoid robot [75]. A final example worth citing is the OmniWristIII design by Rosheim [102].

The R1 humanoid robot (shown in Fig.5.1) was designed and constructed with the purpose of bringing humanoid robots capable of effective manipulation affordable in the commercial market. The robot has an expected manufacturing cost of €12,000 if produced in large quantities (for an estimated minimum of 1000 units). For this project a compact, dexterous wrist design that could be constructed with limited cost while providing key manipulation capabilities was envisioned. The system that was developed is described in detail hereafter.

5.2 Conceptual Design

The main goal of the conceptual design phase was to make a detailed list of requirements and formulate a solution to this technical problem.

5.2.1 Requirements

The primary design approach of the R1 wrist was to keep it simplistic and cost-efficient. Other requirements were derived from the list of high-level user needs for R1. The user needs are discussed more in detail below:

- **the wrist has to be affordable**: the R1 robot is set at €12,000 and the two wrists should cost around €1200 each
- **the wrist has to be extensible**: the R1 robot should pick objects off of the floor. Given the robot's other requirements' limitations, the best possibility would be to extend the forearm
- **the wrist has to be compact**: a design team first conceptualized the look of the robot and proposed a shape for the entire robot. The wrist had to fit inside this volume (diameter: 80 mm, length: 200 mm)
- **the wrist should have an acceptable dexterity**: the robot should be able to manipulate objects effectively. For this purpose, the wrist flexion/extension and abduction/adduction motions was set at ± 40 [deg]
- **the wrist should have an acceptable payload**: considering that the R1 should be able to pick a 0.5 l water bottle off a table, and that the estimated hand weight is 0.5 [kg], the wrist shall have a payload of at least 1 [kg]
- **the wrist should have an acceptable operational speed**: the speed of wrist movements should be comparable to a humans wrist during normal manipulation tasks (approximately 2 s to move sideways)
- **the wrist should be light**: the target weight for R1 is 50 [kg]. The maximum allowed weight for each wrist is 1 [kg]

Furthermore, a list of secondary requirements was also defined:

- **the wrist should be stiff and with minimal backlash**: a stiff structure increases the accuracy of hand positioning
- **the wrist should have a platform large enough to easily mount and dismount the hand**

To achieve these goals, a novel joint design is to be developed with special attention to cost and space constraints.

5.2.2 Kinematic Structure Selection

The wrist extension was a major user requirement that limited the use of actuation methods available. Extension is considered to be achieved in two different ways: The first involves using a linear joint in series with other rotational joints, the second solution is to use a parallel kinematic structure. Given the space and cost constraints, it was decided to explore a design based on a parallel kinematic structure with affordable linear actuators.

Before selecting the kinematic structure, a detailed comparison between series and parallel structures was performed. In particular, the following advantages in parallel actuation were identified:

- it doesn't suffer from cumulative position errors
- it offers higher rigidity and hence higher payloads
- its centre of mass is closer to the base and adds stability as the actuators are placed closer to the base
- its synergistic behavior results in the total effort being distributed among all the actuators of the system. This allows for using smaller actuators with respect to serial arrangements

The parallel kinematic mechanism also have their drawbacks as defined by [85], [20], [91], some of those drawbacks include:

- it is more complex to model and design
- it is kinematically challenging since they tend to have multiple solutions
- it can have a higher instance of singularities with respect to serial actuation
- the range of motion of parallel mechanisms can be limited

A parallel kinematic manipulator is usually constituted by a base, a platform and a set of kinematic chains called "leg" connecting the base to the platform. Each leg can comprise one or more actuators in series, with linkages connected through passive joints. The position and orientation of the platform is usually a non linear function of the position of actuated joints. In literature many different parallel manipulator designs have been proposed. As an example, the Steward platform [114] is a 6 DoF

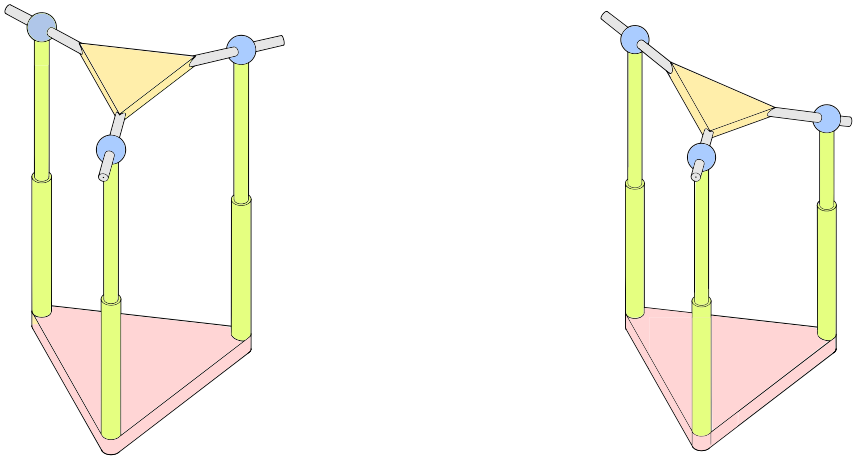

Fig. 5.2 The conceptual design of the parallel structure in two different configurations. The colors identify the core components of the system, red: the base, green: linear actuators, blue: passive spherical joints, gray: passive prismatic joints and yellow: the platform. When the platform is tilted, its centre also moves in the horizontal plane.

system that exploits 6 linear actuators to control independently the position and orientation of the platform. For the R1 wrist the focus was on a simpler design with only 3 DoF [98]. As shown in Fig. 5.2, the base of this parallel manipulator is an equilateral triangle. Three linear actuators were fixed perpendicular to the base, one on each vertex of the triangle. The actuators are connected to the platform through a passive spherical joint in series with a passive prismatic joint. The main advantages of this system is its simple mechanical design, the absence of singularities within its workspace and the possibility of controlling the platform height (the wrist extension for the R1) and the platform inclination (wrist flexion/extension and abduction/adduction) independently.

In particular, if all the three linear actuators move together, the platform moves vertically without changing its orientation. And if the actuators move separately the platform tilts back and forth or sideways.

5.2.3 Load Path Analysis

During the conceptual design the loads paths among the whole system had to be considered. Having selected a parallel structure with the actuators fixed to the base, all the forces acting on the platform have to be supported by the linear actuators itself. As depicted in Fig. 5.3, the major drawback is that the rod of the linear actuator has

to bear not only axial forces but also radial forces[1]. Furthermore, the loads acting on the actuator rod are configuration dependent. In particular, if the platform is horizontal, a flexion moment generates only axial loads on the rod.

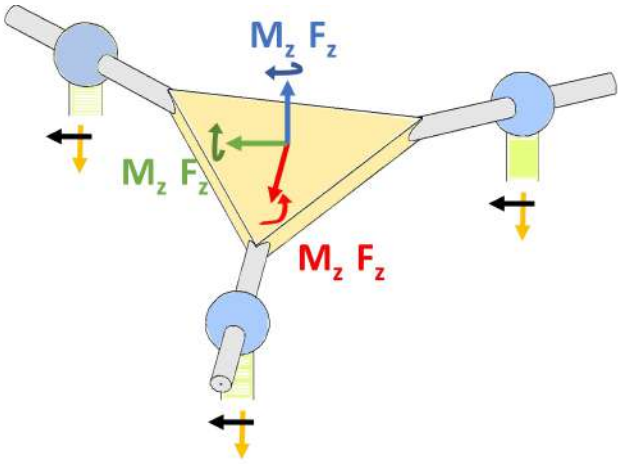

Fig. 5.3 Load analysis: the spherical joints don't produce any reaction moment on the actuator rods. Due to this decoupling mechanism, the only forces acting on the rods are either pure axial loads (yellow arrow) or radial loads (black arrow).

Conversely, when the platform is tilted the same moments also generate a radial load. The magnitude of the axial and radial loads for a flexion moment is computed by solving a moment balance equation. However, the case of the platform loaded by a torsional moment and a radial force is a more complex one. In this case the load is equally distributed among the three rods, and can be computed by solving (variables are as shown in Fig. 5.4) the following system of equations:

$$\sum_y : -Fcos(\vartheta) - R_1 + \frac{1}{2}R_2 + \frac{1}{2}R_3 = 0 \tag{5.1}$$

$$\sum_x : -Fsin(\vartheta) - \frac{\sqrt{3}}{2}R_2 + \frac{\sqrt{3}}{2}R_3 = 0 \tag{5.2}$$

$$\sum_M : M_z - Fcos(\vartheta)l + \frac{3}{2}l\left(\frac{1}{2}R_2 + \frac{1}{2}R_3\right) = 0 \tag{5.3}$$

Another attribute in this design was that the linear actuator can only bear axial loads. To solve this problem custom linear guides supporting the rod of each linear actuator was constructed. Each linear guide has been designed considering the target payload of the wrist and a security coefficient.

[1]In parallel manipulators like the Steward one, each linear actuator is decoupled from the base and the platform through a spherical joint. In such cases the only forces acting on the linear actuator rod is a pure axial force.

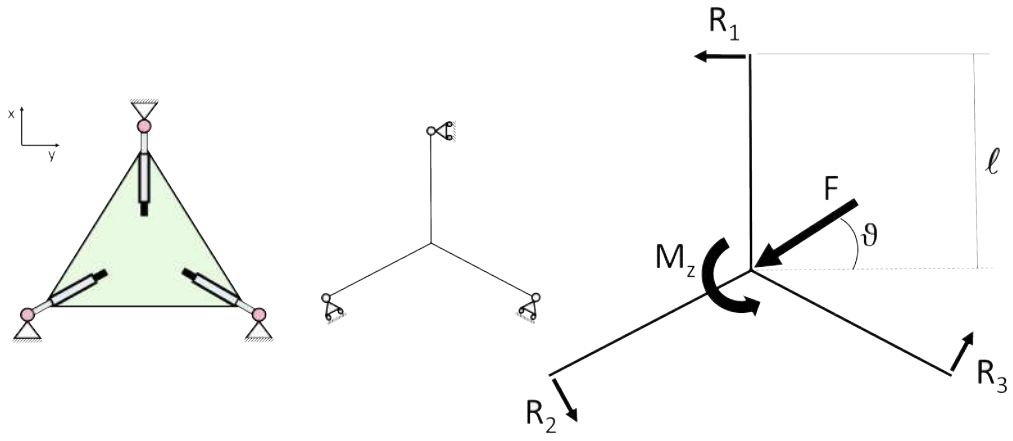

Fig. 5.4 The left image represents a 2D model of the platform. The middle image represents the equivalent model, while the image on the right represents its free body diagram. M_z is the torsional moment, while F is a generic radial load. The three forces R_i represent the radial load acting on the actuator rods.

5.3 Embodiment Design

A top down approach was adopted to design the system. A skeleton outlining the major moving components were designed to fit inside the surfaces provided by the designer. The starting point was the volume as defined by the designers. All other subsystems were designed keeping this in mind and the kinematics were completely controlled by the skeleton that was developed for this.

5.3.1 Hardware

The three linear actuators, as discussed in the previous section, were spaced equally around the circumference of a circle with rod end bearings (employing the heim or rose joint) attached to the end of each actuator. A rigid plate (shown in yellow in Fig.5.2) with three shafts extending with an angle of 120between each other on the plane of the platform connects the three rod end bearings and provides a mounting platform for the hand.

As the linear actuators extend and retract together, the platform moves up and down providing 130mm of extension of the forearm length. As the linear actuators extend and retract with respect to each other, the rods rotate and slide inside the rod end bearings, allowing the platform to angle. This provides the wrist with ±30of flexion/extension and abduction/adduction. A support structure was constructed to

house and orient the components within the covers.

Since one of the driving design decisions was that of reducing costs, minimizing the number of custom parts was a priority, along with an initial design encompassing commercial off the shelf (COTS) linear guides and actuators. However, using COTS components suffered from some drawbacks such as lateral vibrations and structural bending. The actuators and initial frame design were then built with a central frame that supports each of the linear actuators. Each of these linear actuating assemblies comprised a Canon DG16L-24-242 brushed DC motor with an integrated planetary gear transmission. The motors where then coupled to a precision leadscrew through a timing belt transmission. For the lead screws, COTS miniature leadscrews from MISUMI were used. These miniature leadscrews were stainless steel screw shafts with right hand dry screw nuts and are corrosion resistant and quiet.

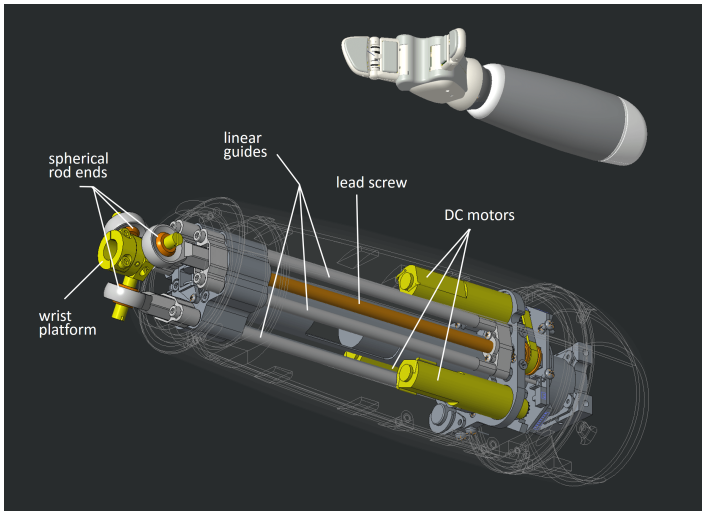

Fig. 5.5 Wrist design. The wrist platform is assembled as shown with the covers assembled on top of it. In picture is the assembled version with the hand mounted on top.

These leadscrews were then used in conjunction with guiding rods from IGUS, which are precision anodized aluminium shafts. The nuts are connected rigidly to spherical bearings made from the IGUS KBRM line of rod ends. A linear shaft slides on these rod ends; one end of these shafts is attached to the wrist platform and the other end is free to slide in and out of the spherical bearing. This saved space occupied by the mechanism in general, since this led the actuation mechanism to be moved close together. This way, independent movement is achieved at each of the three joints depending on which actuator is being run. The entire assembly is as

shown in the CAD view in Fig.5.5.

The wrist undergoes three stages of transmission, the first through the planetary gears of the DC motors (242:1), the next through the belt transmission at the base of the forearm (1.43:1) and finally through the lead-screw mechanism (349:1) employed in the forearm. The wrist heave has a nominal force of 126 [N] after reduction.

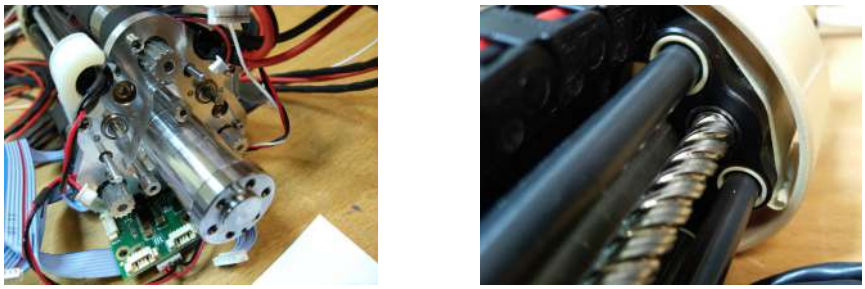

(a) Bottom view (b) Lead screw

Fig. 5.6 Transmission design. On the left side, the bottom of the wrist base can be seen before the transmission belt is mounted, it can be seen how the motor shafts and the guiding rods are assembled onto the bottom plate. On the right, the lead screw with its guide rods can be seen entering the top part of the wrist through IGUS bushings.

The robot had to be completely enclosed, and not to have any possible pinch point for safety reasons. All robot parts, thus also the forearm, were covered with plastic shells. The covers were attached to the wrist platform and slide on plastic IGUS bushings. The rigid cover is attached to the wrist platform by means of three suspension springs. The wrist also has a spherical cup shaped cover to accommodate as well as facilitate the wrist motion.

5.3.2 Electronics

There are two main electronic boards housed within the forearm structure, namely:

MC4-Plus : This board is a small motor controller [95] capable of driving up to four DC motor, using 100 Mbps Ethernet communication for commands and control data exchange. It is powered by an ARM®Cortex®-M4 microcontroller and a 12V supply voltage. It houses a STM32F407 chipset and other components including a 9 axis IMU and a CAN BUS with choke filter. It is connected to the motors, all the position sensors in series, and to the MTB boards that interfaces all the tactile sensing points of the skin.

CER-WPS : This is the position sensor board for the wrist, it comprises a magnetic encoder based on the AS5040 absolute rotary position encoder which is used to acquire the position information from the magnet placed at the rotor of the DC motors. This board reads the orientation of the magnetic field generated by the magnet, digitalizes it and sends it over an SPI protocol to the MC4Plus control board to close the position control loop.

It also consists of optical sensors which detect the proximity of the linear guides. They act as calibration sensors for the linear guides.

5.4 Evaluation

The forearm was built and assembled on to the robot. It was then tested extensively against each of the design requirements prescribed in Section II. The weight of the

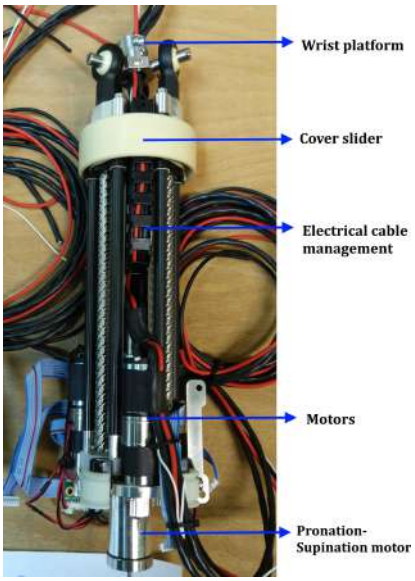

Fig. 5.7 Completed design of the R1 wrist. The completely mounted wrist is as shown. On the top part is the wrist platform on which the hand will be mounted, this is supported by the three IGUS rod ends that have the telescoping shafts mounted on them. Below the platform is the IGUS bushing that allows sliding of the forearm cover on the entire structure as the wrist moves up and down. The electronic cables is grouped together and moves along with the platform by means of a cable carrier. All the actuators and transmission are finally attached at the bottom. The motor for pronation and supination is mounted at the centre of the base platform as shown.

forearm was within the design requirements and weighed an estimated 1.25 [kg] as

extracted from the CAD parameters. The other tests are described more in detail in the follow sections.

Table 5.1 Cost breakdown.

Parts	**Cost(€)**
Actuators	160.00
Commercials	240.00
Custom molded parts	180.00
Custom machined parts	440.00
Electronics	260.00
Others	60.00
Assembly and wiring	80.00
Total	1,420.00

5.4.1 Cost Evaluation

The R1 is intended to be a commercial robot. A scaling up of all incurred costs was hence deemed necessary. All COTS components costs were then scaled up for a minimum of 1000 units. The forearm base structures are mostly made of metal components. The central support structure and the base were from custom machined parts. The covers were made predominantly out of plastic parts, except for the textile skin wrap.

The forearm manufacturing costs were also scaled up to a minimum of 1000 units and is listed as shown in Tab.5.1. These are for all components that are to be purchased or manufactured as was generated by the bill of materials. The corresponding costs were much more in accordance with the design cost estimate that was initially made. The estimation of all the machined and molded parts were from Proto Labs[2].

5.4.2 Payload

The forearm of the R1 robot weighs about 1.25 [kg]. The total expected payload of the forearm in the retracted position was about 1.6 [kg], which exceeded the initial requirement. In the extended position it was able to carry a full 0.5 l bottle of water

[2]https://www.protolabs.co.uk/

as shown in Fig.5.8. The hand weighs 400 grams which accounts for a cumulative payload for 1.6 [kg] of attainable payload by the wrist.

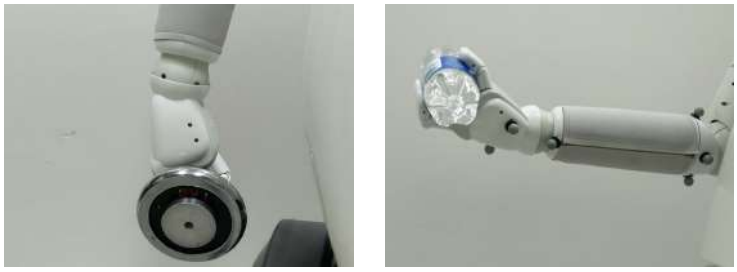

(a) (b)

Fig. 5.8 Payload. The forearm was put through a number of tests with varying payloads held in the hand (a)1.2 [kg] payload pointing downwards to the ground, it was tested along with the heave of the forearm and in (b) the forearm was tested by carrying a 0.5 l bottle and performed both heave and tilt actions in the horizontal position.

5.4.3 Range of Motion

The forearm structure, due its complex covers, had to limit its wrist roll and pitch angles to ±30 degrees. Forward bending of your wrist is called flexion. Normal wrist flexion is approximately 70 to 90 degrees. Extension: backward bending of your wrist, is necessary for tasks like pushing a door close. Normal wrist extension is approximately 65 to 85 degrees.

This difference in range was employed in the R1 wrist by introducing a pre-tilt of 15 degrees of the R1 hand to give it a natural range of motion, comparable to that of the human wrist during everyday grasp tasks. The forearm (as shown in Fig.5.9) can extend to a maximum of 130 mm from its initial rest pose. The R1 was also tested successfully for its operable reach in various scenarios including reaching for bottles placed on tables and from the ground.

5.4.4 Performance Analysis

The performance analysis was done by running the forearm through a number of tests using motion capture, namely VICON technologies. The robot was tested mainly for accuracy and repeatability in position and dexterity in movement. Four markers were placed at the bottom of the forearm (wrist markers) for reference and three markers

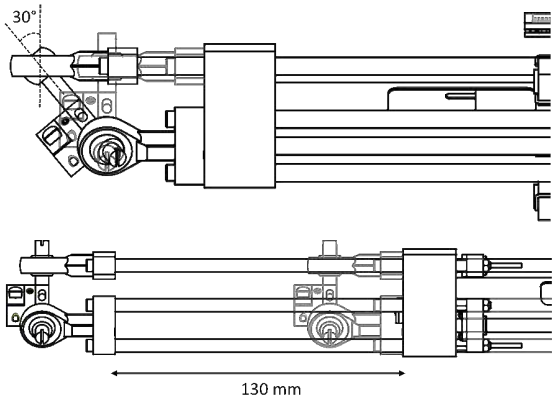

Fig. 5.9 Range of motion. The wrist platform exhibits a pitch-roll deflection of 30 degrees and an extension of 130 mm

were placed on known positions on the hand (hand markers) as shown in Fig.5.10. A few other markers (base markers) were also placed as references to retrieve the position and orientation of the robot root frame. This way, the model is firmly placed with all required references and a snapshot of all markers in the correct poses were used as an initial reference for the tests performed.

The experimental setup can be described as follows. Two sets of wrist data were collected by the hand markers as shown in Fig.5.10. These markers were placed in known positions with a known transform to the wrist platform (as defined by the wrist markers). This way a set of wrist platform poses was obtained by sampling a desired platform trajectory expressed in Cartesian space. For each of the poses, equivalent

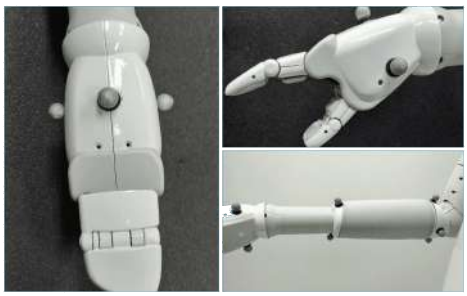

Fig. 5.10 Marker positions. Three markers were placed on the hand, four near the elbow as a reference for the base. All other markers were supplementary references.

linear actuator strokes have been computed exploiting the mapping described by the inverse geometric model. The joint space trajectories which were acquired by software were used to drive the linear actuators thanks to a simple PID control loop.

Repeatability

The repeatability of the forearm was determined by comparing the measured position of the hand markers for four different poses for a given cycle. For this analysis, all other joints were locked in a defined position and activated only the wrist tripod joints and actuated them in turns to match the predefined points in space. This cycle was then repeated for 15 iterations. Their positions were recorded, analyzed and were super-imposed on top of each other.

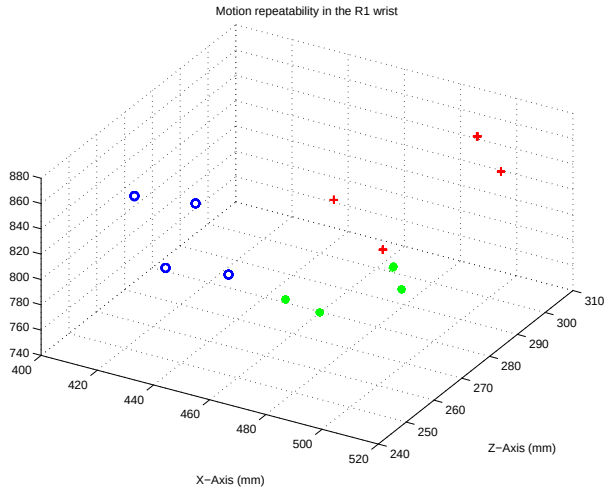

Fig. 5.11 Repeatability. The forearm performed as expected. Each marker went through four discrete poses. The points overlapped each other in most cases.

As can be seen in Fig.5.11, the R1 was able to achieve very good repetitions of its points in space. The points had an accuracy error of less than 3mm for all the points every-time.

The position average of each discrete point from the hand markers were calculated. An array of these averaged coordinates of the four discrete point positions were then calculated. This gave a single set of points for all the markers. The maximum error across the four points for any given co-ordinate was calculated to be less than 3 mm.

Radial Force Loading

In the preliminary stages of the design, the wrist-forearm assembly was subject to cantilever loading to check its radial deviation and the efficacy of its support rods as shown in Fig.5.12. Weights of increasing magnitude were hung from the platform and the corresponding deflection was measured to check the cantilever effect and the robustness of the system. These deflections were later minimized further by adding

Fig. 5.12 Radial force loading. The wrist-forearm assembly at its first stages of design was tested for cantilever bending when subject to radial loads.

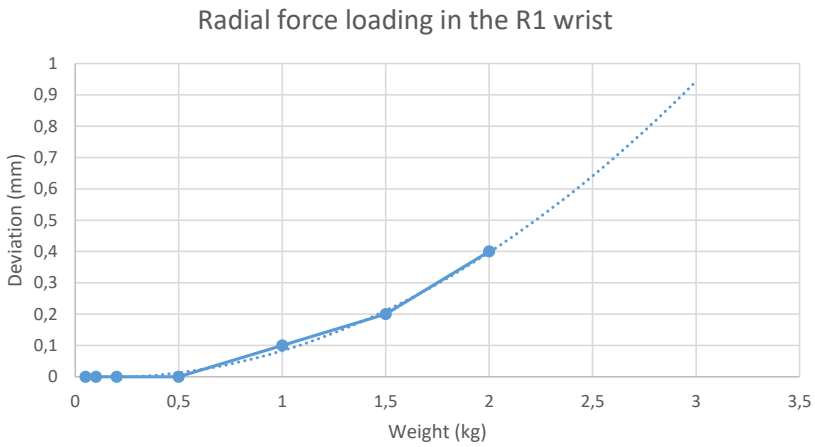

Fig. 5.13 Radial loading was done by attaching weights to the platform of increasing magnitude. The deflection was recorded as shown and a polynomial line of the second degree was fit to show the behavior.

stiffer guide rods and providing linear bushings at both the base and platform of the wrist-forearm assembly.

Accuracy

The accuracy of the forearm was evaluated by comparing the measured position of the markers with the desired position in Cartesian space. The same hand markers' position from the previous tests were used. Fig.5.14 shows the trajectory followed by the central marker in the hand. The recorded trajectory was offset from the desired by less than 5mm at any given instant. This shows that the wrist was developed is fairly accurate for the basic user tasks the robot is expected to perform.

This chapter discussed the wrist-forearm assembly that was developed for the R1

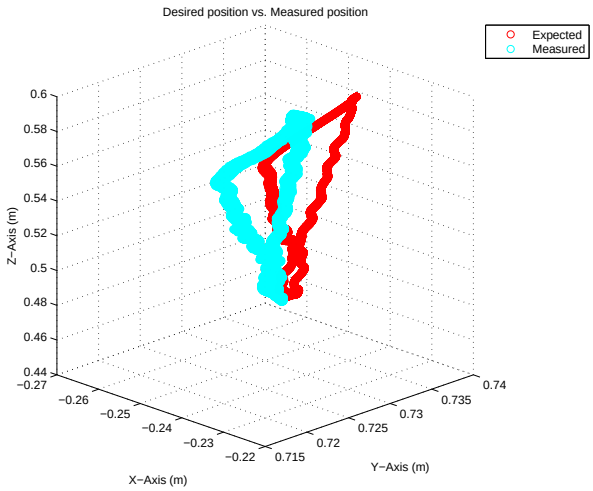

Fig. 5.14 Wrist accuracy. The recorded trajectory tracking in Cartesian space shows an overall error of less than 5mm from the computed trajectory.

humanoid robot. The following chapter starts describing the design of the R1 hand, it is mounted on the wrist platform and is a standalone system. The next chapter starts with the design decisions that was made into constructing the hand and the design of a new series elastic module that aids in force sensing and goes on to analyse each of its features in detail.

Chapter 6

The R1 Hand

The previous chapter defined the R1 wrist on which the hand will be mounted. The hand design will be discussed in more detail in this chapter. In the first part, the conceptual design of the hand will be explained along with the kinematics. The theory behind the force sensing elements, i.e., the series elastic module will also be briefly discussed. The second part will explain the embodiment design of each of these components and explain the overall design of the hand in a lot more detail. The final section will explain the evaluation done on the hand to test its various features and also its grasping and payload capabilities.

6.0.1 Design philosophy

The design of the R1 hand is outlined by a similar design philosophy as set in the previous chapters. The high-level user needs are extracted from this, which can be summarized as follows:

- **the hand is affordable**, costing around 10% of the total unit cost of a robot
- **the hand should be able to pick a water bottle from a table**, it has a minimum payload of 700 [g]
- **the hand is compliant and safe enough**, to minimize damage to itself and the environment
- **the hand should be sufficiently dexterous**, it is able to open doors and toggle switches
- **the hand is able to perform everyday tasks**

- **the hand is robust**

For the last item, a set of 12 grasps as identified by Bullock et al. [21] was considered, where the most common grasps employed in everyday tasks were listed. This is considered as the standard grasp requirement for the R1 robot, while all other grasps were treated as supplementary.

6.1 Conceptual Design

The R1 hand was designed to be semi-anthropomorphic but without individual fingers to decrease user expectation. The user needs were then stated to the industrial design team who developed the aesthetics of the robot. It was decided the hand will have two main digits which called the "paddle" and "thumb". It was decided that the R1 hand would be underactuated and have four DOF and two DOA. The return of the phalanges to the open position was achieved with torsional springs located at the hand joints. Measuring the grasping force was an important factor. At the same time the hand had to be compliant to impact loads. Both of these requirements were achieved by incorporating series elasticity into the system.

The hand hardware had to be completely self-contained, comprising all needed control boards and motors. The design had to be predominantly in plastic to cut costs. To this end, based off of work[115] spectra tendons were employed for actuation. An easy to attach interface to the wrist was also required for ease of troubleshooting and maintenance. One of the most interesting features of the iCub is the tactile sensing skin technology[25]; it was decided to use this on all the individual phalanges of the hand.

Table 6.1 DH parameters of the R1 hand

Phalange	**i**	A_i **(mm)**	d_i **(mm)**	α_i **(deg)**	θ_i **(deg)**
Paddle	i = 0	42	0	0	0 - 70
	i = 1	44	0	0	0 - 70
Thumb	i = 0	42	0	0	0 - 60
	i = 1	34	0	0	0 - 70

6.1.1 Kinematics

The kinematics was initially approximated from the shape suggested by the design team and fine tuned by building a mock-up hand and grasping objects with this hand to see what had to be changed. The range of motion, link lengths and joint positions were then decided from this analysis. The corresponding Denavit-Hartenberg (DH) parameters are as shown in Table 6.1. The hand was assembled with a tilt of 15° with respect to the perpendicular of the principal axis of the wrist[121]. This was done

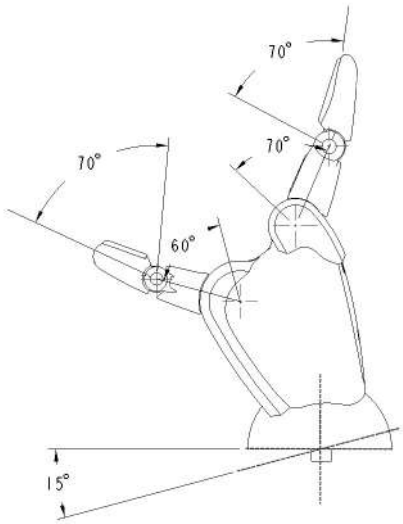

Fig. 6.1 Hand Kinematics. The figure shows the four DOF of the proposed hand and their ranges of motion (ROM). The two digits "thumb" and "paddle" can be identified with their corresponding labels.

to provide an extra 15° flexion to the hand, since an extension of 30° was deemed unnecessary for our grasp requirements. This effectively provided the hand with 45° of flexion and 15° of extension. This is lower than the human wrist, but imitates the range of motion with a ratio similar to that employed in human hands for most tasks (shown in Fig.6.1).

6.1.2 Series Elastic Elements

Placing a robot in a human-centric environment poses many safety related issues since hazardous threats arise from unintended contact between these robots and humans [119]. These occur more frequently during manipulation tasks in unstructured settings. For safer human-robot interaction or even robot-environment interaction, there arises

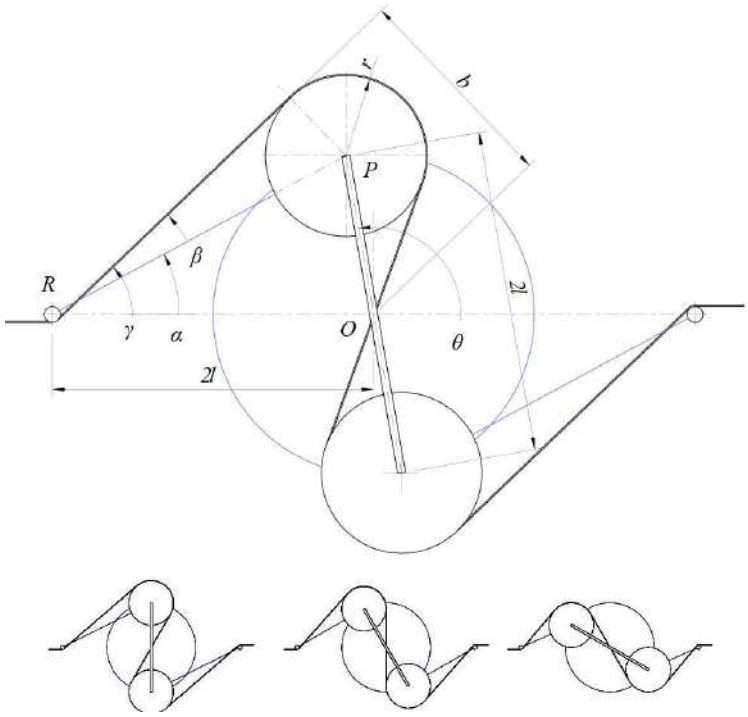

Fig. 6.2 SEE module geometry. The figure shows the simplified geometry of the series elastic element.

a need for compliance. A series elastic elements (SEE) module for the R1 hand was designed with this in mind.

The SEE module is used to allow force control of the hand during grasping tasks. It also acts to store the energy during impact loads and prevents the robot's hand from damage. The degree of compliance shall both enable safe interaction and grasping of fragile objects.

The concept behind the SEE module as shown in Fig.6.2, consists of a lever arm with two pulleys of radius r on either ends. The lever arm is mounted with a central torsional spring of a given spring constant (k_{el}); the spring deflection is θ. The tendons of the hand winds around directional bushings, onto the pulleys and is fastened to the distal phalanges of the fingers. The radii of directional bushings is neglected for simplicity. The length of the lever arm is given as $2l$.

The coordinates of the centre of the pulley P and that of the directional bushing R are:

$$P = \begin{bmatrix} l\cos(\theta) \\ l\sin(\theta) \end{bmatrix}; R = \begin{bmatrix} -2l \\ 0 \end{bmatrix}. \tag{6.1}$$

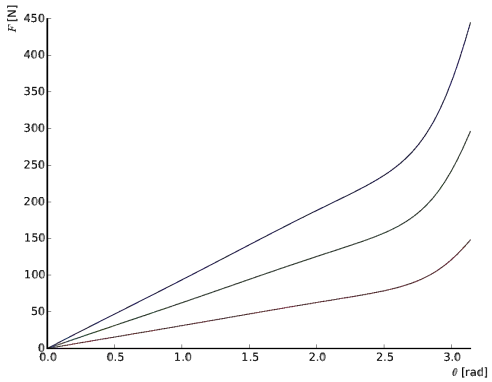

Fig. 6.3 SEE stiffness curves. The figure shows the theoretical force F to angular deflection θ curves for a range of stiffness of the torsional spring. The red curve is for a value k_{el}=0.5[Nm/rad], the green one for k_{el}=1.0[Nm/rad], the blue one for k_{el}=1.5[Nm/rad], where r = 0.006 [m] and l = 0.008 [m].
As can be seen the stiffness characteristic is asymptotic with a steep increase in the final part of the SEE range of motion.

$$L = \begin{bmatrix} l\cos(\theta) + 2l \\ l\sin(\theta) \end{bmatrix} \tag{6.2}$$

where α is given by:

$$\alpha = \operatorname{asin}\left(\frac{l\sin(\theta)}{\sqrt{l^2\sin^2(\theta) + (l\cos(\theta) + 2l)^2}}\right) \tag{6.3}$$

and β is given by:

$$\beta = \operatorname{acos}\left(\frac{r}{l\sqrt{4\cos(\theta) + 5}}\right) \tag{6.4}$$

from which γ can be computed as:

$$\gamma = \operatorname{acos}\left(\frac{r}{l\sqrt{4\cos(\theta) + 5}}\right) + \operatorname{asin}\left(\frac{\sin(\theta)}{\sqrt{4\cos(\theta) + 5}}\right) \tag{6.5}$$

Now b can be computed as :

$$b = 2 * l * sin(\gamma)$$

Solving for b, from Eq 6.5:

$$b = 2l\sin\left(\operatorname{acos}\left(\frac{r}{l\sqrt{4\cos(\theta)+5}}\right)+\operatorname{asin}\left(\frac{\sin(\theta)}{\sqrt{4\cos(\theta)+5}}\right)\right) \tag{6.6}$$

The pulling force F can be given by simplifying:

$$F = (k_{el} * \theta)/b$$

as a pulling force is applied on the tendon, the lever arm begins to deflect and the torque around the centre can be given as :

$$\tau_{el} = k_{el} \cdot \theta = F * 2l\sin\left(\operatorname{acos}\left(\frac{r}{l\sqrt{4\cos(\theta)+5}}\right)+\operatorname{asin}\left(\frac{\sin(\theta)}{\sqrt{4\cos(\theta)+5}}\right)\right) \tag{6.7}$$

and solving for the tendon pulling force "F" using torsional spring force equations, the simplified force equilibrium equation are as shown in Eq.6.8 where k_{el} is the torsional spring constant and F is the tendon pulling force. All the additional parameters are as shown in the Fig.6.2.

$$F = \frac{k_{el}\theta}{2l\sin\left(\operatorname{acos}\left(\frac{r}{l\sqrt{4\cos(\theta)+5}}\right)+\operatorname{asin}\left(\frac{\sin(\theta)}{\sqrt{4\cos(\theta)+5}}\right)\right)} \tag{6.8}$$

From the above equation, the appropriate "k_{el}" value was derived for the torsional spring for a given range of input pulling force as shown in Fig.6.3.

Also shown is the non-linear behavior of the spring. This is advantageous for force sensing since it allows a varying measurement resolution depending on the force magnitude. The lower force range of the spring behaves linearly with higher resolution. In the high force range the measured forces' resolution decreases effectively increasing the range of measurable forces.

In this way it is possible to design a spring suited for a corresponding force. The overall joint deflection of each link is independent of the SEE module design as long as the force required for the deflection remains within the estimated range. In this case a stainless steel torsional spring with a spring co-efficient of 0.925 [Nm/rad] was employed.

6.2 Embodiment Design

6.2.1 Hardware

The design philosophy of the R1 hand has always been to use cost-effective materials and manufacturing processes. The design of the hand is started with the help of the space and shape derived from the surfaces suggested by the design team.

The hand consists of a central part made of machined plastic (Dupont DELRIN) which houses the series elastic module. The proximal phalanges are also machined from the same material and mounted on this central part. The MC2Plus motor control board (discussed in the following sections) and the motors are mounted on sheet metal parts which are fastened to this central part. The distal phalanges are made from rapid-prototyped ABS plastic. The covers are then mounted onto the central part and the phalanges. The only metal parts are the joint shafts since they will have to undergo considerable stresses and will also have to house the magnets for the joint position encoders. They also act as a centring support for the return springs which help in the agonistic actuation of the R1 hand. Textile covers are utilized as an interface

Fig. 6.4 Skin assembly on the R1 hand.

for the skin and to provide grip. The textile-skin assembly is made as a modular setup which is separately assembled. The tactile sensing PCB takes the same shape as the phalanges and is mounted onto a piece of plastic. This is then assembled onto the phalanges as a snap-fit. A survey of all motors that are available in the market for our purposes was carried out. The Canon DG16L-24-0410 was selected for its cost to performance ratio. The hand is mostly self-contained with only the Ethernet and power cables extending into the forearm. An easy to attach interface with four fasteners facilitates access to the hand for troubleshooting and testing.

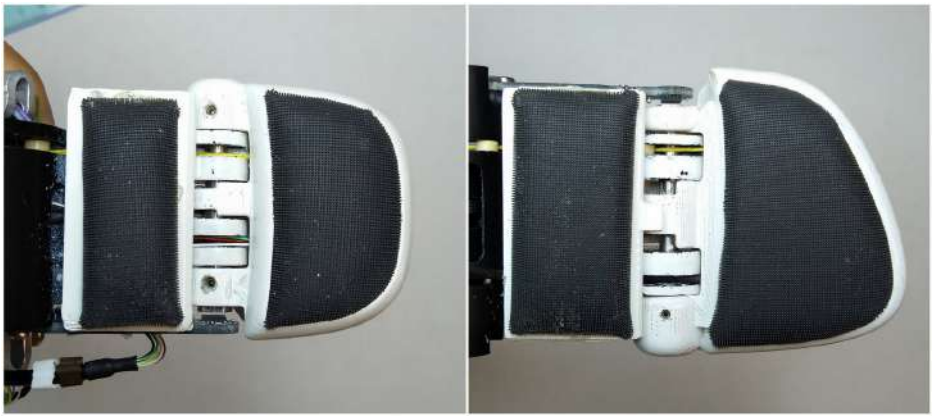

Fig. 6.5 Skin padding. The R1 hand has both its paddle and thumb padded with a deformable 3M gripping material that has micro-fibers for improved friction properties.

6.2.2 Friction Management

A Spectra wire of 110 [kg] load capacity and 0.8 [mm] thickness is wound around the capstan of the actuation motors. The wire then winds around a directional bushing and then through the pulleys of the SEE module before being pivoted on the central part and wound through the phalanges. It is then finally attached to the proximal phalange of both the paddle and the thumb. To help tendon sliding and to prevent cutting of the plastic material due to tendon movements, metal dowel pins are placed at all entry and exit ports of the phalanges. In addition to this, IGUS bushings were placed at calculated intervals to facilitate smooth sliding of the tendons.

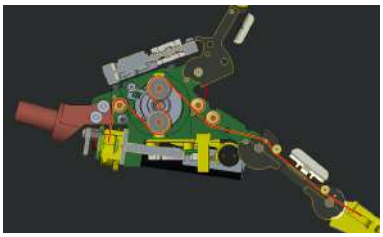

(a) Tendon routing - paddle

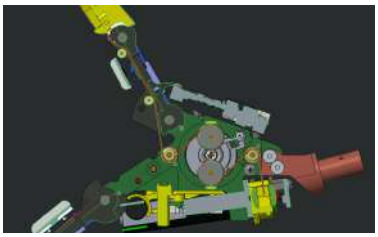

(b) Tendon routing - thumb

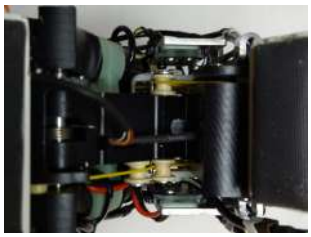

(c) On the hand

Fig. 6.6 Tendon management. The tendon routing through the system (a) on the paddle (b) on the thumb

6.2.3 Coupling and Actuation

Since the hand is underactuated, the motion of the phalanges are predetermined and coupled by control. The paddle and the thumb both have coupled joints. In both cases

the coupling method is the same, where the proximal and distal phalanges are driven by the wires wound around the same motor. A torsional spring is placed on the joint shaft which accumulates energy with flexion and helps facilitate the extension of these joints. In the absence of external forces, the position of the proximal (θ_{pp}) (Eq.(6.9)) and the distal (θ_{dp}) (Eq.(6.10)) joints can be written in relation to the motor position (θ_m) as:

$$\theta_{pp} = \frac{k_{dp}}{k_{dp} + k_{pp}} \frac{r_m}{l_{pp}} \theta_m, \tag{6.9}$$

$$\theta_{dp} = \frac{k_{pp}}{k_{dp} + k_{pp}} \frac{r_m}{l_{dp}} \theta_m \tag{6.10}$$

where k_{pp} and k_{dp} are the spring co-efficients of the return springs of the proximal and the distal phalanges respectively, and r_m is the radius of the motor capstan, l_{pp} and l_{dp} are the distances of the tendon from the centre of their respective joint shafts of the proximal and distal joints. This way, the spring co-efficient is chosen to control the wrap sequence and is used to provide an uniform wrap motion of the phalanges for the hand.

6.2.4 Design of the Series Elastic Elements

The series elastic module comprises a torsional spring (as discussed in Section 6.1.2) that is mounted on the central part (Fig.6.7) of the hand. A shaft acts as the centering element for this spring. A lever arm with two pulleys on either end is then mounted on to the central shaft: this routes the actuation tendon. This way, every grasp force has a corresponding angle deviation at the rotation axis of the SEE module which is measured by joint position sensors. This k value was carefully chosen to allow complete deviation for the desired range of grasp force. Hence, a unique deflection can be mapped for a corresponding pulling force.

The lever arm is supported by the hollow shaft that is double supported by deep groove ball bearings as shown in Fig.6.7a and is mirrored on the other side. The lever arms are then axially locked by a single screw which can be fastened on either side of the assembly. The spring is pre-loaded by 5° to accommodate a favorable range of motion for the given range of input force.

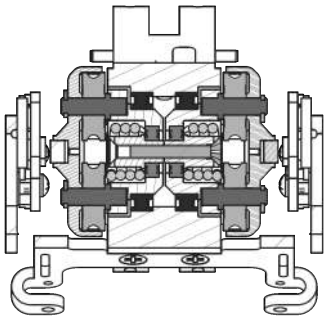

(a) Cross section

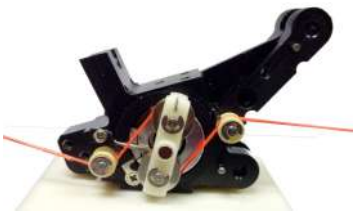

(b) Stand-alone

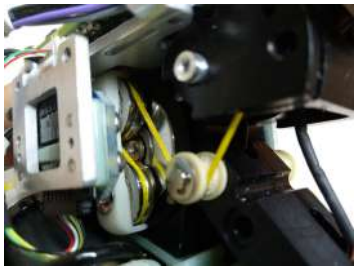

(c) Assembled on the hand

Fig. 6.7 SEE module construction. Cross section (a) and prototype (b) stand-alone construction of the SEE module and (c) the module mounted on the hand.

6.2.5 Electronics

The hand is a self-contained system; all the sensors and control boards were contained within the structure. Since the hand is underactuated, care was taken to provide the hand with enough sensors to control it reliably. The hand comprises a central MC2Plus motor control board with an Ethernet interface. The board reads the position sensors of the fingers, the motor encoders, the series elastic elements and drives the two motors. It also has a CAN interface to connect the tactile sensors board (MTB board) to the MC2Plus.

The tactile sensors are distributed in the proximal and distal phalanges of both digits. The hand has four absolute position encoders based on magnetic hall effect sensors connected in daisy chain. The same sensor has been used for reading the deflection of the spring in the SEE module. The encoder of the motor has been designed in order to fit it on the central part of the hand and to read the incremental position of the shaft after the gearbox.

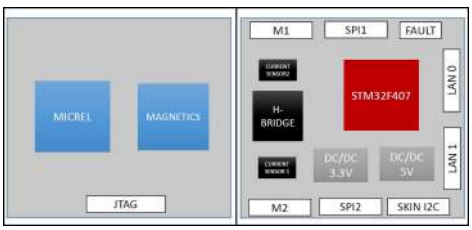

(a) Architecture

(b) Actual board

Fig. 6.8 The MC2Plus electronic board

The MC2Plus Board

The MC2Plus board is mounted on the thumb side of the hand. It is powered by an ARM®Cortex®-M4 microcontroller, Ethernet and power driver for 2 DC motors, two SPI BUS for reading 4 absolute encoder sensors, 2 analog channels and a 12V supply voltage. It houses a STM32F407 chipset and multiple other components including a BNO055 9 axis IMU and a CAN BUS. It is connected to the motors, all the position sensors in series, and to the MTB board that interfaces all the tactile sensing points of the skin. It is as shown in Fig.6.8. Current measurement for each motor is based on Hall Effect sensor (ACS711).

The MTB board was placed in the middle of the hand, on top of the motors for ease of access for wiring.

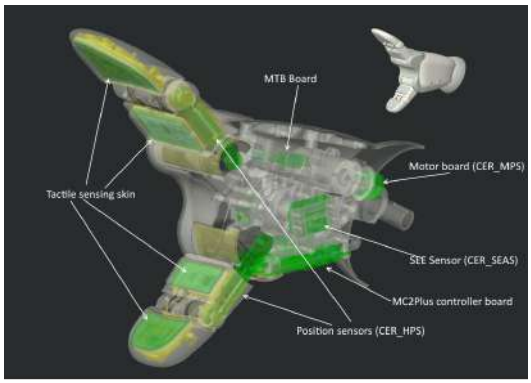

Fig. 6.9 Electronic boards layout. All electronic boards are in green. The MC2Plus board was placed at the bottom, and directly above the CER_SEAS boards that read the SEE module deflection. On the phalanges' side, the CER_HPS was placed as a single board for joint measurement, one each for paddle and thumb. The tactile sensing boards were placed in front on the phalanges.

Position Sensors

Four (as shown in Fig.6.9) standard boards are designed using a 10 bit AMS AS5055A absolute encoder chip. They are placed at the joints of each phalanges and are co-denamed CER_HPS for clarity. The encoders read the rotation of a diametrically magnetized, cylindrical N40 Neodymium magnet of 3.2 [mm] diameter housed inside the joint shaft.

Series Elastic Sensor

Two absolute hall effect sensors using 10 bit AMS AS5055A absolute encoder chips were placed on the rotation axis of the series elastic setup in the centre of the hand to measure the deflection of the lever arm of the SEE module, and are codenamed CER_SEAS.

Motor Encoder

A board based on incremental magnetic encoders is also designed. The board (MIE) uses a 10 bit incremental encoder chip that reads the revolutions of the motor capstan. This measurement is important for not losing the control of the tension of the tendon.

Skin

The skin as shown in Fig.6.9 is based on the existing tactile skin technology of the iCub robot [25]. The R1 robot has tactile sensors on the gripping side of its phalanges and also on the entirety of its forearm. This provides the robot with an additional force sensor and is extremely useful for grasping tasks of any given object.

Table 6.2 Tactile sensing points on the hand skin

Part	Sensing points	CDC chips
Paddle Proximal	21	2
Paddle Distal	27	3
Thumb Proximal	12	1
Thumb Distal	15	2
Total (two hands)	150	16

However, differently from [105] which used flexible triangle PCBs, rigid PCB boards were employed here. It gives more freedom in assembly on the phalange and an atypical arrangement of the tactile sensing points. The details of the sensing points and the number of CDC chips used on each phalange is shown in Tab.6.2. This board is covered by a deformable foam which is covered by an electrically conductive textile material coupled with an external protective fabric layer, that has also a gripping finish. This tri-laminate is laser cut and is pasted onto the boards to cover all the tactile sensing points. All four boards are controlled by a single MTB board (a microcontroller board that interfaces the tactile sensor) which is placed in the palm on top of the SEE module.

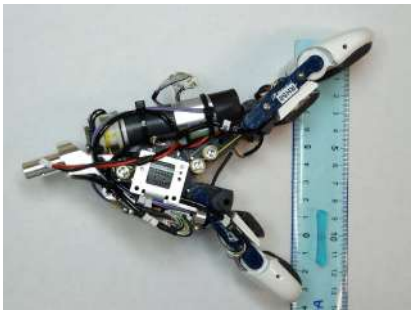

(a) R1 hand without covers

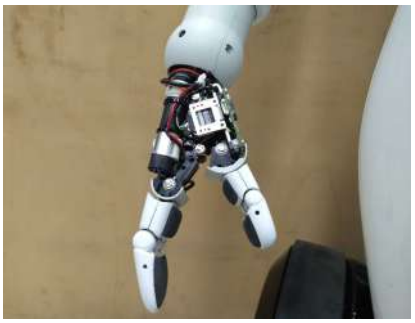

(b) Hand mounted on the wrist

Fig. 6.10 The R1 hand without covers. The completely mounted hand can be seen on the left, it can be seen that it has an effective opening of about 13cm. On the right is the hand mounted on the robot and interface to the wrist. It can be seen how the hand cables are interfaced to the electronics in the wrist.

6.3 Evaluation

The hand was tested against the user needs that was initially listed (Section 6.0.1). The hand was able to grasp a wide range of objects. It was able to carry 700 [g] of weight without assistance and a peak weight of 1 [kg] with added grip material to the object to prevent slippage. A challenging grasp was the hammer swing where the velocity was very limited as a quick transition of the CoM of the hammer caused both friction problems as well as over-extension of the wrist joints.

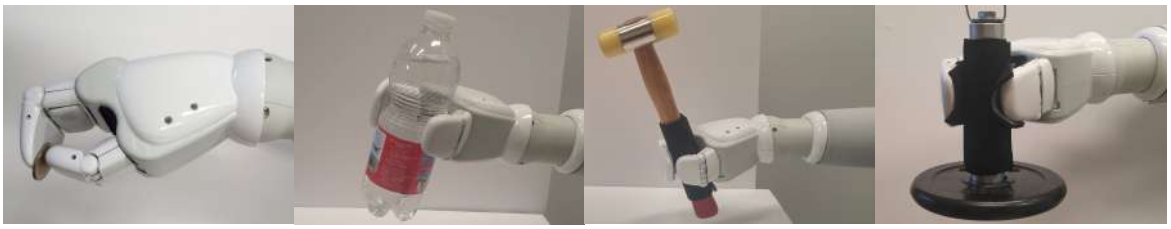

(a) Coin (b) Bottle (c) Hammer (d) 1kg weight

Fig. 6.11 Grasps with payloads. The hand successfully carried objects of varying weights, including a coin (a), a 0.5 [l] water bottle (b), a 0.35 [kg] hammer (c), and a peak payload (d) of 1 [kg] (with additional gripping material).

The tip pinch of the key (Fig.6.15e) and coin (Fig.6.11a) was also carried out successfully, but the process of picking it off the table was complicated without added friction due to the polished fingertips. There was a higher rate of success on the pinch grasps when a thermoplastic polyurethane gripping polymer (3M-GM400) was added on the polished fingertips of the hand. The same material was then pasted to the palm

of the hand to aid in lifting the 1 [kg] weight as shown in Fig.6.11d.

The hand performed well in most cases and was able to open most types of doors and toggle switches.

The prototype cost was more than our predicted costs. A scaling up of the cost for production, according to our market research, gave us a price range of €1400 for both hands. This was consistent with our requirements.

6.3.1 Performance Analysis

A SEE module characterization experiment were conducted where the tendon pulling forces was compared to the mechanical elastic deformation of the spring. Increasing forces of up to 45 [N] were applied and the corresponding spring deflection value was recorded. A fifth polynomial line was then fit to the result, given the output data points, to draw a comparison with the theoretical values.

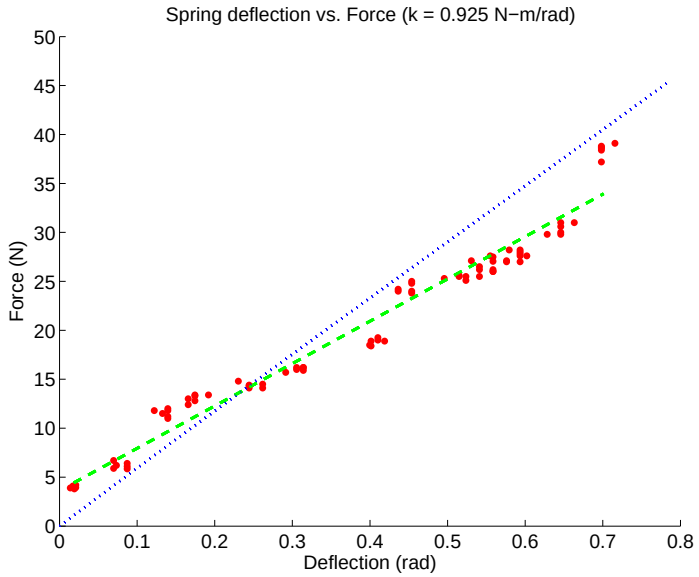

Fig. 6.12 Tendon force vs. SEE module deflection. The blue dotted line was the theoretical response of the selected spring and the green line shows the fitted response as measured for corresponding input force.

The result, as shown in Fig.6.12, provided the SEE deflection behavior for a given range of input tendon forces. Each tendon was capable of a maximum pulling force of 45 [N], but the SEE module returned maximum deflection of the spring at 36 [N].

This was due to the safe travel range restrictions imposed by the torsional spring. In effect a hardware limit of 40° deflection was set for the spring as opposed to the

calculated 45°. As a consequence the spring did not have the full operational range that was originally envisioned in the calculations. Beyond this range, the SEE module was at full deflection and the hand behaved rigidly without any compliance.

The hand employs the SEE module for force control. The tactile skin on the phalanges are used for finer force measurements and for determining unique characteristics of the objects being grasped, the demonstration of which are beyond the scope of this paper.

6.3.2 Grasp Force Sensing

The grasp force of the hand was tested by squeezing a rigid ball that housed a force torque sensor in its centre. The ball was 34 [mm] in diameter and housed an *F/T Sensor Nano17* from ATI Industrial Automation. The ball was placed in the hand at

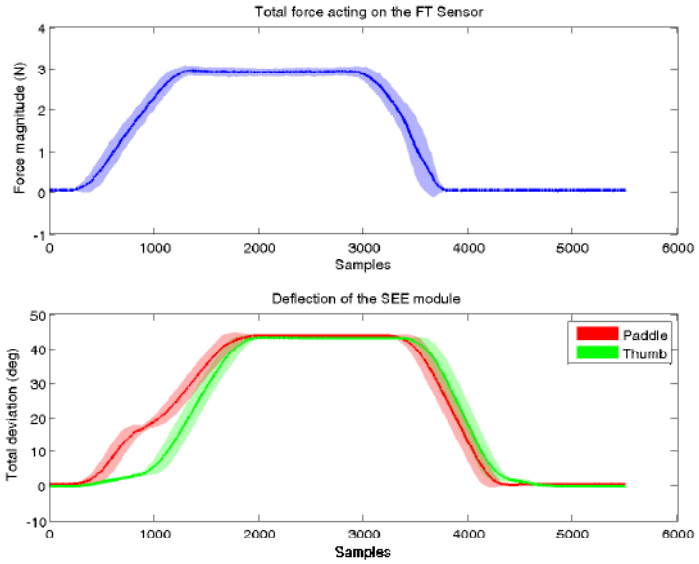

Fig. 6.13 Sphere grasping experiment. The figure shows the sensor readings for the sphere grasping experiment described in the main text. The top graph (blue) shows the grasping force magnitude measured by the force-torque sensor. The bottom graph shows the values of the two SEE sensor readings (red and green for paddle and thumb respectively). The lines are the average of 15 different trials and the data were sampled at 1 KHz. The standard deviation is represented by the shaded region.

a resting position and was squeezed to maximum deflection of the SEE module. The corresponding values of the force-torque sensor was then recorded (Fig.6.13), the safe travel range of the torsion spring limited the maximum allowable deflection to 40°. As can be observed from the graph, the module corresponds to the force applied to

the force-torque sensor. It can be seen that the performance is regular and does not exhibit any significant drift or hysteresis.

6.3.3 Load Response

The hand was tested for impact loads and incidental force impacts. The paddle struck an FT sensor repeatedly from the top in a way that the joints were restricted in their motion. As shown in Fig.6.14 the excess force was redirected to the SEE module which stored the excess energy till the incidental load was relieved.

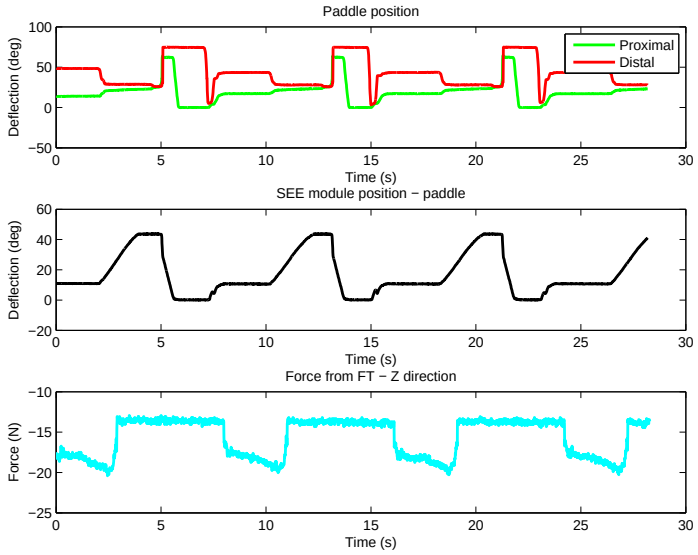

Fig. 6.14 External force response. The SEE module response when there is force loading on position locked joints of the paddle. Paddle joints (top) are locked at limits as external force (shown as FT sensor values in cyan) continues to be applied. To prevent damage to the hand structure, the SEE module deflects (black) and acts like an energy storing mechanism that absorbs the excess force.

The energy stored in the SEE module is released immediately after the incidental force was removed, which can be seen in the joint deflection of the paddle joints. All elements then immediately recover their set positions. This was also observed for higher impact loads which are known to be highly detrimental in rigid designs. This was in accordance to the initial requirement of the hand being able to handle impact loads without causing damage to the hand structure and to the environment it is working in.

6.3.4 Grasping Analysis

The R1 humanoid robot was designed to aid people in their day to day activities. It was therefore essential the hand perform the most basic grasps. As stated in the introduction, a minimal set of grasps was selected from the analysis of Bullock et al.[21]. One limitation was the force with which the objects are to be grasped. The SEE module deflection measurements was used to limit the maximum applicable force on each object as shown in Fig.6.13. This way successful grasps of objects of different weights and densities were carried out without damaging them.

(a) Medium wrap

(b) Power disk

(c) Palmar pinch

(d) Light tool

(e) Tip pinch

(f) Tripod

(g) Thumb finger

(h) Power sphere

(i) Palmar

(j) Tip pinch

Fig. 6.15 Grasping. A select number of grasps based on the work of Bullock et al.[21] was carried out.

As seen in Fig.6.15, the hand was able to perform most of the key grasps that were listed by Bullock except for those that involved lateral support (lateral pinch and tripod), this accounts for more than 80% of all grasps.

6.3.5 Robustness

The hand was subject to a continuous operation of about 5000 cycles, without any load, to test the reliability of the structure and tendon wear before mounting. The R1

hand was then mounted and has been under continuous operation for more than a year, grasping various objects on a daily basis without any significant drop in performance or hardware repairs. This shows the robustness of the system.

6.3.6 Weight

The hand had an estimated weight of 460[g] (on CAD) and an actual weight of 420[g] including all electronic boards and covers which is within the required limit of 600[g].

6.3.7 FFP Evaluation of the R1 hand

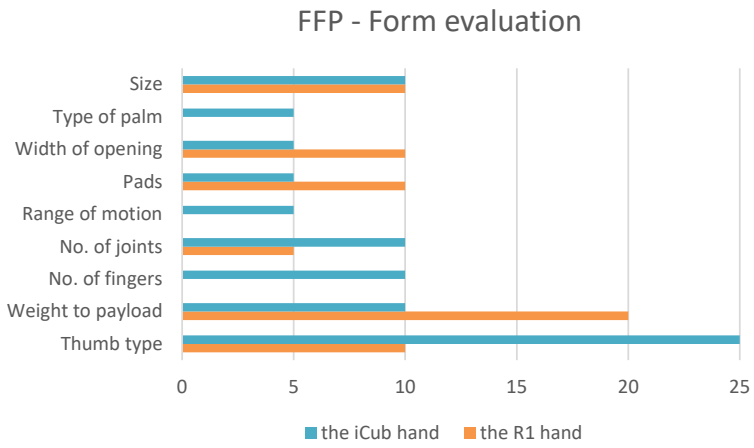

Fig. 6.16 The form breakdown of the R1 hand as compared to the iCub 2 hand.

The FFP evaluation of the R1 hand was also carried out. The hand performed poorly when it came to gestures and manipulation tasks. But it was able to perform satisfactorily when it came to grasping. As mentioned earlier, it was able to do most of the essential grasps as defined by Bullock et al., but the objects as defined by the FFP evaluation were more challenging. The hand performance was low when it came to pinch grasps, especially.

It got a performance score of only 58% as it was unable to perform the key categories of gestures and manipulation effectively.

A detailed breakdown of the performance of the R1 hand as compared to the iCub hand is shown in Fig.6.18. It can be seen that although the hand was able to perform satisfactorily when it came to grasping objects and did well with power grasps, it underperformed at non-prehensile tasks and failed at the manipulation tasks and gestures. However, the R1 was not built to perform any human like gestures or

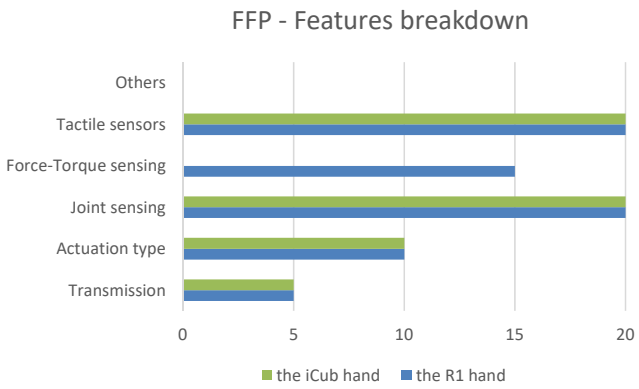

Fig. 6.17 The features breakdown of the R1 hand as compared to the iCub 2 hand.

complex manipulation. Under the context of the guidelines set initially, the R1 hand performed quite satisfactorily.

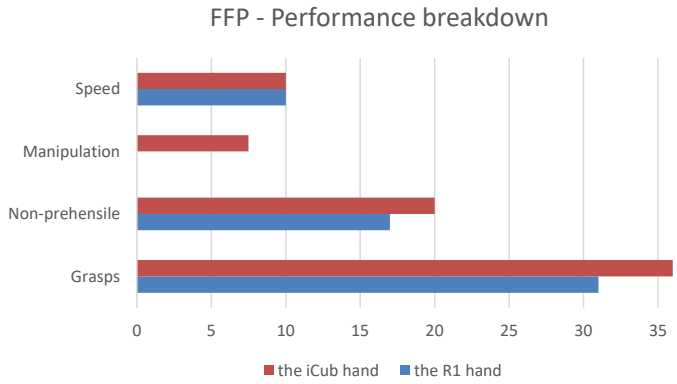

Fig. 6.18 The performance breakdown of the R1 hand as compared to the iCub 2 hand.

The lack of anthropomorphic features (shown in Fig.6.16) such as multiple fingers and an articulated thumb also led to just an average score when it came to form. The form score for the R1 hand was 62%, which is passable but can still be improved upon.

Since the R1 hand is underactuated and has only two phalanges, the control becomes harder. For this purpose, it was equipped with a number of sensors, which helped in boosting its features score (as shown in Fig.6.17) up to 70% which is a much better score than that of the iCub hand. The R1 hand, is a fully observable system. It contains motor position sensors, hall effect joint position sensors, position sensors for monitoring the series elastic module for force sensing and tactile sensors on all the phalanges. Applying the recommended biases for a domestic robot in the FFP index for the R1 hand gave it an overall score of 62.5%. This chapter discussed the hand that was developed for the R1 humanoid robot. The following chapter starts

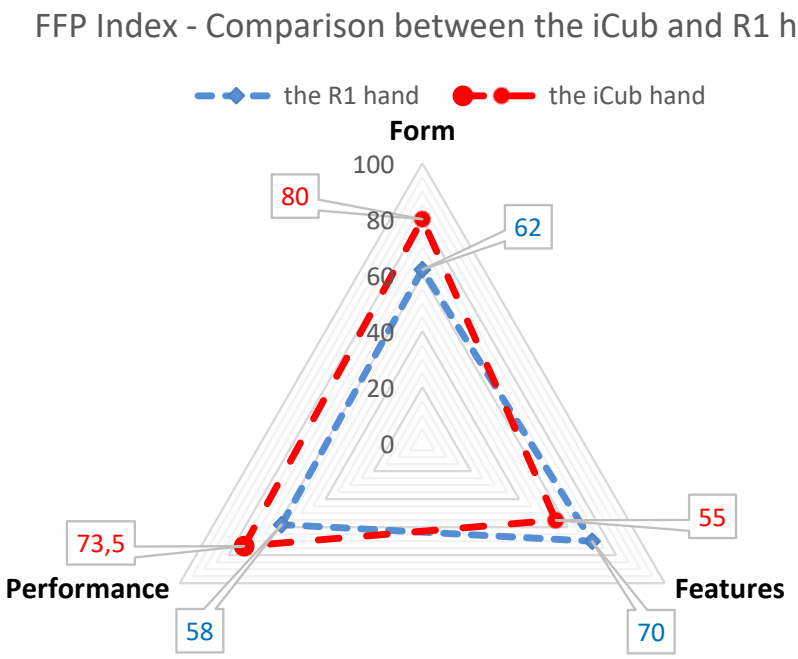

Fig. 6.19 The FFP evaluation of the R1 hand as compared to the iCub hand

describing the design of the iCub plastic hand, starting with the design decisions and design of the series elastic module for the iCub plastic hand.

Chapter 7

The iCub Plastic Hand

The previous chapter explained the development of the R1 hand in detail. It was a good platform for basic grasping and for low level manipulation tasks. The R1 hand was a good learning platform for many diverse domains in robotic hand design. Iterative design using polymeric materials using rapid prototyping was a good learning curve. Certain best design practices were set in place that was learnt during the development of the R1 hand.

A new experimental prototype plastic hand that employs the design decisions that was made for the R1 was developed also for the iCub platform. The current iCub hand has a few major drawbacks that has to be addressed in this new prototype plastic hand. The new hand, for clarity purposes, will be called the iCub plastic hand from here on.

7.0.1 Lessons Learnt from the R1 Hand

Some of the key lessons we learnt from the R1 hand were:

- The use of polymer materials allows making lightweight hands
- The use of additive manufacturing allows the manufacture of components that are unique in design and can't be produced otherwise
- Use of sheet metal components and its corresponding manufacturing processes for cost-cutting and ease of manufacturing
- Integrated design of the tactile skin
- Issues with fingertip modelling and skin surfaces

- Stack design where the hand can be maintained individually without having to be disassembled or dismounted

The above mentioned pointers led to improving design objectives and addressing previously undetermined problems.

7.0.2 The iCub Hand

The hand of the iCub robot always come with a prerequisite that all of its features be anthropomorphic. Hence, a hand similar to that of the R1 robot is automatically ruled out when it comes to form. The iCub hand [106] has 20 joints organized in 9 degrees of freedom. Its dimensions (50mm long, 34mm wide at the wrist, 60mm wide at the fingers and 25mm thick) and ranges of motion were inspired by those of a human hand. These 20 joints are actuated using 9 DC motors (resulting in 9 DOAs) 7 of which are embedded in the forearm and 2 in the hand. Therefore, certain DOFs are obtained by coupling different joints (either tightly or elastically) so that they are actuated using a single motor in a synergistic fashion.

Drawbacks

Many of the major features of the iCub hand are discussed in Chapter 4. Some of the major drawbacks that were recorded from experimentation and experience, which were extracted from different platforms are:

- tactile sensing is present only on the proximal phalange fingertips
- the thumb has an extra phalange and does not correlate with its anthropomorphic equivalent, this consequently makes it longer and afflicts the effective grasping space of the hand
- the steel tendons get damaged quite often
- the repair and maintenance is messy and arduous as the entire forearm has to be dismounted to extract the hand
- the hand, thus far has little to no force sensing and the only potential for force sensing is through its tactile skin
- the position sensing is quite non-linear and relies on outdated technology

- the recommended maximum payload of the hand is quite low (around 300 grams)

Keeping these drawbacks in mind, there arose a need for a better and generally more robust hand. The use of polymeric materials was also considered advantageous with the advent of additive manufacturing techniques. The higher level user needs remained the same, but the iCub plastic hand requires more dexterity than the R1 hand since it has to perform basic gestures in an anthropomorphic manner.

The iCub plastic hand is a completely anthropomorphic hand when it comes to shape, it has five fingers which includes an articulated thumb. The hand has been specifically designed for the iCub and therefore an exceptional level of integration can be expected from it. This version also acts as an experimental prototype, which will be further refined for cost and manufacturing efficiency in further iterations before being integrated into the iCub robot.

The chapter is organized as follows: the first section illustrates the hand kinematics, actuation system, the series elastic module design which is followed by the overall design of the hand, the following section goes into more detail with the design of the fingers and the design decisions that went into selecting the parameters and components employed in the fingers and the hand. The final section explores the design in detail where the hand and the finger designs and the integration of the finger electronics into its design are explained in detail. The hand contains a singular flex PCB running inside the fingers leading to a more integrated design. Its details, along with its design intricacies are also discussed. The tendon and slack management throughout the hand is also discussed and the integration of the series elastic module is also explained.

7.1 Conceptual Design

The iCub plastic hand is designed to be anthropomorphic and has finger ratios that are similar to that of the human hand. The hand has five fingers and two phalanges (proximal and distal) on each of its fingers, except for the thumb. Some similarities carried over from the design of the R1 hand are that the return of the phalanges to the open position is achieved with return springs contained within the finger. The hand will be tendon driven like in the previous version and the design had to be predominantly in plastic to cut costs. However, differently from R1, the hand hardware does not need to be completely self-contained within the hand. All the required actuators and control electronics are contained within the forearm.

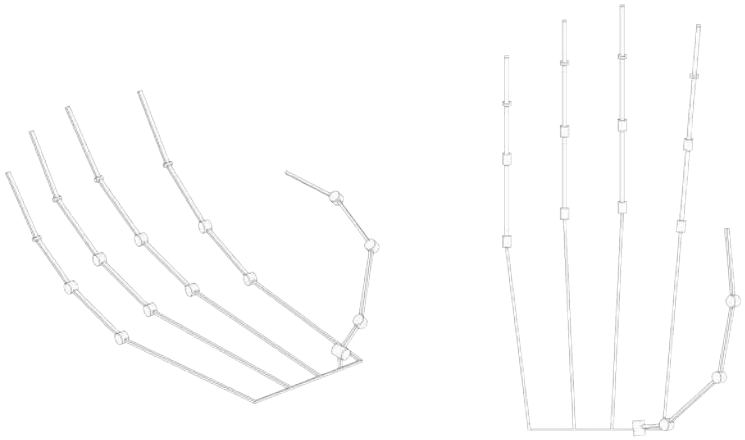

Fig. 7.1 The iCub plastic hand: Basic outline of the proposed kinematics

A skeleton based on the derived kinematics from the following section is designed and acts as the system's overview. The design is then carried top-down, by predefining the position of all subsystems while not going into finer details. This way, it gives a clear overview of the system and makes modification a lot easier. This is discussed in more detail in the embodiment design.

A basic overview of the kinematics is first designed as shown in 7.1, where the type of joints are first determined, as well as the overall shape and size of the hand.

7.1.1 Kinematics

The link lengths of all the fingers were obtained from the human hand data from Buryanov and Kotiuk [22]. An important thing to note is that the represented data is of the lengths of the human hand bones. When the human hand is considered in its final form with muscle and skin, there exists an added padding, covered with glabrous as discussed in Chapter4. This padding at the base of the proximal phalange of about 10mm was excluded and the fingertip padding on the distal phalange was added by about 5mm on average from the quoted lengths. Another motivation to test the parts quickly and to reduce manufacturing constraints was by making all fingers except the thumb of the same length. Since the little finger varies from the other fingers by a large degree, it was excluded, and the other fingers : the index, middle and thumb, were averaged to obtain the phalange lengths of all four fingers.

The thumb however, is unique from the other fingers, but the proximal phalange of the thumb is kept the same size as the proximal of the fingers. The metacarpal joint was split into two, one for rotation and the other for reduced flexion to facilitate in

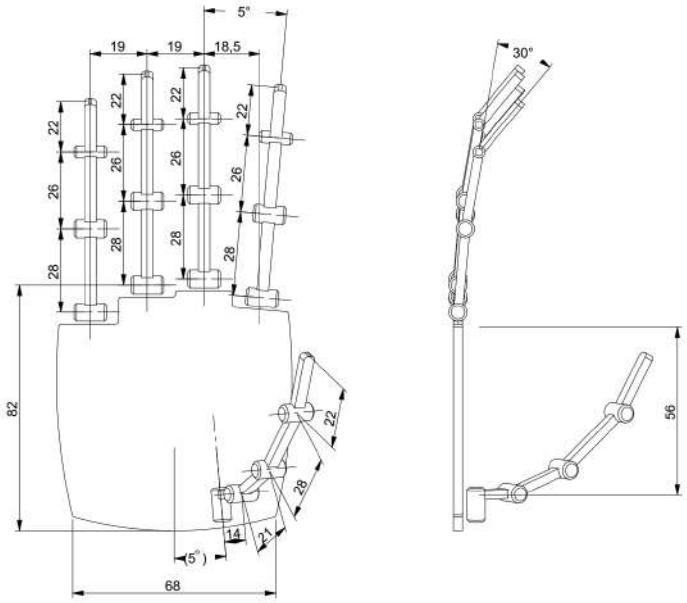

Fig. 7.2 The iCub plastic hand kinematics: This defines the rotational joints (big joints), rigidly coupled joints (smaller joints) and link lengths

adapting the thumb to a better degree. The overall length of the thumb, was however kept congruent to that of human data. The corresponding Denavit-Hartenberg (DH) parameters are as shown in Table 7.1 and 7.2.

Table 7.1 Finger kinematics

Link i / H − D	A_i **(mm)**	d_{i+1} **(mm)**	α_i **(rad)**	θ_{i+1} **(deg)**
i = 1	28	0	0	0 -> 80
i = 2	26	0	0	0 -> 80
i = 3	22	0	0	30

Both the proximal and distal phalanges has a flexion range of 80°. The intermedial phalange and the distal phalange were fused to form a single distal phalange. The distal phalange was fused to the intermedial at a fixed angle of 30°. A detailed diagram of the kinematics of the iCub plastic hand is given in Fig.7.2.

The thumb rotates from 0° (parallel to the palm plane) to about 110°. The metacarpal phalange is broken in two, one fixed to the rotation link and the second with a flexion range of 45° and the proximal and distal phalange have equal flexion ranges of 80°.

Table 7.2 Thumb kinematics.

Link i / H – D	A_i **(mm)**	d_{i+1} **(mm)**	α_i **(rad)**	θ_{i+1} **(deg)**
i = 0	0	0	-pi/2	0 -> 110
i = 1	14	0	0	0
i = 2	18	0	0	0 -> 45
i = 3	28	0	0	0 -> 80
i = 4	22	0	0	0 -> 80

7.1.2 Overall Design

The iCub plastic hand is intended to be an experimental prototype. The main motivation behind the design lies in testing new concepts and efficient kinematics. All the

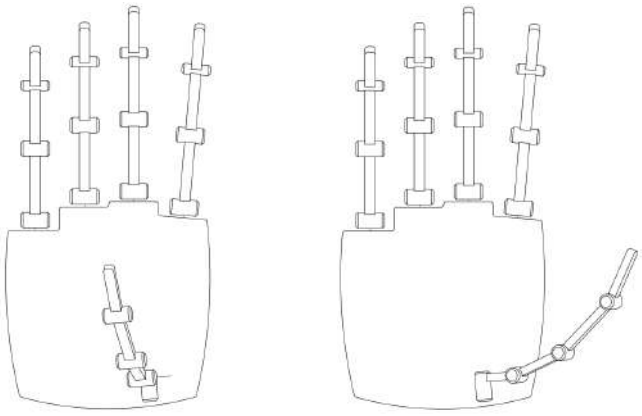

(a) Thumb rotation of 110° (b) Thumb rotation of 15°

Fig. 7.3 Proposed hand thumb positions, at 110° and 15°

finger and thumb placements are inspired from human hand kinematics. However, the fingers have been made identical for cost reduction. The hand, especially the palm structure is also fashioned as a stack design, where each layer serves a primary purpose that makes troubleshooting the hand easier.

7.1.3 Transmission

The design of the grasp transmission mechanism is fully based on the theoretical analysis and design of under-actuated hands proposed by Birglen et al. [15].

In classical under-actuated mechanisms, coupled joints always remain passive and

the coupling ratios fixed. Autonomous finger adaptation is obtained by introducing elastic elements in the transmission chain so that fingers can be always brought back to a known configuration. Spring stiffnesses are chosen to counterbalance finger weight and inertial effects and, at the same time, to oppose the least torque against actuation while grasping.

Any system when interacting with any other system where there exists a force exchange undergoes slight deformation in multiple planes, referred to as contact geometry. No friction and contact geometry are involved in this analysis since the objective is to characterize the normal forces developed by the fingers according to their designs. Fingers are modeled in accordance to the quasi-static analysis proposed by [15]:

$$t^T \omega_a = \sum_{i=1}^{n} \xi_i \circ \zeta_i \tag{7.1}$$

where t is the input torque vector exerted by the actuator and the springs located between the phalanges , ω_a is the corresponding joint velocity vector, ξ_i is the twist of the i^{th} contact point on the i^{th} phalange with ζ_i being the corresponding wrench and $\circ$ being the scalar product between the two states.

Now :

$$t = \begin{bmatrix} \tau_a \\ T_2 \end{bmatrix} = \begin{bmatrix} \tau_a \\ -k_2 \Delta\theta_2 \end{bmatrix} \tag{7.2}$$

$$\omega_a = \begin{bmatrix} \dot{\theta_a} \\ \dot{\theta_2} \end{bmatrix} \tag{7.3}$$

where τ_a is the actuation torque applied at the base of the finger, T_2 is the torque at the distal joint, k_2 is the stiffness co-efficient of the distal return spring and $\Delta\theta_2$ is the deviation from the fully extended position of the distal joint. Virtual power can be written as:

$$t^T \omega_a = f^T J \dot{\theta} = f^T J T \omega_a \tag{7.4}$$

where T is the so called transmission matrix which relates the input velocity vector to the joint velocities: $\dot{\theta} = T\omega_a$. Therefore, given the input torque, vector contact forces are computed as follows:

$$f = J^{-T} T^{-T} t \tag{7.5}$$

where f only accounts for the normal contact forces (since no torques and friction

forces are assumed at contact) and J (the Jacobian matrix) is simply defined as:

$$J = \begin{bmatrix} k_1 & 0 \\ k_2 + l_1 cos(\theta_2) & k_2 \end{bmatrix} \tag{7.6}$$

where k_i is the distance between the i_{th} contact point and the base (frame origin) of the i_{th} phalanx. This formulation isolates the transmission mechanism T from the finger kinematic structure allowing to analyze the influence of the transmission type and its corresponding geometry can play a role in grasping force.

Transmission Mechanism

The transmission mechanism required to propogate the actuation torque to all the phalanges of the proposed finger mechanism is given briefly in this section. The

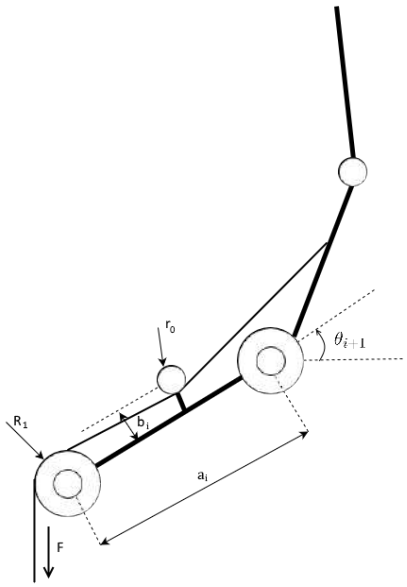

Fig. 7.4 The proposed transmission mechanism of the iCub plastic hand. Here $R1$ is the radius of the pin at the distal joint and r_0 is the radius of the pin at the proximal joint.

proposed finger mechanism is similar to that of the Da Vinci finger mechanism and is as shown in Fig.7.4.

In our case the tendon slides on pins at a fixed distance away from the joints. When the tendon is in tension, the only sliding surface should be on the pins, however in practice there occurs some other frictional losses too. But for this analyses, those frictional losses are considered negligible and is ignored. While the matrix of J remains

unchanged, the matrix T is given by:

$$T = \begin{bmatrix} 1 & \frac{R1}{r_0} \\ 0 & 1 \end{bmatrix} \tag{7.7}$$

where $R1$ is the radius of the pin at the distal joint and r_0 is the radius of the pin at the proximal joint. From the relation between actuation and contact forces, the equation can be split as:

$$\tau = T^{-T} t \tag{7.8}$$

$$f = J^{-T} \tau \tag{7.9}$$

where Eq.7.8 shows the actuation torque distribution according to the transmission mechanism and Eq.7.9 represents the effects that finger and contact geometries exert on grasping forces. The key factors which determine contact forces are: the contact point positions, the joint configurations, the link lengths and the distance from the link joints. The contact point positions and the joint configurations are determined by the object being grasped and will have sensors to monitor them. Meanwhile, the link lengths are subject to anthropomorphic constraints. The link joints and to a certain extent the pulley diameter at the joints are the only major parameter that can be optimized.

7.1.4 Finger Design

As mentioned in previous sections, one of the key parameters that can be optimized in this finger design is the distance of the rolling pins from the central link. This can be assumed as a overhang beam problem where the finger joint torque is given as:

$$\tau_f = m_f \cdot (l_f/2) + p_f \cdot l_f \tag{7.10}$$

where m_f is the mass of the finger, p_f and l_f are the finger payload and length of the finger respectively.

Considering a finger length of 70[mm] which weighs about 60[g] and a payload at the end of the finger estimated around 500[g].

The resultant torque required can be computed as:

$$M_f = 0.36[Nm] \tag{7.11}$$

This is the required torque to actuate the finger from the point of an overhanging beam. Optimizing the distance $R1$ to get the right range of torque, it can be inferred that,

$$M_f = F/R1 \tag{7.12}$$

Given these requirements, a DC MAXON motor with a nominal torque of around 0.005 [Nm] before reduction was chosen(including efficiency assumptions). The motor is then coupled with a gear head that has a gear ratio of 103:1 that gives 0.50161 [Nm] nominal torque available to actuate the finger. Including a 75% gearhead efficiency, the expected nominal output torque is around 0.39 [Nm]. The next step would be to compute the right motor carrier diameter to avail the right range of tendon pulling forces.

7.1.5 Actuator and Motor Carrier Design

To determine the tendon pulling force is straightforward. Given the motor torque and the distance of the tendon from the motor carrier, it can be determined that:

$$\tau_m = F_t \cdot x_t \tag{7.13}$$

where x_t is the distance from the joint, τ_m is the motor torque and F_j tendon pulling force

it is calculated that the optimal diameter for the motor carrier is around $6mm$. The resulting pulling force for a distance of 6mm from the joint is :

$$F_t = 65[N]$$

Assuming friction losses, of about 20%, it is assumed the effective tendon pulling force is

$$F_t = 54.2[N]$$

The final step in the actuation design process is to determine the right distance of the sliding pin from the joint pulley centre. Given the pulling force and the desired range of torques capable of being handled at the finger joint, the optimal distance can be determined and the resulting range is depicted in Fig.7.5.

For the range of tendon pulling forces that was estimated previously and the given

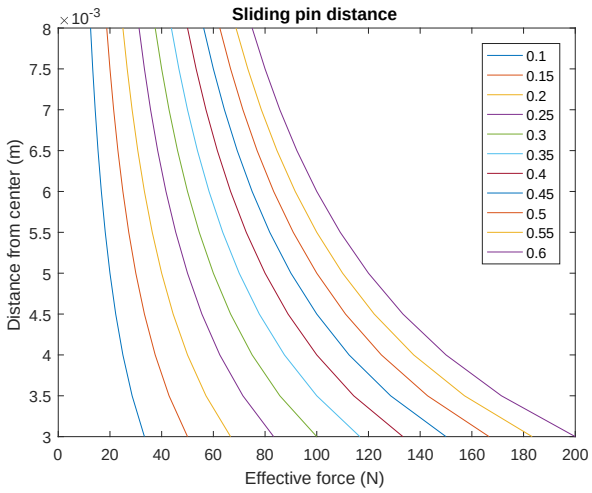

Fig. 7.5 Sliding pin distance calculation. The tendon runs on rails inside the phalanges of the hand. To minimize friction, entry and exit sliding pins are placed inside the fingers. Given the distance of the pin from the joint center, the optimum distance for the placement of the pins is selected.

design constraints, the distance was selected to be around 7mm.

7.1.6 Return Spring

A typical closed-loop actuation structure in hand design relies on a pulley attached to the motor: a stainless steel tendon is entwined around the pulley and is routed to the joint and back to the motor using sheaths. These sheaths are basically any kind of structure that help the tendon to slide. In this way, a closed-loop configuration exploits the tendon for moving the joint in the two directions of motion. On the contrary, in the open-ended actuation system the tendon only contributes to rotating the joint in one direction (usually flexion) while a spring-return is in charge of rotating the joint back (corresponding extension). The rotation of the motor flexes the joint and compresses the spring; the counter-rotation releases the potential energy accumulated in the spring and extends the joint.

For the iCub plastic hand, the open-ended actuation system is proposed where a leaf spring runs all across the spine of the finger and acts as a return spring. The rotation of the motor flexes this joint and when the force is released, the bent leaf spring releases the accumulated energy from the bending of the spring and consequently extends the finger.

This needs to compensate only for the weight of the finger, in accordance with previous assumptions, let us say that each phalange weighs about 20g and the average

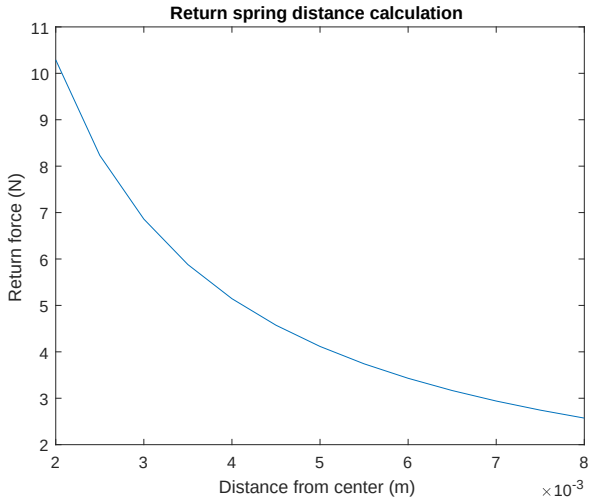

Fig. 7.6 Return spring selection given the distance from joint

phalange is 24mm in length.

Then we have the momentum to be

$$M_{ph1} = 0.0024[Nm]$$

And for the whole finger, the torque required at the joint for return to the extended position is given as

$$M_{fr} = m_f \cdot (l_f/2) \tag{7.14}$$

which gives :

$$M_{fr} = 0.012[Nm]$$

Leaf springs were used for generating the return force in this design, considering the spring is mounted about a distance x_{cf} away from the joint.

$$\tau_{cf} = F_{cf} \cdot x_{cf} \tag{7.15}$$

Substituting the value of x_{cf} we get

$$0.012 = F_{cf} \cdot 0.007$$

$$F_{cf} = 1.72[N]$$

This is the minimum force the leaf spring needs to generate due to flexion at the joint, to be used to bring back the fingers to its fully extended position. Weighing

in a safety factor of about 1.2, the selected spring should have a constant pulling force about 2.1[N]. A stainless constant force spring with a pulling force of 2.2[N] was selected for this design as a return spring.

7.1.7 Series Elastic Module

In this section, the importance of series elastic elements is discussed alongwith its design for the iCub plastic hand. The introduction of series elastic components in the system allows for compliance in the joints' transmission which in turn allows to decouple the inertia of the drive from the inertia of the link, effectively reducing the peak force transmissibility. This is typically done by putting a spring in series and the deflection of this spring can be measured, which is effectively proportional to the force in the system.

Force sensing, specifically the grasping force and tendon slack monitoring is considered an important factor. At the same time the hand had to be compliant to impact loads as in the R1 hand. All of these requirements were achieved by incorporating series elasticity into the system.

Robotic hands which incorporate this kind of force sensing is not common. There are some examples such as [53] [33] [50]. There are different types of series elastic elements that can be incorporated, depending on the functionality, the shape, the transmission elements and the actuation methodology [97] [90] [123].

There are increased instances of force sensing and SEA design in general in prosthetics and hand exoskeleton design [4]. It is important to consider these into account since they give a comparable metric to those used in robotic hands since they have comparable size and force ranges.

Linear Spring Design

There are three stages for the series elastic module design. In the first stage, there should be just slack monitoring. Considering no friction in the system, this should be pretty straightforward. Let force during this phase be f_{p0}. The second stage should be where there should be a desired minor deflection in the elastic module for complete actuation of the finger for its entire range of motion but without payload, let the force required to actuate be f_{p1} and finally, there should be the maximum possible range of deflection for f_{p1} where there is force loading due to payload and external disturbances. For simplification, let f_{p0}, f_{p1}, f_{p2} be the force required at different

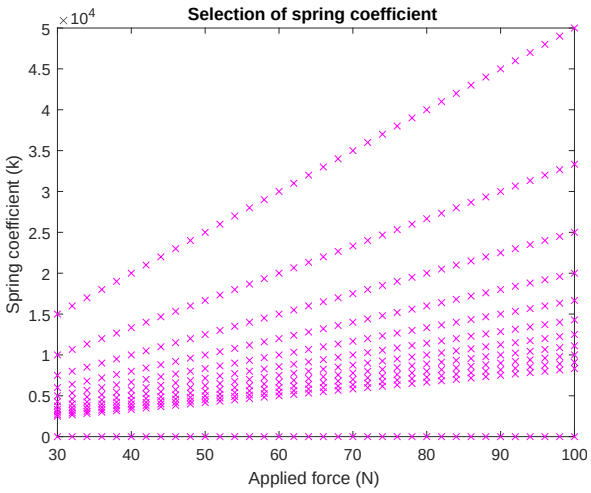

Fig. 7.7 Series elastic module 'k' value estimation

phases that the linear spring undergoes. Let r_f be the radius of the finger joint; r_m be the radius of the motor pulley and θ_{m0} be the initial motor angle (at no load), θ_m be final motor angle and r_m be the radius of the motor carrier.

$$f_{p0} \geq 0; \tag{7.16}$$

The next stage would be actuation phase where there should be deflection where

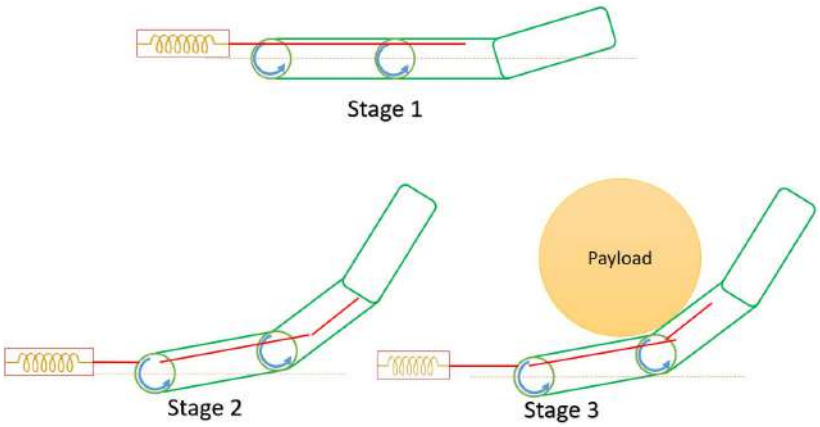

Fig. 7.8 Series elastic module spring stages. In the first stage, there should be just slack monitoring. The second stage should be where there should be a desired minor deflection in the elastic module for complete actuation of the finger for its entire range of motion but without payload, and the final stage there should be maximum possible range of deflection for where there is force loading due to payload and external disturbances.

the finger is not supporting any external load but supports only its own weight and friction.

$$f_{p1} = f_m - f_f \tag{7.17}$$

In the second stage, the pulling force is subject to the weight of the finger and its joint friction properties. Without any friction in the system, the force required should be around the same as f_m as the weight of the finger is quite negligible

$$f_{p1} \lesssim f_m$$

But this is usually not the case, the finger has sliding tendons on pins and in the final deflection pulley in the distal phalange, there tends to be a fair amount of friction as the tendon winds around the finger and slides to and fro across the phalanges. Considering these friction losses f_f to be about 20% of f_m, we get :

$$f_{p1} = f_m - f_f \tag{7.18}$$

$$f_{p1} = \frac{f_m}{1.2} \tag{7.19}$$

Now the last phase is for determining external loads, the nominal pulling force of the motor should correspond with an equivalent force that provides the maximum safe travel range of the spring f_{p2}.

$$max.f_{p2} = f_m = \tau_m / r_m \tag{7.20}$$

It should generally be capable of withstanding higher forces for impact loads, but there is no necessity for sustaining those loads for long periods of time.

The kinematic relationship in the system with the two springs of same effective stiffness values (k1 = k2 = k) (assuming the stretch in the cable to be negligible at the operating loads) is given by :

$$\Delta l = r_f(\theta_f - \theta_{f0}) - r_m\theta_m \tag{7.21}$$

where Δl is the extension in spring with length l. The maximum torque $max.\tau_m$ of the motor as discussed earlier is 0.39[N-m]. And the corresponding pulling force capable by the motor is given by:

$$max.f_m = \frac{max.\tau_m}{r_m} \tag{7.22}$$

And substituting this maximum force achievable by the motor in Hooke's law, the equation can be re-written as :

$$f_m = 2 \cdot k \cdot \Delta l$$

The maximum safe travel range of the spring then should be given as :

$$\Delta l = \frac{f_m}{2 \cdot k} \tag{7.23}$$

So at force f_{p2} the maximum deflection should be Δl and the force should be equal to $max.f_m$.

Analysis

The motor torque before reduction is 0.00487 [Nm], considering motor and gear efficiencies, and with a gear ratio of 103:1 it was calculated as 0.39 [Nm]. Let f_{sp} be the pulling force in the system.

$$f_{sp} = \frac{\tau_m}{r_m}$$
$$f_{sp} = \frac{0.39}{0.007}$$
$$f_{sp} = 55.8[N]$$

Considering a safety factor of about 1.1

$$f_{sp} = 61.3[N] \tag{7.24}$$

This gives an indication of what can be expected to be the maximum pulling force of the selected motor. And the spring should be at full deflection. This way, the springs can be selected in a way that is tuned to any force range that is required to be measured by the user.

Now, the spring can be tuned in such a way that the k value selected, behaves in a way as required by the user. For this, two unique cases are explored: one in the high range and one in the lower range. A single spring that performs well across the entire range of operation as defined in the previous section is difficult to avail commercially due to the limited size available within the hand for maximum length of compression springs and its corresponding deflection.

There is never going to be zero friction in the system. Assuming basic friction

losses and finger actuation forces, it is safe to ignore the lower force range for both cases. One possibility as a spring is to select a k value that works along the entire possible force range capable by the motor. A second possibility is to select a spring that works only on the higher force range capable by the motor and extending further to compensate for man-made force exertion and impact loads. In this case, the high force range springs help in determining high forces, human intervention and compensating for impact loading, the force bandwidth is small and is above the actuation force of the hand. The low range has a high bandwidth and works for almost the entire force bandwidth capable by the hand, but is not particularly good at impact force loading and becomes rigid at higher forces.

By tuning the spring stiffness according to the desired bandwidth, these two springs can serve two different purposes in the hand design. The stiffer, high range spring is used for power grasps in all fingers except the index, while the low range is used in the index finger to estimate forces during precision grasps.

7.2 Embodiment Design

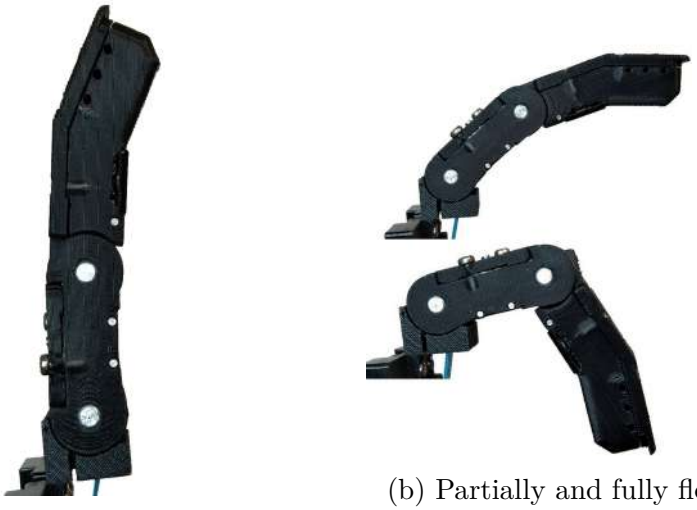

(a) Finger-fully extended

(b) Partially and fully flexed

Fig. 7.9 The finger is constructed and its bend behavior is shown

For the design of the iCub plastic hand, similar to that of the R1 hand, the top down design approach is adopted. Starting from the proposed kinematics, the SEA module size and placement, to deflection and transmission are all designed as part

of a skeleton model on top of which all other components and sub-assemblies will be mounted upon.

The design philosophy too, follows the same as the R1 hand, with optimizing cost, assembly and repair of the hand. The design process is broken down further as shown in the following sections.

7.2.1 Finger Design

The design of the finger is quite straightforward. It consists of two distinct phalanges: the proximal and the distal, which are mounted on the metacarpal joint which interfaces to the palm of the hand as shown in Fig.7.9. For the prototype, all components of the finger were rapid prototyped.

(a) Hard limits enforced on the finger

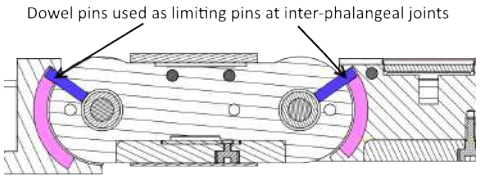

(b) Hard limit for 80% flexion on phalanges

Fig. 7.10 The hard limits enforced on the phalanges

The proximal phalange will eventually be machined in DELRIN. It consists of three distinct components: the main phalange, the clamping sheet and the dorsal cover. The proximal phalange contains most of the important components of the finger. It has the limit pins as shown in Fig.7.10. It also houses the joint shaft that interfaces with the metacarpal and the distal phalanges. The joint shaft in the metacarpal-proximal (MP) joint rotates with respect to the deflection of the proximal phalange to the metacarpal, while the proximal-distal (DP) joint shaft rotates with respect to the deflection of the distal phalange. The shafts are fastened to the metacarpal and the distal phalange respectively by means of set screws.

The shafts also house a diametrically charged magnet of 3mm diameter. The deflection of the shaft is recorded by a hall effect IC from AMS5055a which is mounted

on the same axes as that of the magnet and reads its deflection directly as a digital output.

Tendon Management

Tendon selection and studying its corresponding friction parameters have been discussed several times in previous work [54] [29]. For the purposes of this study, as in the R1 hand, Dyneema cables are used for their desirable properties. The actuation tendons enter from the palm through the metacarapal phalange and slide onto the rails of the proximal phalange, directed by the deflection pints in the entry and exit ports. They then go on into the distal phalange where in the lower half, there is a deflection pulley present as shown in Fig.7.11.

The deflection pulley is mounted atop a ball bearing and clamped down with a top plate which is in turn fastened to the shaft of the ball bearing. The shaft is press fit on to the phalange and helps to limit the tendon from escaping due to transverse loads.

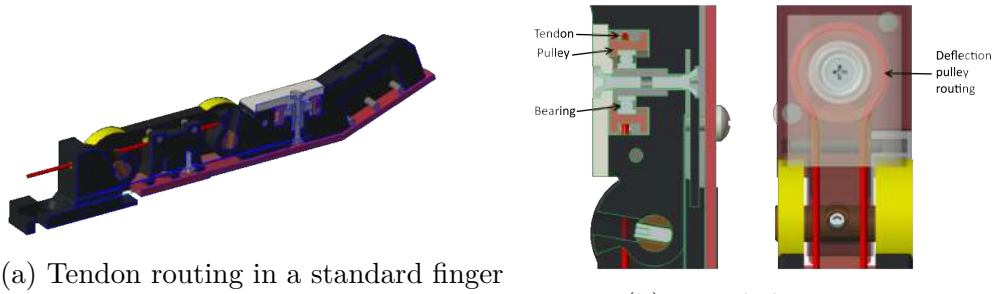

(a) Tendon routing in a standard finger

(b) Detailed cross section

Fig. 7.11 Tendon routing in a standard finger of the iCub plastic hand

The tendon slides on the rails provided in the proximal phalange. To prevent wear of material and to reduce friction, there are entry and exit pins on all entry and exit ports of both phalanges. Although, this does not completely rid the finger of sliding friction, it helps in minimizing and controlling it. The tendon direction is then reversed and follows the distal-proximal-metacarpal path, exiting the metacarpal joint and is wound around the shaft of the series elastic module.

Return Spring

The finger extends back into place after the torque is relieved from its joints using a return spring, which is mounted at the back along the spine of the finger.

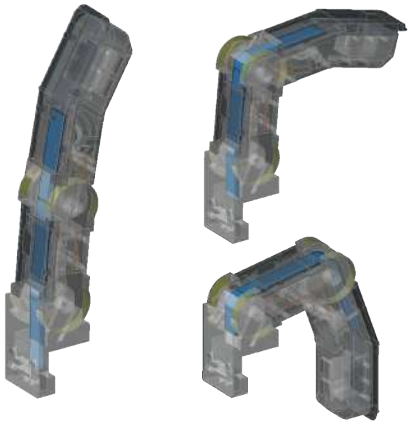

Fig. 7.12 Behavior of the return spring on the spine of the finger

The spring selection is as discussed in Sec.7.1.6. A drawback in this type of spring is that it essentially slides all along the surface of the spine, thereby increasing the friction in the system. This could be largely confined to the joints, but given the property of constant force springs, they need to always curve around the joints, further limiting the design of the phalanges.

Another problem to be addressed was locking the force direction of the spring under pressure. It tended to 'fold' under lateral force and permanently deforming, rendering it useless. This is controlled by limiting its sliding surface between the anterior and posterior sections of the proximal phalange. It is attached by a rivet in the proximal phalange and free sliding in the metacarpal phalange towards the end to make up for the joint radii during deflection.

7.2.2 Palm Design

The palm has four main functions. Firstly, it has to provide a friction surface to perform all the grasps as defined in the previous sections of different sizes and shapes. Secondly, it has to route the tendons from the forearm to the fingers with minimal friction losses. Thirdly, the fingers are all mounted onto the palm structure and finally, it houses all the sensor and integration boards which allow for data collection from all the sensors mounted on the fingers and the palm.

The palm has a stacked design to it, i.e., the palm has three distinct stacks. From back to front: the first stack acts as a support structure for housing all the finger sub-assemblies. The second stack or the central assembly is deemed the most important as it contains all the deflection pulleys and acts as the base structure on which the elastic

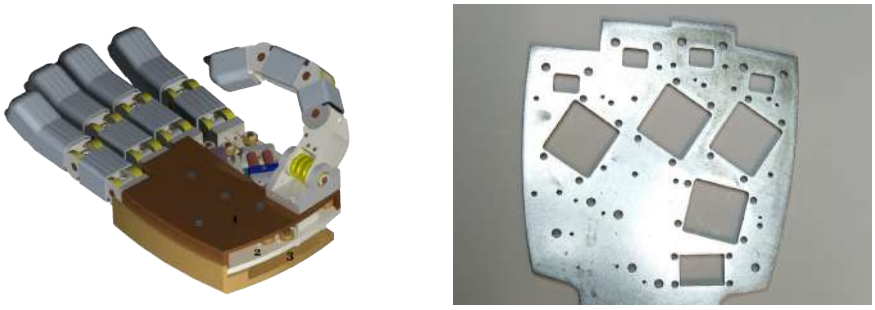

(a) The different palm stacks (b) The central stack element

Fig. 7.13 Palm design of the iCub plastic hand. The anterior part has the thumb mounted on it, the middle stack houses all the tendon routing and the series elastic modules, while the fingers are mounted onto the posterior stack of the palm.

modules are mounted on. This is the central part which adds rigidity to the entire palm structure and is made of waterjet-cut ERGAL material. The first and third layer of the sub-assembly stacks mount onto this central structure. The motivation behind this kind of structure is to trouble shoot the hand and to make maintenance easier. The sensor system of the elastic module can be dismounted along-with the thumb assembly by removing the first layer. All the transmission and elastic modules can be maintained this way, while the finger electronics can be mounted and repaired by not dismounting any of the other stacks.

Transmission Management

The tendon transmission is a complex problem to be addressed as the tendon has to be routed to the fingers and brought back into the palm to be attached to the series elastic module. The tendon transmission system needs to have three main characteristics:

- It needs to minimize friction between the tendons and the other components
- The tendons should be accessible and easy to fix within the palm
- It should act as an interface between the actuation system and the fingers

It is necessary to determine the amount of friction involved in the system during the routing of the tendon around the palm. An effective way to reduce frictions is to minimize cable re-directions and to use free-wheel pulleys (or rotating axes) rather than sliding surfaces (e.g. simple fixed axes). In fact, force loss non-linearly varies with the turning angle if the cable jointly moves with a bearing (as shown in Eq.7.25),

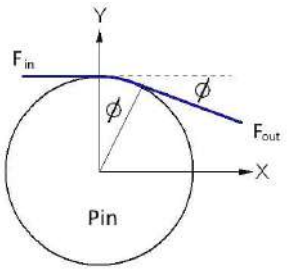

Fig. 7.14 Tendon friction force calculation [34]. Here the tendon is wrapped around a pin or pulley with a wrap angle of ϕ, and a tendon tension T

while it varies exponentially if the cable slides on a fixed surface using the Capstan equation as shown in Eq.7.26.

$$F_{in} = F_{out} \cdot \frac{1 + cos(\frac{\pi}{2} - \frac{\phi}{2} \cdot \mu)}{1 - cos(\frac{\pi}{2} - \frac{\phi}{2} \cdot \mu)} \tag{7.25}$$

$$F_{in} = F_{out} e^{\mu\phi} \tag{7.26}$$

where F_{in} and F_{out} are the tension forces at equilibrium before and after cable bending, μ is the friction coefficient and ϕ the angle of redirection. In the former case the friction coefficient is determined by the pulley and axis materials while, in the latter, it is determined by the tendon and pin materials. This way the frictional forces at each pin and pulley can be calculated and the effective pulling force can be determined after frictional losses. Considering the number of routing pins and pulleys during the tendon transmission in the palm, the frictional losses are quite considerable and are estimated to be around 40% for each finger. This is quite significant and the tendon transmission needs to be optimized in further iterations.

The tendon transmission within the palm is as shown in Fig.7.15 where the entry pulleys direct the tendons to the fingers using deflection pulleys. The elastic modules are skewed at an angle to facilitate easier access and to prevent contact between the tendons and the other sub-components. This is also to minimize the number of deflection pulleys, thereby minimizing friction present in the system. The anterior stack of the palm also mounts the thumb system. The tendon is redirected from the palm to the thumb through the anterior stack which is then wound around pulleys mounted at the base of the metacarpal phalange of the thumb. The tendon then winds around the thumb like in the normal fingers and re-enters the central stack and onto its elastic module.

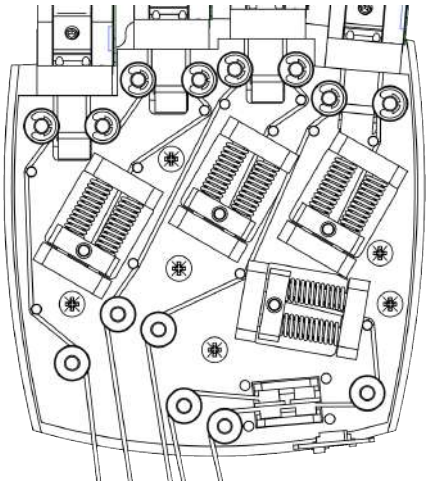

Fig. 7.15 Tendon management in the palm

7.2.3 Series Elastic Module Design

For the design of the series elastic module, compression springs were employed to achieve the desired deflection as discussed in Sec.7.1.7. Compression springs deflect along a straight line, whether it might be in the vertical or horizontal direction. One of the key design aspects to be explored would be the spring index of a given compression spring. It is the ratio of the outer diameter of a spring to its wire diameter, the formula for spring index can be given as :

Index = (Outer Diameter – Wire Diameter) ÷ Wire Diameter

A 4:1 index is difficult to manufacture commercially while springs higher than 15:1 index have low spring stiffness. This can be used as a guideline for selecting commercially available springs. A comparison of the two selected spring is as shown in Fig:7.16. The high range spring has a k value of 5N/m and the low range spring has a given k value of around 0.9N/m. These selected springs is estimated to work within the high and low range springs as defined previously. Since higher range performances are of particular interest, its response to impact loads and human interference needs to be explore further. The high range spring is selected in this design. The selected springs' behavior is first studied in the engineering simulation software ANSYS, for its stress, displacement and fatigue behavior. The spring index for the selected high range spring is 5 while that of the lower range spring is 9, this makes it good candidates for use in this design.

For this design, the high range force spring is mounted in series with all fingers except the index, this helps in impact load compensation during power grasps. The

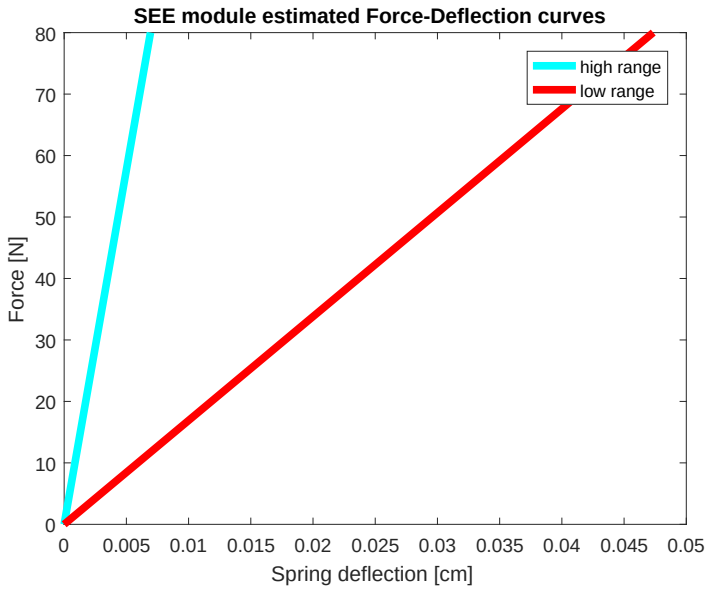

Fig. 7.16 Series elastic module estimated force deflection for a high range spring with k value as 5.8 [N/m] and a low range spring with k value as 0.845 [N/m]

lower range spring is mounted on the index's series elastic module, to aid in precision grasps. Both types of springs are mounted as shown in Fig.7.17a where the spring is held between two fixed components and the springs themselves are mounted on a slider which slides along two guiding shafts, depending on the pull of the tendon. The tendon is knotted and glued onto a central shaft on the slider. This slider shaft houses a rolling ball mounted on a spring, this is done to exert the right amount of pressure on the linear potentiometer which measure the deflection of the spring for a given force.

7.3 Electronics

One of the major aspects explored was the design of the flexible PCB and its design integration on the iCub plastic hand. The current iCub hand, similar to that of the R1 hand from the previous chapters, suffer from troubleshooting problems as they require the electronics to be mounted in series with the mechanical components. This way of cabling tends to make the assembly disorderly and time-consuming. This problem is addressed in this design by the incorporation of a single PCB running along the length of the finger, covering all taxels and joint position sensors in a single board. This flex circuit board is connected to the motor control boards (same as the ones explained in Chapter.5) in the forearm. The flex circuit design architecture is as shown in Fig.7.18a

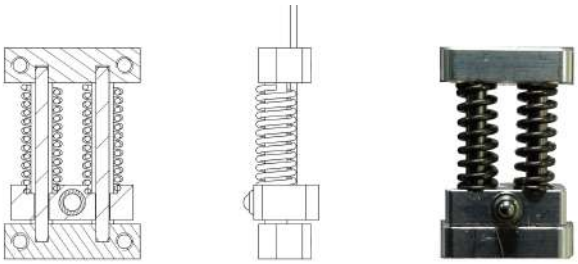

(a) Series elastic module - Linear design

(b) Series elastic module - preloaded shaft

Fig. 7.17 Series elastic module. The series elastic module assembly consists of a central component on which a shaft containing a preloaded spring is mounted. The tendon is attached to this shaft and as the tendon pulls on the shaft, this component rises up and consequently loads the springs. The springs are mounted on linear guides. The pre-loaded spring in the shaft is to apply the right force on the linear potentiometer that measures the spring deflection.

and is discussed in more detail in the following section.

7.3.1 Finger Flex Circuit Design

The finger flex circuit was developed in tandem with the mechanical design of the finger. Flexible PCB or flex circuits offer the same advantages of a printed circuit board: repeatability, reliability, and high density but with flexibility and vibration resistance. The most important reason to adopt flex circuit technology is the capability of the flex circuit to assume three-dimensional configurations and to avoid smaller cables from being untethered or broken. For this design, a blend of rigid and flex emphasizing the best of both constructions, adding synergistic capabilities is adopted. In its most typical configuration, the rigid-flex is a series of rigid PCBs joined by integrated flex circuits. Rigid areas provide excellent hard mount points for components, connectors and chassis while flex areas offer dynamic flexing, flex to fit, and component mounting. Hence, by careful design of zones, it is possible to vary the flex layers by giving the best of both worlds. This is achieved by adopting thinner flex circuits in zones that have low mass and require vibration resistance. The design of the flex circuit for the

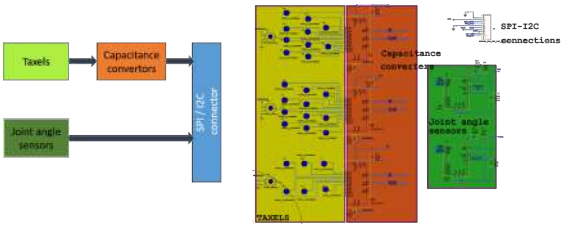

(a) Finger flex circuit architecture.

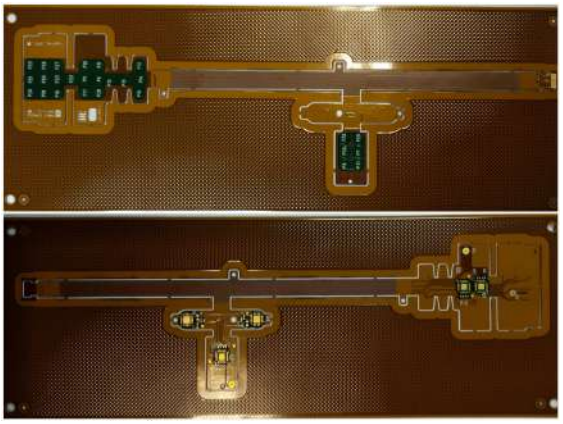

(b) Completed board without component mount.

Fig. 7.18 The completed design of the flex PCB is as shown. On top is the architecture of the board and in the bottom is the manufactured flex PCB without the ICs mounted.

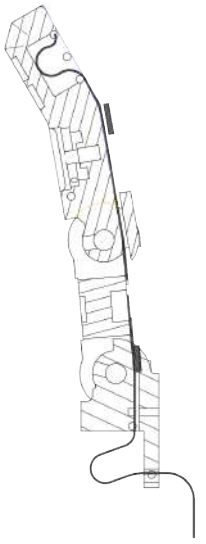

(a) Fully extended

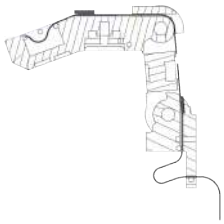

(b) Distal flexed

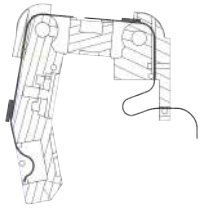

(c) All joints flexed

Fig. 7.19 Slack maintenance for flex PCB. The distal finger phalange is designed to have a cavity that allows the excess slack to be re-routed into it. The slack between the metacarpal and the proximal phalange is accommodated in the palm. As the finger flexes, these slacks are straightened and upon release go back into their cavities.

Table 7.3 Tactile sensing points on the finger skin as part of the flex PCB

Part	Sensing points	CDC chips
Finger Proximal	6	1
Finger Distal	21	2

finger was done by copying the external surface of the completed design of the distal phalange. This surface acts as the first bed of capacitive taxels for touch and force sensing of the finger. It is then drawn to the back and fixed with mounting points on the top of the distal phalange and a couple of others on the proximal phalange. Now, to achieve flexing, the PCB needs some slack maintenance. This is done by classfiying two zones where the slack will be controlled, one in the distal phalange and one after the metacarpal link. This entire zone of the PCB design is to carry the traces that connect each component to the other and is referred to as wire tracks hereafter.

After the initial mounting point, the flex circuit is led into the first 'slack zone' and is locked with limiting pins to prevent it from exiting. The circuit runs all along the spine of the finger, similar to that of the return spring. It is then deviated onto the front of the proximal phalange to form the joint position sensing part of the PCB. This measures the joint position of both the proximal and distal phalanges by reading the shaft deflection by means of the magnet installed in the joint shaft. This is read by hall-effect absolute position sensors (4096 counts per revolution).

This section of the PCB goes around one more time and constrained as a wrap with the front section of the PCB acting as a bed of nine capacitive taxels. The wire tracks continue on down into the metacarpal and exit from behind the finger and to the back of the palm, from where it connects to the motor controller board.

Silicone molds are utilized as an interface for the skin and to provide grip. The silicone based assembly acts as a slip on fit for the prototype. The tactile sensing PCB takes the same shape as the phalanges and is mounted directly onto the phalanges. A survey of all motors that are available in the market for our purposes was carried out. The MAXON-DCMAX16KL with a gear transmission ratio of 103:1 was selected for its desirable characteristics as discussed in the previous sections. All the motors required to actuate the hand is housed in the forearm along with the motor control boards. An easy to attach interface with four fasteners facilitates access to the hand for troubleshooting and testing.

The hand is designed as shown in Fig.7.21. It has the fingers mounted on the

(a) Assembly wrap of flex PCB (b) Completed flex PCB routing

Fig. 7.20 The finger flex PCB is assembled as shown.

posterior stack and mated with the middle stack that facilitates the tendon transmission. Both these stacks then assemble onto the front stack which houses the linear potentiometers to measure the series elastic deflection. The front stack of the palm also assembles mounts the thumb. The tendons enter the palm and are routed to the fingers as discussed in the previous sections. The thumb has two tendon actuated joints, one for rotation and the other for flexion. The finger PCBs assemble onto the

(a) Full CAD model (b) Exploded CAD model

Fig. 7.21 The completed CAD model of the hand

phalanges of the four fingers. Since, this is an experimental prototype, the PCB design will be further extended to the thumb. All the phalanges are then covered with silicone molded skin, whose deflection gives a corresponding taxel activation and force measure on the taxel sensor arrays. A silicone padding is also provided on the palm surface to aid in gripping objects.

7.4 Evaluation

Typically, the hand is tested against the user needs that was initially listed (Section 4.5.1). But in this case, the electronics, namely the finger PCB is still under production. Hence the hand is broken down into its major sub-assemblies and tested separately.

7.4.1 Force sensing

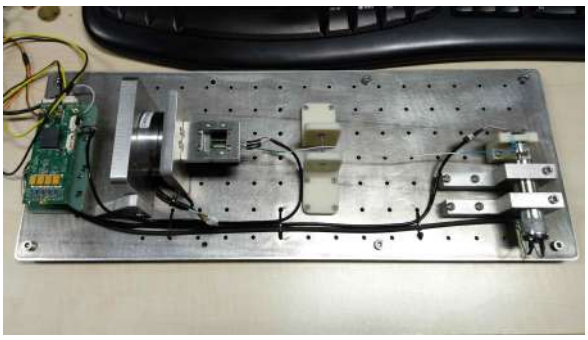

Fig. 7.22 The series elastic module test setup

A test for characterization of the series elastic module was designed. The tendon pulling forces were compared to the mechanical elastic deformation of the linear springs in the series elastic module. Increasing forces of up to nearly 70 [N] was applied and the corresponding spring deflection value was recorded. A quadratic fitting line across the recorded value was then superimposed, given the output data points, to draw a comparison with the predicted theoretical values. The test setup for this experiment is as shown in Fig.7.22. The series elastic module is mounted on to an FT sensor and pulled, the corresponding recorded force values are registered and compared with spring deflection which is recorded by the linear potentiometer.

The result, as shown in Fig.7.23, provided the series elastic module deflection behavior for a given range of input tendon forces. Each tendon was capable of a maximum pulling force of around 70 [N], and the corresponding spring deflection response for a low range spring as characterized in the previous section is shown. As expected, there is a slightly non-linear behavior in the spring, which largely lies under the expected values from the system.

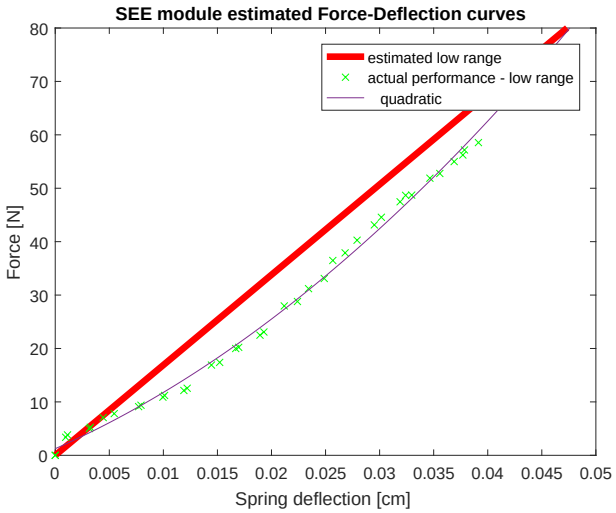

Fig. 7.23 Series elastic module estimated force deflection for a low range spring with k value as 0.845 [N/m]

7.4.2 Tactile Sensing

One of the key improvements from the previous design is taxel placement in the finger phalanges. As can be seen from Fig.7.24, the taxels do not lie on the center of the phalange plane. This has always lead to inefficient contact and force sensing in the previous design. In the iCub plastic hand prototype, the taxels are specifically placed

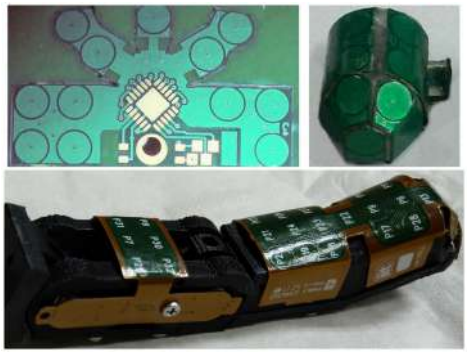

Fig. 7.24 The distribution of taxels on the fingertips in the iCub 2 hand

to achieve maximum gripping surface all along the phalanges. Moreover, taxels are present on both the proximal and distal phalanges, providing a uniform distribution of capacitive sensor arrays on the finger.

7.4.3 Cost

The iCub plastic hand being an experimental prototype, is deemed to be quite expensive. A detailed cost breakdwon is given in Table.7.4. Most of the mechanical components were rapid prototyped except for the shafts and the central stack of the palm, which were machined or waterjet cut. The control boards and the flex PCB of the fingers were deemed to be the most expensive part of the hand. However, scaling the hand manufacturing for larger quantities, reduces the price significantly. By developing molds for all the parts of the hand[1], the cost of the mechanical parts can be significantly reduced.

Table 7.4 A tentative cost breakdown of the iCub plastic hand

Particulars	**Prototype cost(€)**	**Projected cost(€)**
Mechanical components	2600	500
Electronics	5000	450
Motors	800	400
Commercials	800	800
Other	800	400
Assembly	500	250
Total	10500	2800

The electronics too is much easier to assemble and requires minimal cabling as compared to the R1 hand, as it employs well integrated flex circuits. Due to this, the cabling and assembly work required is also reduced, thereby cutting on assembly expenses.

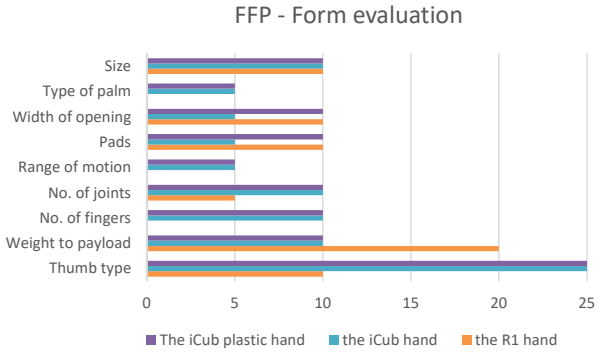

Fig. 7.25 The form breakdown of the iCub plastic hand as compared to the R1 and the iCub 2 hand.

[1]scaled up costs from: https://www.protolabs.com

7.4.4 FFP Evaluation

A partial FFP evaluation of the iCub plastic hand was carried out. The iCub plastic hand is endowed with a number of anthropomorphic features such as multiple fingers, an articulated thumb, friction grasp surfaces etc. The form score for the iCub plastic hand was hence evaluated to be 95%, which is excellent, the only major drawback being the number of joints in each finger.

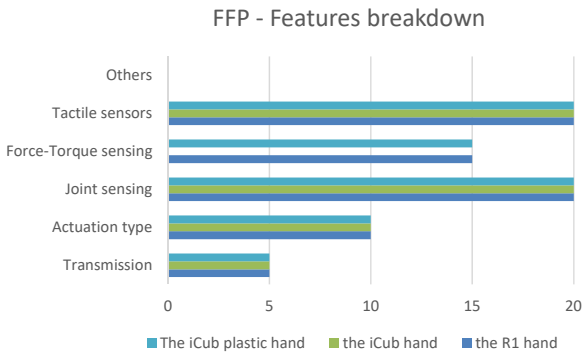

Fig. 7.26 The features breakdown of the iCub plastic hand as compared to the R1 and the iCub 2 hand.

The iCub plastic hand too is underactuated and has only two phalanges, hence it is better suited if it was a completely observable system. For this purpose, it was equipped with a number of sensors, which helped in boosting its features score up to 70% which is a much better score than that of the iCub hand and quite similar to that of the R1 hand. It contains motor position sensors, hall effect joint position sensors, position sensors for monitoring the series elastic module for force sensing and tactile sensors on all the phalanges.

Chapter 8

Conclusion

In this thesis a number of challenges were addressed. A new evaluation method was formulated and its different aspects were discussed. A new hand and wrist design for a new humanoid robot, the R1 was also explored in detail. Finally, an experimental prototype hand for the iCub hand was developed. The majority of this thesis presented was in the R1 platform and continued on to make an experimental prototype of the iCub hand.

8.1 Summary of Contributions

The work done in this thesis is composed of three major topics. Chapters 2 and 3 provided a context for this research and help set up the problem. A good way to explore solutions to these problems is the first main topic, where an evaluation index was proposed as envisioned in Chapter 4. The FFP index identified major evaluation criteria in robotic hands and explored the different aspects of anthropomorphism and the role it plays in increasing user expectations and different ways to evaluate robotic hands performance. This was then put into practice by first designing the R1 wrist, detailed in Chapter 5. It is based on a parallel kinematic structure with 3 DOF comprising of a pitch-roll movement comparable to humans in addition to an extensible structure. The constraints of constructing a commercially viable robot forced us to find the best trade-off between cost, functionality and payload. This helped to move beyond traditional solutions and opt for a parallel kinematic structure. The weight, cost, payload, accuracy and repeatability of the wrist were evaluated. Later, the R1 hand was detailed in Chapter 6, which was very user-centric and although capable of performing only a limited number of grasps, emphasis was put on affecting these

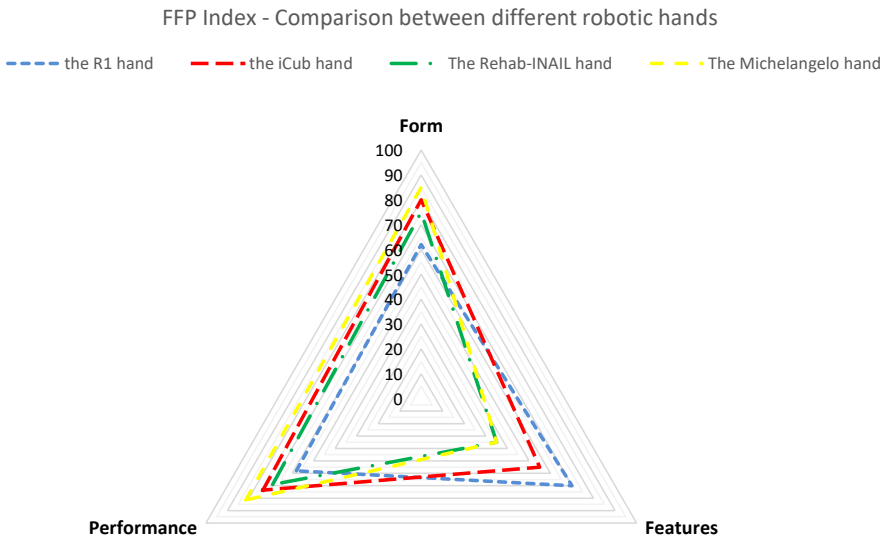

Fig. 8.1 FFP Evaluation and comparison between different hands

grasps effectively. It was highly robust and incorporated force sensing capabilities in the form of the SEE module and the tactile skin on the phalanges. Both the R1 wrist and hand aimed at making cost-effective systems that worked within its designed objectives.

Finally, the iCub plastic hand was developed and explained in Chapter 7 to explore all the three major aspects of the evaluation index, the form, features and performance, while still staying within the initial requirements of cost-cutting, use of polymers and underactuated systems. The iCub plastic hand was designed to explore the possibility of incorporating new techniques into the existing iCub platform.

8.2 Other Contributions

Some other contributions to the R1 humanoid robot project done by the author during the PhD includes the design of the R1 head display [122] (refer to Appendix.B for more details) and developing the expressions for it [74]. Another project of note was the design of a calibration device for quick calibration of tactile sensor arrays. More details on these devices can be found in the Appendix.

Fig. 8.2 The face display of the R1 humanoid

8.3 Reached Goals

The initial research objectives for this thesis as defined in Chapter.1 is summarized below:

- **Challenge 1**
  A humanoid robot that is easy to assemble and repair, which also happens to be cost-effective

- **Challenge 2**
  A method of evaluating the key characteristics that make up a good robotic hand that can be objectively evaluated from a hardware perspective.

- **Challenge 3**
  It aims to achieve a middle ground between compactness, weight, sensor-less safety, actuation and power of the hand. A trade-off between the number of actuators, the hand's dexterity and its payload should also be achieved.

- **Challenge 4**
  A hand that can move beyond just the classical grasping methodologies and to being an effective agent for human-like interaction.

- **Challenge 5**
  New and effective methods of sensor-less safety and inherent safety measures need to be explored. A robotic hand that aids safe human interaction by providing compliance and aiding in sensing the forces from its external environment and its internal system becomes mandatory.

[1] to be calculated : the experiments are currently being carried out

Table 8.1 Validation of the designed robotic hands

Challenges	R1	iCub plastic hand
easy to assemble and repair	≈	✓
cost-effective	✓	≈
gestures	X	✓
safe human agent interaction	✓	✓
easy integration	✓	✓
robust	✓	≈
silent	✓	✓
self-contained	✓	X
form	62	85
features	70	70
performance	58	*tbc*[1]
FFP score	62,4	*tbc*

All the different challenges that were envisioned were largely addressed during the course of the thesis. A summary of the challenges and their platform specific results is given in Table.8.1. The prototype iCub plastic hand is still undergoing tests and a final summary will be done in time. However, the preliminary results show a good improvement over the existing iCub hand while cutting down on costs. The R1 hand and wrist performed well within the parameters set for the R1 humanoid, under the context of being a domestic robot. However, several improvements can be made, which will be discussed in more detail in the following sections.

8.4 Lessons Learnt

Over the course of the thesis work, several challenges were addressed and consequent observations were made.

The use of force sensing components in the hand was a key concept, that turned out to be a useful addition to the framework of humanoid robots. It worked well as tendon tension monitoring systems, compensating also for the inherent elastic deformation in Dyneema tendons. It also aids the system in compensating impact force unloading and depending on the force range of the elastic element, can be tuned to sense forces in a given range.

Another interesting factor in efficient grasping was the design of the tactile skin. The existing capacitive sensing skin works well, but the accompanying dielectric mate-

rial is set in its physical properties and proved detrimental to effective grasping since it combined with textile covers which had smooth surfaces inefficient for grasping. These were substituted with 3M gripping material, which doubled as deformable di-electric material, whose shore hardness can be chosen. This is effective, since the deformation level to forces can be chosen this way, depending on the application.

A major lesson from the research is the use of two digit, semi-anthropomorphic hands. Grippers work due to the independence and range in movement, this was not the case in the R1 hand which was confined to a semi-anthropomorphic shape. This caused a lot of difficulties in performing finer grasps in an underactuated system. One of the options that was looked at was the use of split fingers, which is discussed a bit more in detail in the following section.

8.4.1 On the Use of Polymeric Materials

Most of the components on both these hands were built using polymeric materials, i.e: plastics. They come with their own set of advantages such as making transparent components, providing a wide range of colors, a wide variety of manufacturing methods, they are comparatively lighter with strengths approaching (depending on the polymer) equivalent metal components etc. In addition to this, they can also act as shields to some types of chemicals and function as thermal and electrical insulators.

However, the use of plastics in robotic hands proved to be quite challenging. Mostly due to the size of the components that went into a robotic hand. The final version of the R1 hand was mostly machined in DELRIN that had favorable physical properties. But most of the prototype components during testing was done in rapid prototyped plastic. This was always limited in one way or the other. Materials high on strength such as ABS had lower resolution due to FDM prints, while PLA printed materials suffered from strength issues. The quality of printers played a big role in determining tolerances, and components that assembled on high tolerances were difficult to produce. In addition, the orientation of the print played a key role due to the amount of moving components within the hand. All these issues need to be addressed before opting to construct a robotic hand using polymeric materials.

8.5 Future Work

Although there were a number of final products that came out as a result of this work, there still exists enough room for improvement. Some of the avenues that are being currently explored are listed below.

8.5.1 The FFP Evaluation Index

The FFP evaluation index needs to be tested in varied domains and not just humanoid robotics. One such domain that could be explored would be prosthesis. This evaluation can then be adapted to suit the domain and other parameters, previously unforeseen can be added to the evaluation.

8.5.2 The R1 Hand

The R1 hand is a key aspect of the R1 humanoid robot. Hence, a design rethink is required. The SEE module can be improved as it needs to be stronger and operational across the entire force range. The springs currently employed were limited by what was available commercially. A novel elastic element which can solve this problem while occupying less volume is being developed.

Another important aspect of the design overhaul of the R1 hand are its digits. From the experiments carried out in the previous sections, it was clear that at least one more digit that facilitates pinch grasp is required. Hence, to try this theory, multiple

Fig. 8.3 The different mock-ups for evaluating the improved version of the R1 hand

mock-up hands, that respect the size constraints of the R1 robot were constructed. They were made as diverse in design as possible and four different mock-ups were selected as shown in Fig.8.3. These hands were then tested in real life scenarios by

picking up objects from the Yale grasping dataset and carrying out non-prehensile and manipulation tasks from the FFP index.

A final design that gave the best results was then selected and chosen to be developed further. This design (a concept sketch of which is shown in Fig.8.4) is to be

(a) Back view (b) Front view

Fig. 8.4 Concept sketches of the improved version of the R1 hand

in accordance with the previous design of the R1 hand in aesthetics, while adding an extra digit to the hand for finer grasping and also to help in conforming to the grasp objects better.

8.5.3 The R1 Wrist

Since one of our main objectives has been cost reduction, custom machined metal parts will be replaced with machined plastic and eventually molded plastic. Care is being taken to design better cable routing facilities inside the wrist and to better incorporate the proposed skin to wrap around the entirety of its length. Other future objectives would focus on cost-reduction and optimizing manufacturing methods.

8.5.4 The iCub Plastic Hand

The prototype iCub plastic hand is currently being tested across all design parameters. However, some suggested improvements to the final design would be to incorporate force variable lattice meshes as the external skin interface, which would be capable of giving a linear force output on the capacitive taxel side with varying shapes on the

environment side. Some other suggestions would be to include the optimization of electronic component sizes and shapes. Currently, most electronic components apart from the finger flex circuit are placed outside the hand and, a part of them, should be integrated in the palm for a proper integration on the robot arm.

References

[1] American sign language dictionary. Website. URL `http://www.lifeprint.com/dictionary.htm`. Sign languages.

[2] Metropolis, 1927.

[3] Star wars:episode iv - a new hope, 1977.

[4] Priyanshu Agarwal, Jonas Fox, Youngmok Yun, Marcia K Malley, and Ashish D Deshpande. An index finger exoskeleton with series elastic actuation for rehabilitation: Design, control and performance characterization. *The International Journal of Robotics Research*, 34(14):1747–1772, 2015.

[5] Emre Akyürek, Anthony Huynh, and Tatiana Kalganova. Control of an asymmetrical design of a pneumatically actuated ambidextrous robot hand. 2014.

[6] Albert Albers, Christian Sander, and Akin Simsek. Development of the actuation of a new wrist for the next generation of the humanoid robot ARMAR. In *IEEE/RAS Int. Conf. on Humanoid Robots (HUMANOIDS)*, pages 677–682, 2010.

[7] Suguru Arimoto, Kenji Tahara, J-H Bae, and Morio Yoshida. A stability theory of a manifold: concurrent realization of grasp and orientation control of an object by a pair of robot fingers. *Robotica*, 21(2):163–178, 2003.

[8] Tamim Asfour, Pedram Azad, Niko Vahrenkamp, Kristian Regenstein, Alexander Bierbaum, Kai Welke, Joachim Schroeder, and Ruediger Dillmann. Toward humanoid manipulation in human-centred environments. *Robotics and Autonomous Systems*, 56(1):54–65, 2008.

[9] Kellar Autumn. How gecko toes stick the powerful, fantastic adhesive used by geckos is made of nanoscale hairs that engage tiny forces, inspiring envy among human imitators. *American scientist*, 94(2):124–132, 2006.

[10] Jeff C Becker and Nitish V Thakor. A study of the range of motion of human fingers with application to anthropomorphic designs. *IEEE Transactions on Biomedical Engineering*, 35(2):110–117, 1988.

[11] George A Bekey, Rajko Tomovic, and Ilija Zeljkovic. Control architecture for the belgrade/usc hand. In *Dextrous robot hands*, pages 136–149. Springer, 1990.

[12] L Biagiotti, F Lotti, C Melchiorri, and G Vassura. How far is the human hand. *A review on anthropomorphic robotic end-effectors*, 2004.

[13] Elaine Biddiss and Tom Chau. Upper-limb prosthetics: critical factors in device abandonment. *American journal of physical medicine & rehabilitation*, 86(12): 977–987, 2007.

[14] Elaine Biddiss, Dorcas Beaton, and Tom Chau. Consumer design priorities for upper limb prosthetics. *Disability and Rehabilitation: Assistive Technology*, 2 (6):346–357, 2007.

[15] Lionel Birglen, Thierry Laliberté, and Clément M Gosselin. *Underactuated robotic hands*, volume 40. Springer, 2007.

[16] PIO ENRICO RICCI BITTI and Isabella Poggi. 12. symbolic nonverbal behavior: Talking through gestures. *Fundamentals of nonverbal behavior*, page 433, 1991.

[17] Otto Bock. Michelangelo hand, 2011.

[18] Jonathan Bohren, Radu Bogdan Rusu, E Gil Jones, Eitan Marder-Eppstein, Caroline Pantofaru, Melonee Wise, Lorenz Mösenlechner, Wim Meeussen, and Stefan Holzer. Towards autonomous robotic butlers: Lessons learned with the pr2. In *Robotics and automation (icra), 2011 ieee international conference on*, pages 5568–5575. IEEE, 2011.

[19] Lyndon B Bridgwater, CA Ihrke, Myron A Diftler, Muhammad E Abdallah, Nicolaus A Radford, JM Rogers, S Yayathi, R Scott Askew, and D Marty Linn. The robonaut 2 hand-designed to do work with tools. In *Robotics and Automation (ICRA), 2012 IEEE International Conference on*, pages 3425–3430. IEEE, 2012.

[20] Sebastien Briot and Ilian Bonev. Are parallel robots more accurate than serial robots? *CSME Transactions*, 31(4):445–456, 2007.

[21] Ian M Bullock, Joshua Z Zheng, SDL Rosa, Charlotte Guertler, and Aaron M Dollar. Grasp frequency and usage in daily household and machine shop tasks. *Haptics, IEEE Transactions on*, 6(3):296–308, 2013.

[22] Alexander Buryanov and Viktor Kotiuk. Proporciones de los segmentos de la mano. *International Journal of Morphology*, 28(3):755–758, 2010.

[23] Darwin G Caldwell and Clarence Gosney. Enhanced tactile feedback (tele-taction) using a multi-functional sensory system. In *Robotics and Automation, 1993. Proceedings., 1993 IEEE International Conference on*, pages 955–960. IEEE, 1993.

[24] Berk Calli, Aaron Walsman, Arjun Singh, Siddhartha Srinivasa, Pieter Abbeel, and Aaron M Dollar. Benchmarking in manipulation research: Using the yale-cmu-berkeley object and model set. *IEEE Robotics & Automation Magazine*, 22 (3):36–52, 2015.

[25] Giorgio Cannata, Marco Maggiali, Giorgio Metta, and Giulio Sandini. An embedded artificial skin for humanoid robots. In *Multisensor Fusion and Integration for Intelligent Systems, 2008. MFI 2008. IEEE International Conference on*, pages 434–438. IEEE, 2008.

[26] Karel Capek. *RUR (Rossum's universal robots)*. Penguin, 2004.

[27] Maria Chiara Carrozza, C Suppo, Fabrizio Sebastiani, Bruno Massa, Fabrizio Vecchi, Roberto Lazzarini, Mark R Cutkosky, and Paolo Dario. The spring hand: development of a self-adaptive prosthesis for restoring natural grasping. *Autonomous Robots*, 16(2):125–141, 2004.

[28] MG Catalano, G Grioli, A Serio, E Farnioli, C Piazza, and A Bicchi. Adaptive synergies for a humanoid robot hand. In *IEEE-RAS International conference on humanoid robots*, pages 7–14, 2012.

[29] Giulio Cerruti, Damien Chablat, David Gouaillier, and Sophie Sakka. Alpha: A hybrid self-adaptable hand for a social humanoid robot. In *IEEE/RSJ International Conference on Intelligent Robots and Systems IROS 2016*, 2016.

[30] Maxime Chalon, Armin Wedler, Andreas Baumann, Wieland Bertleff, Alexander Beyer, Joerg Butterfaß, Markus Grebenstein, Robin Gruber, Franz Hacker, Erich Kraemer, et al. Dexhand: A space qualified multi-fingered robotic hand. In *Robotics and Automation (ICRA), 2011 IEEE International Conference*, pages 2204–2210. IEEE, 2011.

[31] K-J Cho, Josiah Rosmarin, and Harry Asada. Sbc hand: A lightweight robotic hand with an sma actuator array implementing c-segmentation. In *Robotics and Automation, 2007 IEEE International Conference on*, pages 921–926. IEEE, 2007.

[32] Young Sang Choi, Travis Deyle, Tiffany Chen, Jonathan D Glass, and Charles C Kemp. A list of household objects for robotic retrieval prioritized by people with als. In *Rehabilitation Robotics, 2009. ICORR 2009. IEEE International Conference on*, pages 510–517. IEEE, 2009.

[33] Christian Cipriani, Marco Controzzi, and Maria Chiara Carrozza. The smarthand transradial prosthesis. *Journal of neuroengineering and rehabilitation*, 8 (1):29, 2011.

[34] Wikipedia contributors. URL `http://en.wikipedia.org`.

[35] Marco Controzzi, Francesco Clemente, Diego Barone, Alessio Ghionzoli, and Christian Cipriani. The sssa-myhand: a dexterous lightweight myoelectric hand prosthesis. *IEEE Transactions on Neural Systems and Rehabilitation Engineering*, 25(5):459–468, 2017.

[36] John J Craig. *Introduction to robotics: mechanics and control*, volume 3. Pearson Prentice Hall Upper Saddle River, 2005.

[37] Mark R Cutkosky. On grasp choice, grasp models, and the design of hands for manufacturing tasks. *IEEE Transactions on robotics and automation*, 5(3): 269–279, 1989.

[38] P Dario, P Ferrante, G Giacalone, L Livaldi, B Allotta, G Buttazzo, and AM Sabatini. Planning and executing tactile exploratory procedures. In *Intelligent Robots and Systems, 1992., Proceedings of the 1992 lEEE/RSJ International Conference on*, volume 3, pages 1896–1903. IEEE, 1992.

[39] Joris De Schutter and Hendrik Van Brussel. Compliant robot motion i. a formalism for specifying compliant motion tasks. *The International Journal of Robotics Research*, 7(4):3–17, 1988.

[40] Myron A Diftler, JS Mehling, Muhammad E Abdallah, Nicolaus A Radford, Lyndon B Bridgwater, Adam M Sanders, Roger Scott Askew, D Marty Linn, John D Yamokoski, FA Permenter, et al. Robonaut 2-the first humanoid robot in space. In *Robotics and Automation (ICRA), 2011 IEEE International Conference on*, pages 2178–2183. IEEE, 2011.

[41] Henry Dreyfuss, R Alvin, et al. The measure of man and woman. *Whitney Library of Design*, 1993.

[42] Paul Ekman, Wallace V Friesen, and Phoebe Ellsworth. *Emotion in the human face: Guidelines for research and an integration of findings*. Elsevier, 2013.

[43] elumotion Ltd. Elu2 hand data sheet. 2010.

[44] Thomas Feix, Roland Pawlik, Heinz-Bodo Schmiedmayer, Javier Romero, and Danica Kragic. A comprehensive grasp taxonomy. In *Robotics, Science and Systems: Workshop on Understanding the Human Hand for Advancing Robotic Manipulation*, pages 2–3, 2009.

[45] Thomas Feix, Javier Romero, Carl Henrik Ek, Heinz-Bodo Schmiedmayer, and Danica Kragic. A metric for comparing the anthropomorphic motion capability of artificial hands. *Robotics, IEEE Transactions on*, 29(1):82–93, 2013.

[46] Jeremy A Fishel and Gerald E Loeb. Sensing tactile microvibrations with the biotac comparison with human sensitivity. In *Biomedical Robotics and Biomechatronics (BioRob), 2012 4th IEEE RAS EMBS International Conference on*, pages 1122–1127. IEEE, 2012.

[47] American Society for Surgery of the Hand et al. *The hand*. Churchill Livingstone, 1990.

[48] Naoki Fukaya, Shigeki Toyama, Tamim Asfour, and Rüdiger Dillmann. Design of the tuat/karlsruhe humanoid hand. In *Intelligent Robots and Systems, 2000.(IROS 2000). Proceedings. 2000 IEEE/RSJ International Conference on*, volume 3, pages 1754–1759. IEEE, 2000.

[49] Immanuel Gaiser, Stefan Schulz, Artem Kargov, Heinrich Klosek, Alexander Bierbaum, Christian Pylatiuk, Reinhold Oberle, Tino Werner, Tamim Asfour, Georg Bretthauer, et al. A new anthropomorphic robotic hand. In *Humanoid Robots, 2008. Humanoids 2008. 8th IEEE-RAS International Conference on*, pages 418–422. IEEE, 2008.

[50] Immanuel Nicolas Gaiser, Christian Pylatiuk, Stefan Schulz, Artem Kargov, Reinhold Oberle, and Tino Werner. The fluidhand iii: A multifunctional prosthetic hand. *JPO: Journal of Prosthetics and Orthotics*, 21(2):91–96, 2009.

[51] DJ Giurintano, AM Hollister, WL Buford, DE Thompson, and LM Myers. A virtual five-link model of the thumb. *Medical engineering & physics*, 17(4):297–303, 1995.

[52] David Gouaillier, Vincent Hugel, Pierre Blazevic, Chris Kilner, Jérôme Monceaux, Pascal Lafourcade, Brice Marnier, Julien Serre, and Bruno Maisonnier. Mechatronic design of nao humanoid. In *Robotics and Automation, 2009. ICRA'09. IEEE International Conference on*, pages 769–774. IEEE, 2009.

[53] Markus Grebenstein, Maxime Chalon, Gerd Hirzinger, and Roland Siegwart. Antagonistically driven finger design for the anthropomorphic dlr hand arm system. In *Humanoid Robots (Humanoids), 2010 10th IEEE-RAS International Conference on*, pages 609–616. IEEE, 2010.

[54] Markus Grebenstein, Alin Albu-Schaffer, Thomas Bahls, Maxime Chalon, Oliver Eiberger, Werner Friedl, Robin Gruber, Sami Haddadin, Ulrich Hagn, Robert Haslinger, et al. The dlr hand arm system. In *Robotics and Automation (ICRA), 2011 IEEE International Conference on*, pages 3175–3182. IEEE, 2011.

[55] Markus Grebenstein, Maxime Chalon, Werner Friedl, Sami Haddadin, Thomas Wimböck, Gerd Hirzinger, and Roland Siegwart. The hand of the dlr hand arm system: Designed for interaction. *International Journal of Robotics Research*, 31(13):1531–1555, 2012.

[56] Shadow Dexterous Hand. C5 technical specification. *Shadow Robot Company*, 2008.

[57] Thea Iberall. Human prehension and dexterous robot hands. *The International Journal of Robotics Research*, 16(3):285–299, 1997.

[58] Jibo Inc. *Jibo info sheet*. URL `www.jibo.com`.

[59] James N Ingram, Konrad P Körding, Ian S Howard, and Daniel M Wolpert. The statistics of natural hand movements. *Experimental brain research*, 188(2): 223–236, 2008.

[60] Hiroyasu Iwata and Shigeki Sugano. Design of anthropomorphic dexterous hand with passive joints and sensitive soft skins. In *System Integration, 2009. SII 2009. IEEE/SICE International Symposium on*, pages 129–134. IEEE, 2009.

[61] SC Jacobsen, EK Iversen, D Knutti, R Johnson, and K Biggers. Design of the utah/mit dextrous hand. In *Robotics and Automation. Proceedings. 1986 IEEE International Conference on*, volume 3, pages 1520–1532. IEEE, 1986.

[62] Matthew S Johannes, John D Bigelow, James M Burck, Stuart D Harshbarger, Matthew V Kozlowski, and Thomas Van Doren. An overview of the developmental process for the modular prosthetic limb. *Johns Hopkins APL Technical Digest*, 30(3):207–216, 2011.

[63] Kenji Kaneko, Fumio Kanehiro, Mitsuharu Morisawa, Kazuhiko Akachi, Gou Miyamori, Atsushi Hayashi, and Noriyuki Kanehira. Humanoid robot hrp-4-humanoid robotics platform with lightweight and slim body. In *Intelligent Robots and Systems (IROS), 2011 IEEE/RSJ International Conference on*, pages 4400–4407. IEEE, 2011.

[64] A Kapandji. Clinical test of apposition and counter-apposition of the thumb. *Annales de chirurgie de la main: organe officiel des societes de chirurgie de la main*, 5(1):67–73, 1985.

[65] Zhanat Kappassov, Yerbolat Khassanov, Artur Saudabayev, Almas Shintemirov, and Huseyin Atakan Varol. Semi-anthropomorphic 3d printed multigrasp hand for industrial and service robots. In *Mechatronics and Automation (ICMA), 2013 IEEE International Conference on*, pages 1697–1702. IEEE, 2013.

[66] Mark Karadesh. Flexor pulley system, February 2014. URL `http://www.orthobullets.com/hand/6004/flexor-pulley-system`.

[67] D Keymeulen and C Assad. Investigation of the harada robot hand for space. 2001.

[68] Yong-Jae Kim, Younbaek Lee, Jiyoung Kim, Ja-Woo Lee, Kang-Min Park, Kyung-Sik Roh, and Jung-Yun Choi. Roboray hand: A highly backdrivable robotic hand with sensorless contact force measurements. In *2014 IEEE International Conference on Robotics and Automation (ICRA)*, pages 6712–6718. IEEE, 2014.

[69] Ralf Kittmann, Tim Frohlich, Johannes Schafer, Ulrich Reiser, Florian Weisshardt, and Andreas Haug. Let me introduce myself: I am care-o-bot 4, a gentleman robot. 09 2015.

[70] George P Kontoudis, Minas V Liarokapis, Agisilaos G Zisimatos, Christoforos I Mavrogiannis, and Kostas J Kyriakopoulos. Open-source, anthropomorphic, underactuated robot hands with a selectively lockable differential mechanism: Towards affordable prostheses. In *Intelligent Robots and Systems (IROS), 2015 IEEE/RSJ International Conference on*, pages 5857–5862. IEEE, 2015.

[71] Nili E Krausz, Ronald AL Rorrer, et al. Design and fabrication of a six degree-of-freedom open source hand. *IEEE Transactions on Neural Systems and Rehabilitation Engineering*, 24(5):562–572, 2016.

[72] Gael Langevin. Inmoov hand. 2011. URL `http://www.inmoov.fr/`.

[73] Steven Michael LaValle. *Planning algorithms*. Cambridge university press, 2006.

[74] Hagen Lehmann, Anand Vazhapilli Sureshbabu, Alberto Parmiggiani, and Giorgio Metta. Head and face design for a new humanoid service robot. In *Social Robotics: 8th International Conference, ICSR 2016, Kansas City, MO, USA, November 1-3, 2016 Proceedings*, volume 9979, page 382. Springer, 2016.

[75] Johannes Lemburg and Frank Kirchner. Conceptual and embodiment design of robotic prototypes. *International Journal of Humanoid Robotics*, 8(03):419–437, 2011.

[76] D. Leyk, W. Gorges, D. Ridder, M. Wunderlich, T. Rüther, A. Sievert, and D. Essfeld. Hand-grip strength of young men, women and highly trained female athletes. *European Journal of Applied Physiology*, 99(4):415–421, Mar 2007. ISSN 1439-6327. doi: 10.1007/s00421-006-0351-1. URL `https://doi.org/10.1007/s00421-006-0351-1`.

[77] H. Liu, K. Wu, P. Meusel, N. Seitz, G. Hirzinger, M. H. Jin, Y. W. Liu, S. W. Fan, T. Lan, and Z. P. Chen. Multisensory five-finger dexterous hand: The dlr/hit hand ii. In *2008 IEEE/RSJ International Conference on Intelligent Robots and Systems*, pages 3692–3697, Sept 2008. doi: 10.1109/IROS.2008.4650624.

[78] Yves Losier, Adam Clawson, Adam Wilson, Erik Scheme, Kevin Englehart, Peter Kyberd, and Bernard Hudgins. An overview of the unb hand system. Myoelectric Symposium, 2011.

[79] Fabrizio Lotti, Paolo Tiezzi, Gabriele Vassura, Luigi Biagiotti, Gianluca Palli, and Claudio Melchiorri. Development of ub hand 3: Early results. In *Robotics and Automation, 2005. ICRA 2005. Proceedings of the 2005 IEEE International Conference on*, pages 4488–4493. IEEE, 2005.

[80] George F Mahl. Gestures and body movements in interviews. In *Research in Psychotherapy Conference, 3rd, May-Jun, 1966, Chicago, IL, US*. American Psychological Association, 1968.

[81] Mary W Marzke and Robert F Marzke. Evolution of the human hand: approaches to acquiring, analysing and interpreting the anatomical evidence. *The Journal of Anatomy*, 197(1):121–140, 2000.

[82] Claire F McCarthy, LK McLean, JF Miller, D Paul-Brown, MA Romski, J Rourk, and D Yoder. *Communication Supports Checklist: For Programs Serving Individuals with Severe Disabilities*. Paul H. Brookes Publishing Company, 1998.

[83] Courtney Medynski and Bruce Rattray. Bebionic prosthetic design. Myoelectric Symposium, 2011.

[84] Claudio Melchiorri, Gianluca Palli, Giovanni Berselli, and Gabriele Vassura. On the development of the ub-hand iv: an overview of design solutions and enabling technologies. 2013.

[85] Jean-Pierre Merlet. *Parallel robots*, volume 74. Springer Science & Business Media, 2012.

[86] Andrew T Miller and Peter K Allen. Graspit! a versatile simulator for robotic grasping. *IEEE Robotics & Automation Magazine*, 11(4):110–122, 2004.

[87] Tetsuya Mouri, Haruhisa Kawasaki, Keisuke Yoshikawa, Jun Takai, and Satoshi Ito. Anthropomorphic robot hand: Gifu hand iii. In *Proc. Int. Conf. ICCAS*, pages 1288–1293, 2002.

[88] Akio Namiki, Yoshiro Imai, Masatoshi Ishikawa, and Makoto Kaneko. Development of a high-speed multifingered hand system and its application to catching. In *Intelligent Robots and Systems, 2003.(IROS 2003). Proceedings. 2003 IEEE/RSJ International Conference on*, volume 3, pages 2666–2671. IEEE, 2003.

[89] John Russell Napier and Russell H Tuttle. *Hands*. Princeton University Press, 1993.

[90] F Negrello, MG Catalano, M Garabini, M Poggiani, DG Caldwell, NG Tsagarakis, and A Bicchi. Design and characterization of a novel high-compliance spring for robots with soft joints. In *Advanced Intelligent Mechatronics (AIM), 2017 IEEE International Conference on*, pages 271–278. IEEE, 2017.

[91] Rolland-Michel Assoumou Nzue, Jean-François Brethé, Eric Vasselin, and Dimitri Lefebvre. Comparison of serial and parallel robot repeatability based on different performance criteria. *Mechanism and Machine Theory*, 61:136–155, 2013.

[92] Lael U Odhner, Leif P Jentoft, Mark R Claffee, Nicholas Corson, Yaroslav Tenzer, Raymond R Ma, Martin Buehler, Robert Kohout, Robert D Howe, and Aaron M Dollar. A compliant, underactuated hand for robust manipulation. *The International Journal of Robotics Research*, 33(5):736–752, 2014.

[93] Gianluca Palli, Gianni Borghesan, and Claudio Melchiorri. Modeling, identification, and control of tendon-based actuation systems. *Robotics, IEEE Transactions on*, 28(2):277–290, 2012.

[94] Ill-Woo Park, Jung-Yup Kim, Jungho Lee, and Jun-Ho Oh. Mechanical design of the humanoid robot platform, hubo. *Advanced Robotics*, 21(11):1305–1322, 2007.

[95] Alberto Parmiggiani, Marco Maggiali, Lorenzo Natale, Francesco Nori, Alexander Schmitz, Nikos Tsagarakis, Joseé Santos Viktor, Francesco Becchi, Giulio Sandini, and Giorgio Metta. The design of the iCub humanoid robot. *International Journal of Humanoid Robotics*, 9, 2012.

[96] Alberto Parmiggiani, Luca Fiorio, Alessandro Scalzo, Anand Vazhapilli Sureshbabu, Marco Randazzo, Marco Maggiali, Ugo Pattacini, Hagen Lehmann, Vadim

Tikhanoff, Daniele Domenichelli, et al. The design and validation of the r1 personal humanoid. In *2017 IEEE/RSJ International Conference on Intelligent Robots and Systems (IROS 2017), Vancouver, Canada*. IEEE, 2017.

[97] Gill A Pratt and Matthew M Williamson. Series elastic actuators. In *Intelligent Robots and Systems 95.'Human Robot Interaction and Cooperative Robots', Proceedings. 1995 IEEE/RSJ International Conference on*, volume 1, pages 399–406. IEEE, 1995.

[98] Bussola R., Faglia R., and Incerti G. A tripod parallel robot as an active suspension for low frequencies damping. In *11th International Workshop On Robotics In Alpe-Adria-Danube Region*, pages 333–338. Budapest Polytechnic - Editor J.K. Tar, 2002. ISBN 9789637154096.

[99] Mayfield Robotics. Kuri : Home robot. URL `https://www.heykuri.com`.

[100] Softbank Robotics. Aldebaran 2.0.6.8 documentation, 2014. URL `http://doc.aldebaran.com/2-0/family/juliette_technical/joints_juliette.html`. visited 03 May 2017.

[101] Michael T Rosenstein and Roderic A Grupen. Velocity-dependent dynamic manipulability. In *Robotics and Automation, 2002. Proceedings. ICRA'02. IEEE International Conference on*, volume 3, pages 2424–2429. IEEE, 2002.

[102] Mark Rosheim. Robotic manipulator, 2003.

[103] J Kenneth Salisbury and John J Craig. Articulated hands: Force control and kinematic issues. *The International journal of Robotics research*, 1(1):4–17, 1982.

[104] Peter Scarfe and Euan Lindsay. Air muscle actuated low cost humanoid hand. *International Journal of Advanced Robotic Systems*, 3(2), 2006.

[105] Alexander Schmitz, Marco Maggiali, Lorenzo Natale, Bruno Bonino, and Giorgio Metta. A tactile sensor for the fingertips of the humanoid robot icub. In *Intelligent Robots and Systems (IROS), 2010 IEEE/RSJ International Conference on*, pages 2212–2217. IEEE, 2010.

[106] Alexander Schmitz, Ugo Pattacini, Francesco Nori, Lorenzo Natale, Giorgio Metta, and Giulio Sandini. Design, realization and sensorization of the dexterous icub hand. In *Humanoid Robots (Humanoids), 2010 10th IEEE-RAS International Conference on*, pages 186–191. IEEE, 2010.

[107] Stefan Schulz. First experiences with the vincent hand. Myoelectric Symposium, 2011.

[108] FAN SHAOWEI, LIU YIWEI, JIN MINGHE, LAN TIAN, and LIU HONG. The anthropomorphic design and experiments of hit/dlr five-fingered dexterous hand. *High technology letters*, 15(3):239–244, 2009.

[109] Gerwin Smit and Dick H Plettenburg. Design of a hydraulic hand prosthesis, with articulating fingers. Myoelectric Symposium, 2011.

[110] Softbank Robotics. How pepper works. URL `https://developer.softbankrobotics.com/us-en/documents/how-pepper-works`.

[111] Prensilia s.r.l. Ih2 azzurra series user guide. 2009-2013.

[112] Prensilia s.r.l. Eh1 milano series data sheet. 2010.

[113] RSL Steeper. Bebionic3 product brochure. *HYPERLINK" http://bebionic.com/distributor/documents/bebionic3_technical_information_-_Lo_Res.pdf"* http://bebionic. com/distributor/documents/bebionic3_technical_information_-_Lo_Res. pdf*, 2012.

[114] Doug Stewart. A platform with six degrees of freedom. *Proceedings of the institution of mechanical engineers*, 180(1):371–386, 1965.

[115] A. V. Sureshbabu, G. Metta, and A. Parmiggiani. A new cost effective robot hand for the icub humanoid. In *2015 IEEE-RAS 15th International Conference on Humanoid Robots (Humanoids)*, pages 750–757, Nov 2015. doi: 10.1109/HUMANOIDS.2015.7363454.

[116] T. Takaki and T. Omata. Load-sensitive continuously variable transmission for robot hands. In *Robotics and Automation, 2004. Proceedings. ICRA '04. 2004 IEEE International Conference on*, volume 4, pages 3391–3396 Vol.4, April 2004. doi: 10.1109/ROBOT.2004.1308778.

[117] Johan Tegin and Jan Wikander. Tactile sensing in intelligent robotic manipulation–a review. *Industrial Robot: An International Journal*, 32(1):64–70, 2005.

[118] Nikolaos G Tsagarakis, Giorgio Metta, Giulio Sandini, David Vernon, Ricardo Beira, Francesco Becchi, Ludovic Righetti, Jose Santos-Victor, Auke Jan Ijspeert, Maria Chiara Carrozza, et al. icub: the design and realization of an open humanoid platform for cognitive and neuroscience research. *Advanced Robotics*, 21(10):1151–1175, 2007.

[119] Milos Vasic and Aude Billard. Safety issues in human-robot interactions. In *Robotics and Automation (ICRA), 2013 IEEE International Conference on*, pages 197–204. IEEE, 2013.

[120] Anand Vazhapilli Sureshbabu, Giorgio Metta, and Alberto Parmiggiani. A new cost effective robot hand for the icub humanoid. In *Humanoid Robots (Humanoids), 2015 IEEE-RAS 15th International Conference on*, pages 750–757. IEEE, 2015.

[121] Anand Vazhapilli Sureshbabu, Jennifer Hong Chang, Luca Fiorio, Alessandro Scalzo, Giorgio Metta, and Alberto Parmiggiani. A parallel kinematic wrist for the r1 humanoid robot. In *Advanced Intelligent Mechatronics (AIM), 2017 IEEE International Conference on*, pages 1215–1220. IEEE, 2017.

[122] Anand Vazhapilli Sureshbabu, Marco Maggiali, Giorgio Metta, and Alberto Parmiggiani. Design of a cost-efficient, double curvature display for robots. In *Advanced Robotics and its Social Impacts (ARSO), 2017 IEEE Workshop on*, pages 1–6. IEEE, 2017.

[123] Anand Vazhapilli Sureshbabu, Marco Maggiali, Giorgio Metta, and Alberto Parmiggiani. Design of a force sensing hand for the r1 humanoid robot. In *Humanoid Robots November 15-17 2017 Birmingham (UK), IEEE RAS International Conference on*. IEEE, 2017.

[124] Richard F Weir and Jonathon W Sensinger. Design of artificial arms and hands for prosthetic applications. *Standard handbook of biomedical engineering and design*, pages 32–1, 2003.

[125] Zhe Xu and Emanuel Todorov. Design of a highly biomimetic anthropomorphic robotic hand towards artificial limb regeneration. In *Robotics and Automation (ICRA), 2016 IEEE International Conference on*, pages 3485–3492. IEEE, 2016.

[126] Zhe Xu, Vikash Kumar, and Emanuel Todorov. A low-cost and modular, 20-dof anthropomorphic robotic hand: Design, actuation and modeling. In *IEEE-RAS International Conference on Humanoid Robots*, 2013.

[127] Hanna Yousef, Mehdi Boukallel, and Kaspar Althoefer. Tactile sensing for dexterous in-hand manipulation in robotics a review. *Sensors and Actuators A: physical*, 167(2):171–187, 2011.

[128] Dachang Zhu, Jianwu Zhu, and Yuefa Fang. Analysis of a novel parallel manipulator for rotary humanoid wrist based on screw theory. In *Robotics and Biomimetics, 2008. ROBIO 2008. IEEE International Conference on*, pages 983–987. IEEE, 2009.

[129] A. G. Zisimatos, M. V. Liarokapis, C. I. Mavrogiannis, and K. J. Kyriakopoulos. Open-source, affordable, modular, light-weight, underactuated robot hands. In *IEEE/RSJ International Conference on Intelligent Robots and Systems*, pages 3207–3212, Sept 2014. doi: 10.1109/IROS.2014.6943007.

Appendix A

FFP Index - Task list

A.1 Grasping dataset for prehensile tasks

List of objects and their recommended grasp type. **Objects from the ALS GATECH dataset:** Bill, Book, Bowl, Can, Cell Phone, Coin, Cordless Phone, Credit Card, Cup / Mug, Dish Plate, Disposable Bottle, Fork, Glasses, Hairbrush, Hand Towel, Lighter, Magazine, Mail, Medicine Box, Medicine Pill, Newspaper, Non-Disposable Bottle, Pants, Purse, Scissors, Shirt, Shoe / Sandal, Small Pillow, Soap, Socks, Spoon, Straw, Table Knife, Toothbrush, Toothpaste, Walking Cane, Wallet, Wrist Watch

Objects from elderly care: Pen / Pencil, Plate, Safety razor, Spectacles case, Toilet paper, Tray, TV Remote

Objects from home or office: Marker, Apple, Banana, Cereal box, Cleaning spray, Cookie box, Flask, Hammer, Ketchup bottle, Key ring/ Keychain, Computer Mouse, Nail, Orange, Peanut/Jam Jar, Plastic Container, Scotch tape, Screwdriver, Spatula, Stapler, Strawberry

A.2 List of non-prehensile tasks

Simple: Sliding mouse, Open door, Emergency handle, Push buttons, Flipping switches, Open refrigerator, Unplug charger, Pull suitcase, Opening mini drawers
Increasing complexity: Pour water from bottle into a glass, Stir water in a glass with a spoon, Embed a screwdriver in its case, Open a jar/bottle
Gestures

Table A.1 Grasping Objects Dataset-1

S.No	Items	Use	Type
1	Apple	Home	Power
2	Banana	Home	Intermediate
3	Bill	ALS	Precision
4	Book	ALS	Power
5	Bowl	ALS	Precision
6	Can	ALS	Power
7	Cell Phone	ALS	Power
8	Cereal box	Home	Power
9	Cleaning spray	Home	Power
10	Coin	ALS	Precision
11	Cookie box	Home	Intermediate
12	Cordless Phone	ALS	Intermediate
13	Credit Card	ALS	Precision
14	Cup / Mug	ALS	Power
15	Dish Plate	ALS	Intermediate
16	Disposable Bottle	ALS	Intermediate
17	Flask	Home	Power
18	Fork	ALS	Precision
19	Glasses	ALS	Intermediate
20	Hairbrush	ALS	Intermediate
21	Hammer	Home	Power
22	Hand Towel	ALS	Power
23	Ketchup bottle	Home	Intermediate
24	Key ring/ Keychain	Home	Precision
25	Lighter	ALS	Precision
26	Magazine	ALS	Intermediate
27	Mail	ALS	Precision
28	Marker	Elderly	Intermediate
29	Medicine Box	ALS	Intermediate
30	Medicine Pill	ALS	Precision
31	Computer Mouse	Home	Intermediate
32	Nail	Home	Precision
33	Newspaper	ALS	Intermediate

Table A.2 Grasping Objects Dataset-2

S.No	Items	Use	Type
34	Non-Disposable Bottle	ALS	Power
35	Orange	Home	Intermediate
36	Pants	ALS	Intermediate
37	Peanut/Jam Jar	Home	Power
38	Pen / Pencil	Elderly	Intermediate
39	Plastic Container	Home	Power
40	Plate	Elderly	Power
41	Purse	ALS	Intermediate
42	Safety razor	Elderly	Precision
43	Scissors	ALS	Power
44	Scotch tape	Home	Precision
45	Screwdriver	Home	Intermediate
46	Shirt	ALS	Intermediate
47	Shoe / Sandal	ALS	Power
48	Small Pillow	ALS	Intermediate
49	Soap	ALS	Power
50	Socks	ALS	Intermediate
51	Spatula	Home	Power
52	Spectacles case	Elderly	Power
53	Spoon	ALS	Precision
54	Stapler	Home	Intermediate
55	Straw	ALS	Precision
56	Strawberry	Home	Precision
57	Table Knife	ALS	Intermediate
58	Toilet paper	Elderly	Power
59	Toothbrush	ALS	Intermediate
60	Toothpaste	ALS	Precision
61	Tray	Elderly	Intermediate
62	TV Remote	Elderly	Power
63	Walking Cane	ALS	Intermediate
64	Wallet	ALS	Power
65	Wrist Watch	ALS	Precision

- All okay
- Thumbs up
- Stop : palm
- Finger pointing
- Stop : closed fist

Fig. A.1 Some gestures

Additional: Counting from one to ten

A.3 Manipulation tasks

Act of changing the state of an object, either picked from the environment or enclosed within the hand. It is divided into the following categories:

A.3.1 In hand manipulation

Translation: Pick a ping-pong ball and move it to the palm and back
Shift: Pick up a pencil and move to its grip

Simple rotation: Unscrew a bottle cap
Complex rotation: Turn a pencil to use the eraser

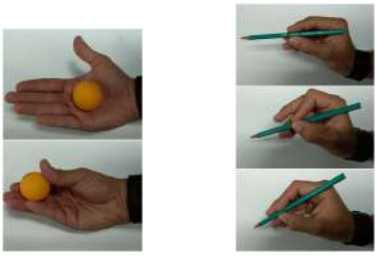

(a) Manipulation - Translation (b) Manipulation - Shift

Fig. A.2 In hand manipulation. In A.2a the hand needs to move a ping pong ball from the palm of the hand to being supported entirely by the fingers, while in A.2b the fingers should move in sync to transfer the grip from the middle of the pencil to the tip.

Fig. A.3 Manipulation task - Simple rotation. Rotate a bottle cap to unscrew and open a plastic bottle.

Fig. A.4 Manipulation task - Complex rotation. Rotate the pencil about the middle to change the use of the pencil from the pencil tip to the eraser tip.

Appendix B

The R1 head display

A low cost head (Fig.B.1) for the R1 robot which is to be employed in human-centric environments is proposed to bridge the gap between the abstract and uncanny representation in humanoid faces. The overall look of the R1 humanoid was conceived

Fig. B.1 Proposed display: The curved display presenting a neutral expression and mounted on the R1 humanoid robot (in picture)

by a design team that took these motivations into consideration. The head also had to be coherent with the overall look of the robot, hence the designers conceived of an abstract head for the R1 humanoid. Drawing from these preliminary guidelines, a list of higher level user requirements were drawn and are enumerated as follows:

- the display outputs a gamut of colors distinguished by the visible spectrum of the human eye
- the color reproduction is discernible and satisfactory; scores more than 80% value on the HSV scale for the core RGB colors
- the display module does not weigh more than 600g

- the display should not cost more than 10% of the total cost of the robot, i.e €1200

- the display should have enough resolution to display expressions efficiently; i.e, expressions displayed should be easily recognizable

To address all these issues a low cost display made from rapid prototyping technologies that enables the projection of images on complex surfaces was selected. This approach had the added advantage of avoiding the reduced intensity and illumination problems in daylight and ambient light that conventional displays suffer. The head and the display were to be curved to give the impression of a 3D surface, while maintaining visibility from different viewing angles. One further design requirement for the display was that it was required to be easily replaced and easy adaptation to allow seamless integration with the rest of the components of the head (e.g. 3D sensors, speakers, cameras etc.).

B.1 Conceptual design

Traditional methods for realizing displays where light projection is decoupled from the light source lie in the use of fiber optic cables due to their superior total internal reflection (TIR) properties. It was decided to further explore this concept to remove the shortcomings in the existing methods. Due to the low cost requirement and the complexity of projecting light on complex surfaces, the use of 3D printed objects was selected. Standard red-green-blue (RGB) light emitting diodes (LED) were chosen as the source of light for the display. The remaining part of the problem was then to transmit the light generated by the LED onto a curved surface; this was solved by creating custom light guides much like a fiber optic cable. Our solution to manufacture these light guides was to create a 3D printed optics module. The main drawback of this approach was that unless a lot of diffusion is applied after the light is conveyed on the projection surface a discrete and "pixelated" output would be seen . This aesthetic effect was nevertheless considered compliant with the overall look of the robot. Finally the requirement for design flexibility was solved by designing a modular display which was capable of conforming to shapes and confined to small spaces.

B.1.1 Printed optics module design

The basic concept of optic fibers is imitated in the new module design by constructing the structure using 3D printing technology. The "light guides" act as the transmission medium or the core. The cladding is then built surrounding the light pipe and it doubles up as the support structure that holds the light pipe in place. The cladding has a lower refractive index, that assists in reflecting back the light rays into the light pipe. When the light rays encounter the cladding at any angle above the "critical" angle, the light achieves total internal reflection. The critical angle θ_c is given by Snell's law,

$$n_1 \sin\theta_i = n_2 \sin\theta_t \tag{B.1}$$

where n_1 and n_2 are the are refractive indices of the light pipe and cladding respectively and θ_i and θ_t are the angle of incident light from the LED and the refracted angle respectively. To find the critical angle, the value for θ_i is determined when $\theta_t = \pi/2$ and thus $\sin\theta_t = 1$. The resulting value of θ_i is equal to the critical angle θ_c. The resulting formula for the critical angle is given by:

$$\theta_c = arcsin\left(\frac{n_2}{n_1}\right) \tag{B.2}$$

The classical structure of fiber optic cables is restructured into just three layers of light pipe (core), support (cladding, coat and support) and a thin layer of air. The efficiency of TIR is controlled by varying the materials to achieve different refractive indices of the cladding and core material. The resulting transmitted light is then

Fig. B.2 Printed optics module structure. It can be observed that the LEDs are set in the "light pipes" structure which is then inserted into the cladding before being covered by the light diffuser or diffusion mask. The "light pipes" are in VeroClear, the cladding in PE and the light diffusion mask made of black Plexiglass.

passed through a light diffuser for better contrast and uniformity in light distribution (as shown in Fig.B.2).

B.2 Embodiment design

The objective of this display is to provide a uniform illumination on multiple curvatures (concave and / or convex). The display as shown in Fig.B.3 is composed of a matrix of RGB light elements (pixels/element 1) that project light on the outer surface of the device. The light passes through the light pipe (element 2) which transfers the light on the outer surface of the display. The support structure (element 3) acts as a cladding and also isolates light passing through the light pipes. The surface is then covered by a transparent or semi-transparent diffusion plate, on which the image is displayed. The display needs to have adequate luminosity to be visible in daylight. As a reference value the reader should consider that the average luminosity in daylight interior is around 500 lumens (lm).

B.2.1 Display Construction

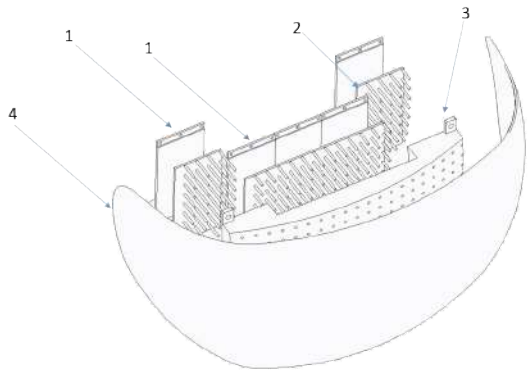

Fig. B.3 Proposed display structure. The FML PCB Board (element 1) is placed on the light pipe structure (element 2) which is then inserted into the cladding (element 3). These are all then covered with a diffusion mask (element 4) which conforms to the shape of the cladding structure.

The light pipe (Fig.B.4) is the mechanical part made of a transparent material. This part can be obtained with different technological processes such as CNC machining, 3D printing or molding. The light source is an RGB LED 2x2mm size. The emitted light is carried by the light guide, that is made of a transparent material. For these purposes the VeroClear® material from Stratasys® was used. Parts were printed on a Stratasys Connex 500 PolyJet® 3D printer; this machine has a print resolution of 0.1mm.

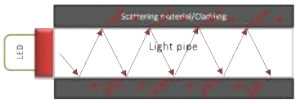

Fig. B.4 Light pipe concept. This shows the total internal reflection concept as applied to our printed optics module.

The terminal part of the guide has a surface roughness specially made to yield a homogeneous diffusion of the light over the end part of the guide. This part is important, because if made differently, would not allow the colors to diffuse effectively. As seen in Section II, to separate the light emitted by the various pixels and to guide the light pipe, another mechanical element, the cladding (element 3) is necessary. This was first tested with a 3D printed structure using VeroBlack. However, this structure was later replaced with a machined Polyethilene (hereafter referred to as PE) for increased robustness and accuracy. PE was specifically selected for its low density to reduce the total weight of the system. It should be noted that this element has holes in which the light pipes are inserted. The PE structure acts as the cladding and has a lower refractive index (around 1.36) compared to that of the light pipe (around 1.53). These guide holes in the cladding have a diameter that is 2mm greater than the light pipes themselves, so that there is a layer of air between the light pipe and the support material. This prevents the light from being absorbed by the support and acts as a second layer of cladding. In this way the cladding also allows the separation of the light that is emitted by adjacent guides. The outermost surface of the display, the light diffusion mask (element 4) will then be the single or double-curved surface which serves as a cover, displays the projected image, and hides the internal structure of the display. The black Plexiglass visor/mask that was used has a reflectance value of 20%.

Fig. B.5 Internal structure. Shows the arrangement of the sensors and the electronic boards in the head structure in conjunction with the display structure(shown in white)

B.2.2 Head Construction

As mentioned earlier the R1 head also houses a number of sensors and control boards as shown in Fig.B.5. The head comprises a frame mounted on a two DOF neck with a pitch and a yaw joint. The display is fixed onto a frame which also houses an ASUS Xtion Pro Live RGBD sensor. The head also houses two Leopard Imaging LI-OV580-STEREO stereo cameras, a microphone and an ABS-229-RC speaker which is situated just below the display module. Finally the head contains a low-cost and high-performance Single Board Computer (SBC) also dubbed "Z-turn board" built around the Xilinx Zynq-7010. This board is placed right behind the display module and controls most of the expression related activities of the robot: it controls the display, through the FML boards via the ZFC electronic board (details regariding these boards will be discussed more in detail in the following section), it processes stereo microphone data, and controls the speaker used to generate the voice of the robot.

B.2.3 Electronics

The electronics architecture of the proposed display is as shown in Fig.B.6. An FPGA-based board Z-turn board controls a number of FML cards (Element 1) connected in a chain. The FML boards are equipped with integrated circuits capable of handling 512 RGB LED present on the same board and arranged in a matrix (16 columns by 32 rows). We can connect up to 16 cards in an FML chain. In the current solution 5 FML boards are used, with a total of 80×32 pixels (2560 pixels). The light sources are RGB LED, 2×2mm in size.

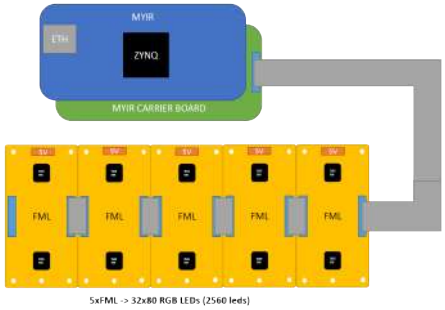

Fig. B.6 Hardware architecture of the display

B.3 Evaluation

The display was tested for its color rendering capabilities, but the most important metric was its capability of displaying the expressions of the R1 humanoid. All the other sensors and electronic boards fit well within the head with no unsightly deviations from the original proposed shapes. Details are discussed in the following sub-sections.

B.3.1 Expression perception

For the purposes of displaying expressions and notifications, the display performed well. The display satisfied the requirement of an effect different enough from that of a traditional LCD or OLED display and had enough resolution to show the images as not excessively disjointed. Some of the sample images of the expressions are as shown in Fig.B.7; these depict the basic human expressions modified for the robot.

(a) Neutral (b) Happy (c) Sad (d) Surprised

Fig. B.7 Sample expressions on the display

A multiple choice survey to study the basic intent behind each expression on the display was carried out. From the survey, 82 replies were received, of which 50 were male and 32 were female. The mean age of the participants was 33.8 years, ranging from 20 to 72. Concerning their experience with robots 37 reported none, 15 reported little, 12 reported some experience, and 18 participants indicated that their experience with robots was substantial. Most of the users who took the survey said they could correlate the face with a particular expression. The survey was done using four designs that indicated “neutrality, happiness, sadness and surprise". Since the exact expression interpretation is influenced by each person’s individual perception, this was not deemed the major intent behind this test. The results of the survey showed that more than 86% agreed on the neutral expression, 60% agreed on happy, 95% on sad and 53% on surprised. But interestingly, the users correlated the displayed face to an expression more than 94% across all given inputs. This shows that the display can be used as an effective HRI interface to display expressions, which remains as the primary objective.

B.3.2 Weight analysis

The display was optimized by the use of low density PE to reduce weight. The other advantage of using machined PE is that it makes cleaning easier as the support material from rapid prototyping methods is absent and does not need to be removed. This was problematic since cleaning the support material after 3D printing was quite a challenge, especially in the cladding. The end weight of the display sub-assembly was in accordance with our initial user requirement of 600g.

B.3.3 Observations

Multichromatic images performed well for color reproduction but were affected by the resolution limitations of the display. The individual LED arrays were previously color calibrated. This study was solely to inspect the overall impact of the light pipes and the surrounding cladding on the reproducibility of colors on the finished screen.

A pixelated display in place of a homogeneous display was successfully built as the focus was on improving clarity and never to provide a replacement for existing display technologies. The cladding acts as an insulator that avoids optical crosstalk and contributes to the pixel effect. The differential refractive indices between the transparent and opaque material facilitates total internal reflection of light which in turn aids in minimizing light leak. This gave clarity in illumination which is further aided by the curved diffusion mask.

Printing both the light pipe (the core) and the cladding together in a single structure with multi-material printing technology was also experimented with. The results were not satisfactory as the air gap proved to be important to reduce scattering losses, and the boundary between the cladding part and the light-guiding part was not sufficiently “sharp” because of the 3D printer resolution limitation. Providing a base structure at the bottom of the light pipes that allows the LED module to “set" inside the light pipes also reduced the scattering effect of the LED light.

Appendix C

A comparison of robotic hands

Table C.1 Robotic hands

Hand	Year	Digits	SC	DOF	DOA	Wt.	PL	Tactile	FS
UTAH/MIT	1986	4	N	16	32	-	3,17	Y	Y
Stanford/JPL Hand	1986	3	Y	9	12	-	-	N	N
Belgrade/USC	1990	5	N	15	4		2,26	Y	Y
GIFU Hand III	2002	5	Y	20	16	1,4	1,5	Y	Y
SPRING	2004	3	Y	8	1	0,4	0,5	N	Y
UB Hand 3	2005	5	N	20	16	3,6	1,2	N	N
Schunk	2006	5	Y	20	9	1,3	1	Y	N
CyberHand	2006	5	Y	16	6	0,36	1,2	N	-
SBC Hand	2007	5	N	16	32	0,8	0,2	N	N
Nao	2008	3	N	4	1	0,19	0,1	N	N
Shadow	2008	5	N	22	44	4,2	3,6	Y	Y
DLR/HIT II	2008	5	N	20	15	1,5	-	N	Y
iLimb	2009	5	Y	11	5	0,46	-	N	-
Vanderbilt	2009	5	Y	16	5	0,5	0,5	N	Y
FluidHand III	2009	5	N	13	8	-	4,5	N	Y
Twendy One	2009	4	Y	16	13	-	-	Y	Y
iCub	2010	5	N	19	9	0,4	0,6	Y	N
Barrett	2010	3	Y	8	4	1,2	6	N	N
Vincent hand	2010	5	N	11	5	1,8	6	N	-
UNB	2010	5	Y	11	3	-	-	N	N
Sonoda Golder	2010	5	Y	14	15	0,8	0,4	N	N

Table C.2 Robotic hands

Hand	Year	Digits	SC	DOF	DOA	Wt.	PL	Tactile	FS
Prensilia -SRI Hand	2011	5	N	16	5	0,55	10	N	Y
Bebionic	2011	5	Y	11	5	0,5	6	N	-
DLR Hand arm	2011	5	N	19	38	0,7	1,5	N	-
Robonaut2	2011	5	Y	12	16	2,1	2,25	N	Y
UNIPI	2012	5	Y	19	1	1	2	N	N
Michelangelo(Ottobock)	2012	5	N	6	2	-	7,5	N	-
PR2- Velo 2G	2012	2	Y	4	1	0,8	0,6	N	N
KITECH	2012	4	Y	16	16	0,9	2	N	N
SRI	2012	4	N	12	4	1,2	1	N	N
SANDIA	2012	4	N	12	4	0,8	1,6	N	N
FESTO - Multichoice	2013	3	N	15	25	-	-	N	-
ZheXU Biomimetic	2013	5	N	20	10	4,6	0,8	N	N
Washington	2013	5	Y	18	36	0,66	2,4	N	N
UB Hand4	2013	5	Y	20	15	3,6	3,5	Y	Y
KAIST	2013	5	N	10	6	0,362	1,1	N	-
YALE	2013	4	Y	8	1	0,4	1	N	N
KU Hybrid	2013	4	N	13	8	1,2	0,75	N	N
Pepper	2014	5	Y	5	1	0,28	0,25	N	N
Care-O-Bot 4	2014	2	N	2	2	0,9	0,5	N	N
iHY	2014	3	Y	8	5	1,35	22	Y	N
Shadow Lite	2015	4	Y	13	13	2,4	4	Y	Y
Openbionics	2015	5	Y	16	2	0,3	1,5	N	N
Brunel	2015	5	Y	13	18	6	0,5	N	Y
ALPHA	2016	5	N	18	7	0,54	0,4	N	N
Colorado	2016	5	N	10	6	0,584	0,8	N	-